NEUTRAL MONOLITHIC CAPILLARY COLUMNS WITH ALKYL AND ARYL LIGANDS FOR REVERSED-PHASE CAPILLARY ELECTROCHROMATOGRAPHY

By

SAMUEL MUKIHA KARENGA

Bachelor of Science in Chemistry
Egerton University
Njoro, Kenya
2002

Master of Science in Chemistry
Egerton University
Njoro, Kenya
2009

Submitted to the Faculty of the
Graduate College of the
Oklahoma State University
in partial fulfillment of
the requirements for
the Degree of
DOCTOR OF PHILOSOPHY
July, 2010

NEUTRAL MONOLITHIC CAPILLARY COLUMNS

WITH ALKYL AND ARYL LIGANDS FOR

REVERSED-PHASE CAPILLARY

ELECTROCHROMATOGRAPHY

Thesis Approved:

Dr. Ziad El Rassi

Thesis Adviser

Dr. Richard A. Bunce

Dr. Jeffery L. White

Dr. Legrande M. Slaughter

Dr. Andrew J. Mort

Dr. Mark E. Payton

ACKNOWLEDGMENTS

To the Glory of God the Father, The Son and The Holy Spirit from whom every good thing comes from, and through whom I can do all things, To Him alone be Glory and honor both now and forever more! It is with great respect and profound gratitude that I wish to recognize the following people without whom, this accomplishment would not have been possible.

I am greatly indebted to my advisor Dr. Ziad El Rassi for his steadfast and diligent instruction during the years under his tutelage. His editorial advice and willingness to share his knowledge and expertise in the field of separation science will always make me feel that he was the best advisor to work under. To all this I say may God keep you safe and healthy Dr. El Rassi.

I am grateful to the members of my graduate advisory committee, Dr. Richard Bunce, Dr. Jeffery White, Dr, Legrande Slaughter and Dr. Andrew Mort. Their advice has gone a long way to teach me immeasurable lessons and insights on the workings of academic research. I particularly feel indebted to Dr. Bunce for providing most of the organic aromatic compounds used in this study and for the Organic Chemistry classes I took from him.

Special thanks to the entire faculty and staff of Oklahoma State University Department of Chemistry without whom this pursuit for higher education would not have

been possible. I am also grateful to the past and present members of Dr. El Rassi's research group for their support and friendship. Special thanks to my brothers Simon Ndung'u, Joseph Murakaru, William Kaboi and sisters Purity Wambui and Rebecca, Nyamiugu for their love, moral, financial and spiritual support throughout my academic endeavors. A big thank you to my nephew Linus Muchugia my friends Jadiel Kibaru, John Gitau, Joseph Nderitu, Josephine Nyakio, Jane Nyaguthii and Karen Nganga for their support and friendship that went a long way to enable me realize this goal. I would like to sincerely thank my cousin Francis Mugo for his encouragement to go for further studies and for his financial assistance. I also thank and appreciate all those people who accompanied me to Jomo Kenyatta International Airport, Nairobi, Kenya on the evening of August 10, 2005 to board a plane to the United States for graduate studies and the small wonderful Presbyterian Church of East Africa that gathers at Gathogorero for their love support, and prayers that went a long way to keep me sound and strong. Thank you to many other friends who through one way or the other contributed to the success of this undertaking and whose names were not listed here due to constraints of space. May the good Lord reward you abundantly for your good work!

Finally, I would like to dedicate this work to my late parents Samson and Agnes Karenga. Dad and Mom, though you never lived to witness this accomplishment by the son you bore in your old age, I will always cherish your love for me, the confidence, belief and the pride you had in me. You taught me to always trust in God, which I cherish as one of the greatest gifts I inherited from you. I will always be proud to be your son!

TABLE OF CONTENTS

Chapter Page

Chapter Page

Chapter Page

Chapter Page

LIST OF FIGURES

Figure Page

CHAPTER I

CHAPTER II

Figure Page

Chapter III

CHAPTER IV

Figure Page

CHAPTER V

Figure Page

CHAPTER VI

CHAPTER VII

Figure Page

LIST OF SYMBOLS AND ABBREVIATIONS

α	selectivity factor
ε	dielectric constant
ε_o	permittivity of the vacuum
ζ	zeta potential
η	viscosity of the electrolyte solution
σ_t	standard deviation of the peak in unit time
σ_L	standard deviation of the peak in unit length
σ^2	peak variance
E	electrical field strength
I	ionic strength of the medium
k'	chromatographic retention factor
k^*	retention factor of a charged solute in CEC
k^*_e	velocity factor of a charged solute in CEC
L	total length of the separation capillary
l	length of the separation capillary from the inlet to the detection
N	number of the theoretical plates
R_s	resolution
t_o	migration time of a neutral solute
t_m	migration time of retained solute
υ_{ep}	electrophoretic velocity

u_{ep}	interstitial electroosmotic velocity
u^{*}_{ep}	apparent electroosmotic velocity
w_b	peak width at the base
w_h	peak width at half height
w_i	peak width at the inflexion point
γ-AMPS	γ-methacyloxy propyl-trimethoxysilane
ABs	alkylbenzenes
ACN	acetonitrile
AETA	[2-(acryloyloxy)ethyl]-trimethylammonium methyl sulfate
AIBN	2,2'-azobis(isobutyronitrile)
AMPS	2-acrylamido-2-methylpropanesulfonic acid
APK	alkyl phenyl ketones
BA	butyl acrylate
BMA	butyl methacrylate
BSA	bovine serum albumin
CE	capillary electrophoresis
CEC	capillary electrochromatography
CZE	capillary zone electrophoresis
DAMA	2-(dimethyl amino) ethyl methacrylate
DMAA	*N*,*N*'dimethyl-acrylamide
DMF	*N*,*N*-dimethylformamide
EDMA	ethylene dimethacrylate
EGDMA	ethyleneglycol dimethacrylate
EOF	electroosmotic flow
ESI	electro spray ionization

GPTMS	3-glycidoxypropyltrimethoxysilane
HEA	2-hydroxyethyl acrylate
HEMA	2-hydroxyethyl methacrylate
HPLC	high performance liquid chromatography
IMA	isobornyl methacylate
LIF	laser-induced fluorescence
LMA	lauryl methacrylate
MAA	methacrylamide
MALDI	matrix-assisted laser desorption/ionization
MEKC	micellar electrokinetic chromatography
MeOH	methanol
MLM	mixed ligand segment
NAPM	2-naphthyl methacrylate
NAs	nitroalkanes
NMM	naphthyl methacrylate monolith
ODA	octadecyl acrylate
ODM	octadecyl acrylate monolith
OMA	octadecyl methacrylate
PAHs	polycyclic aromatic hydrocarbons
pCEC	pressurized capillary electrochromatography
PDA	1,4-phenylene diacrylate
PDMS	poly(dimethylsiloxane)
PEDAS	pentaerythritol diacrylate monostearate
PEI	polyethyleneimine
PETA	pentaerythritol triacrylate

RP-CEC	reversed-phase capillary electrochromatography
RSD	relative standard deviation
SCX	strong cation exchanger
SEM	scanning electron microscope
SMC	segmented monolithic capillary
SSM	single segment monolith
SPMA	3-sulfopropyl methacrylate
SWNTs	single-wall carbon nanotubes
THF	tetrahydrofuran
TRIM	trimethylolpropane trimethacrylate
UV	ultraviolet
VBC	vinylbenzyl chloride
VBSA	vinylbenzenesulfonic acid
VSA	vinyl sulfonic acid

CHAPTER I

BACKGROUND, RATIONALE AND SCOPE OF THE INVESTIGATION

Introduction and Scope of the study

Capillary electrochromatography (CEC) is a separation technique in which the flow of the mobile phase is driven by an electric field through electroosmosis rather than by applied pressure, as it is the case in high performance liquid chromatography (HPLC). In the recent years, CEC has been gaining increased interest because of its ability to combine the selectivity of HPLC with the miniaturization and high separation efficiency of capillary zone electrophoresis (CZE) [1-3].

In CEC, small diameter capillaries (typically 50-100 μm) with large surface area-to-volume ratio are employed to minimize thermal gradients from joule heating. One major difference between CEC and CZE resides in the fact that the separation principle in CEC is based on a dual mechanism whereby neutral analytes are separated according to their chromatographic partitioning between the stationary and mobile phase while charged solutes additionally experience a separation factor based on their differential

electrophoretic migration just like in CZE, the mobile phase in CEC is transported through the capillary column by electroosmotic flow (EOF). The plug flow profile of the EOF decreases band broadening as compared to the laminar flow profile observed with pressure gradient methods such as HPLC. As a result of the plug flow profile, higher separation efficiencies are realized in CEC, which is further enhanced by the use of small diameter packing material, which could otherwise generate high backpressure in HPLC. Miniaturization of electrochromatography in capillary and chip formats has allowed the analysis of small sample volumes and minimized consumption of reagents.

The scope of this dissertation encompasses the development, characterization and applications of novel neutral alkyl and aryl acrylate/methacrylate-based polymers for use as stationary phases for reversed-phase capillary electrochromatography (RP-CEC). Different stationary phases exhibiting either π-π, hydrophobic or a combination of both interaction mechanisms have been developed. Mixed ligand and segmented monolithic stationary phases were also developed as a way of tuning EOF, retention and selectivity. The monolithic columns made from these stationary phases were investigated in terms of their retention, efficiency and selectivity towards various neutral and charged solutes including small molecules such as alkylbenzenes (ABs), nitroalkanes (NAs), alkyl phenyl ketones (APKs) benzene and toluene derivatives, phenols, anilines, pesticides, polycyclic aromatic hydrocarbons (PAHs) and large molecules such as peptides and proteins.

This chapter is an introduction to the fundamental aspects of CEC along with its basic operation principles. It also includes a brief historical introduction to CEC, an overview of its instrumentation and the various column technologies that are currently available, with an emphasis on the recent introduction of neutral organic monoliths.

Furthermore, a discussion of EOF and a review of parameters that will be used in later chapters of the dissertation are provided.

In addition to this introductory chapter, the dissertation contains six other chapters. Chapter II describes the development of a neutral octadecyl acrylate monolith (ODM) for RP-CEC of a wide range of solutes. Several aspects will be described in detail including methods of column design, evaluation and application to the separation of various species. In chapter III, the fabrication of a hydroxylated ODM (ODM-OH) monolith with fast EOF and its application to separation of various solutes including biomolecules will be described. Chapter IV is a detailed study of a naphthyl methacrylate monolithic (NMM) column for RP-CEC exhibiting both π-π and hydrophobic interactions while chapter V discusses a naphthyl-phenylene diacrylate monolith similarly exhibiting π-π and hydrophobic interactions. In chapter VI, segmented monoliths incorporating different ODM and NMM segments are described as a way of controlling retention, selectivity and EOF. The last chapter of this dissertation describes the preparation and chromatographic evaluation of mixed ligand monoliths prepared by mixing both octadecyl acrylate (ODA) and 2-naphthyl methacrylate (NAPM) in different proportions. Their application to the separation of a wide range of solutes is described in detail.

In the following sections, the basic principles and concepts of CEC are summarized. The various components of CEC instrumentation are also provided.

Historical background-The development of CEC

Electrophoresis, which is defined as the migration of analytes within a background electrolyte under the influence of an electrical field was first described by Arne Tiselius, a Swedish scientist in the 1930s [4]. Later, Strain reported the earliest use of electrophoretic and chromatographic forces to the separation of dyes by adsorption chromatography on a column made of alumina using an electric field [5]. In 1950 Mound and Sanger reported the first attempt to use EOF in the separation of polysaccharides on a collodion membrane [6, 7]. The first application of an electrical field to column chromatography was in mid 1974 by Pretorius *et al* [8]. They defined electroosmosis as the flow of liquid in contact with a solid surface under the influence of a tangentially applied electrical field. The authors used 75-125 μm diameter particles packed in 1 mm glass tube to show the smaller band broadening as compared to that observed in pressure driven flow [8]. Jorgenson and Lukacs in 1981 improved on the use of inert tubes by pioneering open-ended glass capillaries, 170 μm i.d. packed with C18 coated silica (ODS) particles. Knox and Grant demonstrated that no overlapping in the electric double layer is detected by using particle diameters as small as 1.5 μm and 0.01 M electrolyte [9, 10].

Instrumentation

Overview of the instrument

The instrument used in CEC is a modified version of the instrument designed for capillary electrophoresis (CE) in which the ability to apply a gas pressure up to 12 bars on the inlet/and or outlet vials is facilitated. Figure 1 is a schematic representation of a

typical instrument used in CE/CEC. A power supply applies the electric field and is capable of delivering up to 30 kV. The inlet high voltage is connected to a platinum electrode while the outlet platinum electrode is grounded to complete the circuit. The separation column is made of a narrow bore fused-silica capillary containing the stationary phase in the case of CEC. A detection window is made by stripping the external polyimide coating of the fused silica capillary to allow the passage of the detector light.

Detection is made either on-column as in the case of UV-Vis and fluorescence or off-column as in the case of mass spectrometry detection. The detector output is transduced and displayed by a computer. Additionally, modern instruments are equipped with auto-samplers [11], control over the column and sample temperature as well as the ability to apply high gas pressure to the inlet and/or outlet vials [11].

Sample injection

Two methods are generally used to introduce the sample into the capillary; hydrodynamically or electrokinetically. In hydrodynamic injection, the sample is introduced by the application of a pressure difference between the two ends of a capillary. In electrokinetic injection, the sample is introduced into the capillary by applying some voltage over a certain period of time. Since each analyte has a different mobility, electrokinetic injection is biased. Although this is not a problem in qualitative

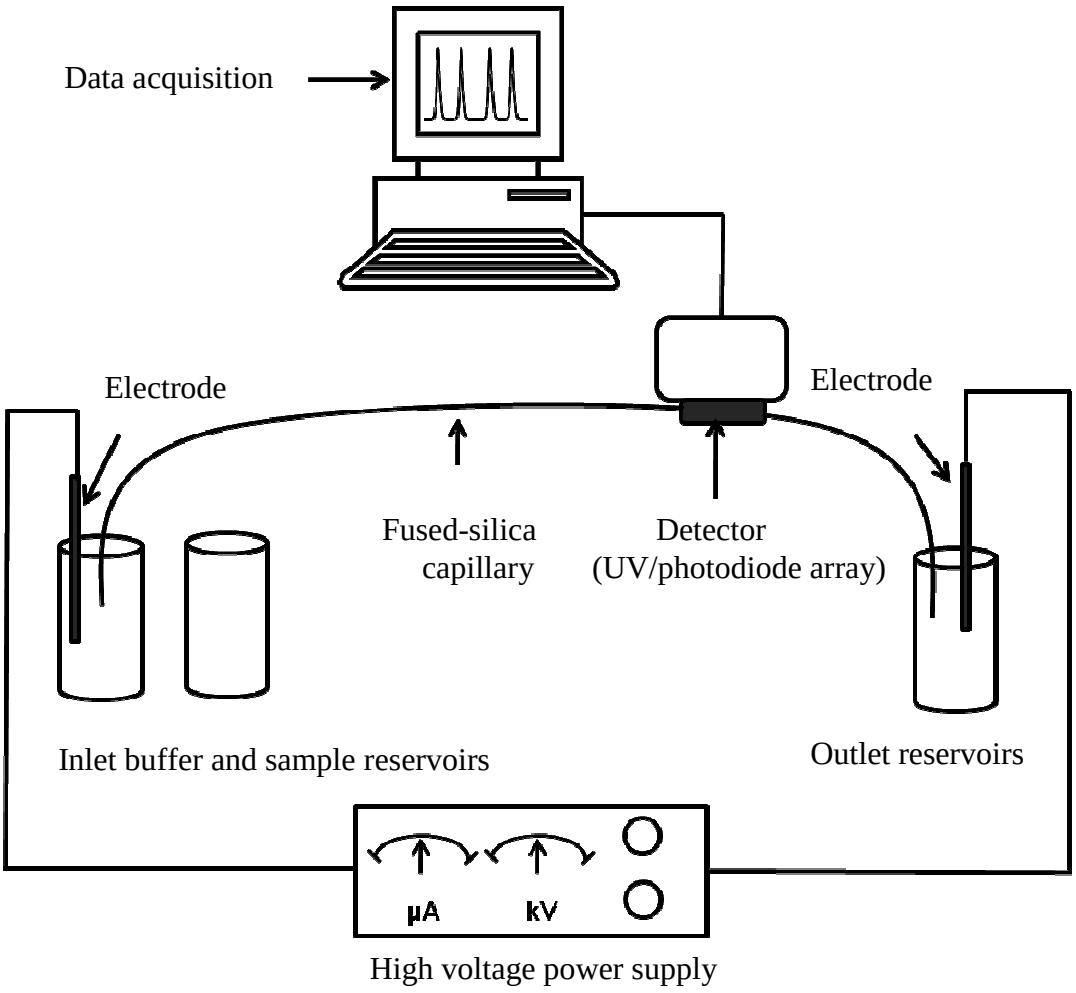

Figure 1. *Schematic representation for an instrument used in CE/CEC.*

analysis it is a drawback in quantitative analysis because the concentration of the injected sample is different from that of the original sample. On the other hand, a limitation to hydrodynamic injection is the fact that the viscosity of the sample matrix and the applied pressure are of importance since there is the possibility of extremely high backpressure resulting from the separation bed or monolith of very low porosity.

Detection in CEC

Optical detection. In CEC, detection based on absorbance of ultraviolet or visible (UV/vis) is the most commonly used. Detection in CE and CEC however, suffers from low sensitivity because of the short path lengths in the range of 50-100 μm. By bending the capillary into a "z" shape with light parallel to the capillary instead of perpendicular to it, the path length can be increased. Moring *et al* [12] used a z-cell with a 3 mm capillary section for path length and obtained approximately a tenfold increase in sensitivity. This "z"geometry however poses a problem since the absorbance is measured along the long axis resulting in band broadening and lower efficiencies. Another way to increase the cell path length is by the use of a bubble cell. In this case, only the inner diameter of the part of the capillary where the light beam goes through is enlarged. Heiger [13] demonstrated a threefold increase in peak height using a 50 μm i.d. capillary with a 150 μm i.d. bubble compared to a 50 μm i.d. straight capillary.

Another popular type of detection method is Laser-induced fluorescence (LIF). It is the most sensitive detection method in chemical analysis [14]. While fluorescence detection provides excellent detection limits, it usually requires the use of derivatization chemistry for analytes that do not possess the required chromophore/fluorophore.

Derivatization of solutes for optical detection. Derivatization has particularly found use in the field of proteomics, where derivatization of proteins and peptides increases the sensitivity of the analysis. The use of pre-, on- and postcolumn derivatization reactions of peptides and proteins can be found in these articles [15-18].

The derivatization of other solutes in CE and CEC has been reported including carbohydrates [19], amines [20] and pesticides [21].

The detection of 2,3-dicarboxaldehyde (NDA)-derivatized amino acids and peptides in CEC with LIF detection was reported on a either negatively or positively charged lauryl acrylate monoliths containing either sulfonic acid groups or quartenary amine moieties. For the separation of the NDA- labeled amino acids, lower limits of detection were achieved [22]. The negatively charged monoliths were also cast in the microchannels of glass chips and were employed to the separation and LIF of three NDA-derivatized bioactive peptides. Peaks of two of the peptides were broad and the authors attributed this to the electrostatic interactions between the positively charged N-terminal arginine residue and the stationary phase [22].

MS and NMR coupling. The recent coupling of MS and NMR to CE/CEC has advanced the detection modes available for these electrokinetic separation methods. These detection methods are unique in that they provide additional structural information about the analytes. Coupling of CEC to MS has generated increased interest in the recent past. This coupling has been accelerated by the nano flow rate and high compatibility of CEC with the ionization techniques of MS especially electrospray ionization (ESI), where sensitivity is not dependent on the detection cell size or path length, and matrix-assisted laser desorption/ionization (MALDI) [23]. Several research articles have been published recently dealing with CEC-MS analysis of peptides [24], drug enantiomers and steroids [25]. A CEC/ESI-MS/MS combined system was developed for the separation of neutral O-linked glycans chemically released from bile-salt-stimulated-lipase. Various types of

isomeric oligosaccharides were first successfully separated by CEC using polar monolithic columns prepared from acrylamide, bisacrylamide and VSA [26].

A novel capillary NMR coupling configuration to CEC was reported. A mixture of five alkyl benzoates was separated in both capillary HPLC-NMR and CEC-NMR. The analysis time in CEC-NMR was reduced by a factor of 2 in comparison with HPLC-NMR [27]. The application of NMR coupled with capillary separation techniques has been described by several authors in the analysis of fatty acids [28] and drug metabolites [29].

Some basic principles of capillary electrochromatography

EOF, the driving force for mass transport and solute differential migration

Electroosmotic flow (EOF) can be defined as the movement of liquid (mobile phase) relative to the stationary phase in the presence of an applied electric field. It arises from the deprotonation of silanol groups (with a pKa value of about 2.2) [30] at high pH thereby becoming negatively charged in the case of bare fused silica capillaries. For packed or monolithic columns the charge may arise from charged moieties that might be intentionally incorporated to support the EOF. Also, the adsorption of ions from the mobile phase creates an adsorbed charged layer of ions on the solid surface.

Under these conditions, and when the surface is in contact with an electrolyte, ions of opposite charge (counter-ions) are attracted to the surface to maintain charge balance while co-ions are repelled from the surface. This leads to the formation of an electric double layer as shown in Fig. 2. The counter-ions are arranged into two layers, fixed and diffuse layer, with a surface of shear at just beyond the surface. The voltage drop between the wall and this surface of shear is referred to as the zeta potential, ζ. At

the application of a an electric field tangentially to the surface, solvated cations in the diffuse layer migrate towards the oppositely charged electrode, dragging the solvent along with them, thereby causing a liquid bulk flow or EOF [31]. The direction of EOF is influenced by the sign of the zeta potential. For a negatively charged solid surface, the zeta potential is negative and consequently, the EOF is cathodal and *vice versa*.

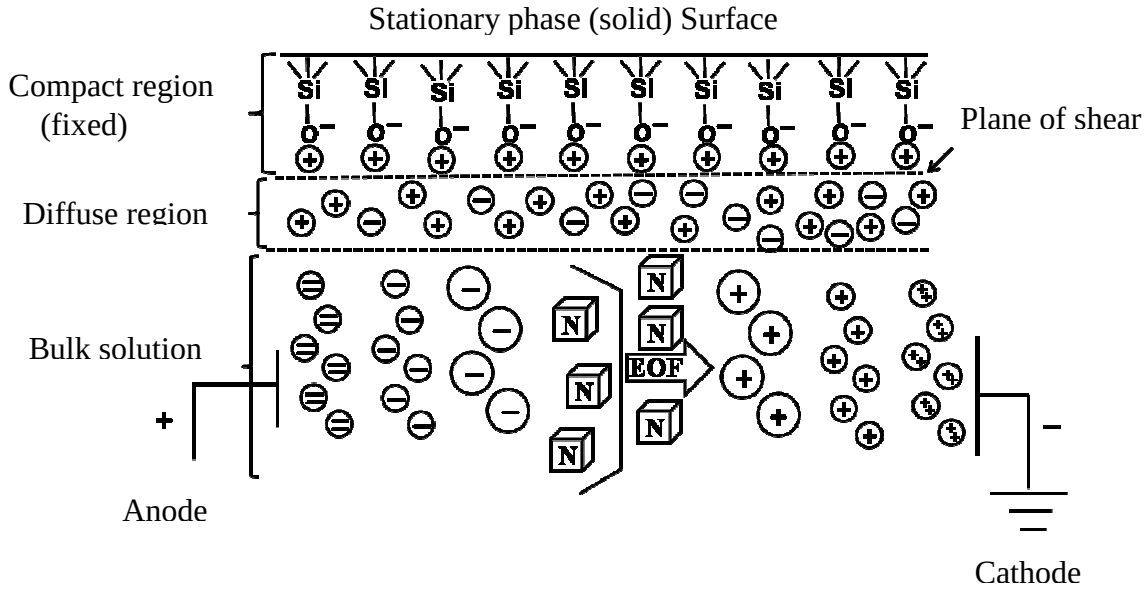

Figure 2: *Illustration of the electric double layer at solid-liquid interface as well as the generation and direction of EOF*.

The mathematical expressions for the EOF in terms of velocity (υ_{eof}) or mobility (μ_{eof}) is given by:

$$\upsilon_{eo} = \frac{\varepsilon\,\zeta}{4\pi\eta}\mathrm{E} \tag{1}$$

or

$$\mu_{eof} = \frac{\varepsilon\zeta}{4\pi\eta}$$

(2)

where the zeta potential is expressed as:

$$\zeta = \frac{4\pi\delta\rho}{\varepsilon}$$

(3)

where ρ is the surface charge density of the capillary surface, δ is the thickness of the double layer and ε is the dielectric constant. Modern electrolyte theory equates δ to *1/k* and therefore equation 3 can be rearranged to:

$$\zeta = \frac{4\pi\delta\rho}{\kappa\varepsilon} \propto \frac{1}{\sqrt{I}}$$

(4)

where I is the ionic strength of the medium. It then follows that increasing the ionic strength of the buffer would decrease EOF, while increasing the surface charge density (by increasing pH), the dielectric constant or the applied voltage would increase EOF.

It should also be mentioned that cations migrate fastest since both EOF and electrophoretic mobility are in the same direction. Neutral molecules move along with the EOF, since they have no electrophoretic mobility. Finally, anions migrate slowest since their electrophoretic mobility is in the opposite direction of EOF. However, they still move toward the detector, because the magnitude of EOF is much greater than their electrophoretic mobility. The separation of ions is also size and charge dependent. Doubly charged cations migrate faster than singly charged cations and similarly, anions migrate. The larger the ion size, the slower is its mobility and *vice versa.* This is clearly illustrated in Fig. 2.

A unique feature of EOF is that since the flow is initiated at the walls of the capillary, it is uniformly distributed along the capillary radial axis which leads to a flat plug-like profile (see Fig. 3b) rather than a parabolic profile that is exhibited by a pressure-driven flow (Fig. 3a), as in high performance liquid chromatography (HPLC). A flat profile of EOF reduces band broadening, enhances fast elution rates, and yields highly efficient peaks as shown in Fig. 3.

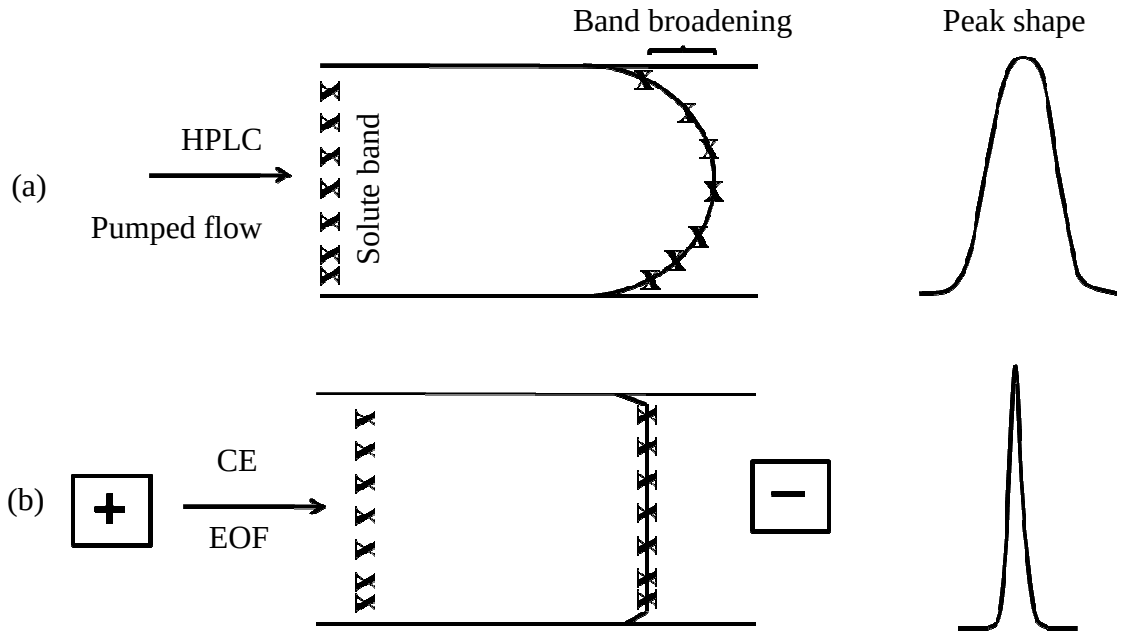

Figure 3. *HPLC and CE flow profiles and the effects of each on the peak shape. (a) Laminar flow observed in pumped flow system and (b) flat/plug flow profile observed in electrically driven methods.*

Retention factor in CEC

Neutral solutes. Since neutral solutes bear no charge, their retention in both CEC and HPLC is due to the difference in partitioning between the stationary and mobile phase. The retention factor for a neutral solute for both CEC and HPLC is computed from the expression:

$$k' = \frac{t_m - t_o}{t_o} \tag{5}$$

where k' is the dimensionless retention factor, t_m is the retention or migration time of the retained solute and t_o is the retention or migration time of the unretained species (i.e., the EOF tracer). To accurately obtain t_o, the EOF tracer must not interact with the stationary phase. Various neutral unretained solutes have been used as EOF markers such as dimethylsulfoxide, acetone, uracil, thiourea, small chain alcohols such as methanol, ethanol, and *n*-propanol [32]. The value of k' can lie anywhere between 0 and ∞, with higher k' value indicating more retardation and interaction with the stationary phase. The retention factor is independent of column length and flow-rate.

Charged solutes. Unlike their neutral counterparts, the retention of charged solutes results from a combination of their electrophoretic migration and chromatographic partitioning. Under these circumstances, the k' defined by equation 3 above is not a measure of chromatographic partitioning as is the case for neutral solutes, but is used as a peak locator. Another retention factor, k*, was introduced by Rathore and Horvath [33, 34] to evaluate the migration of charged solutes in CEC, and is defined by:

$$k^* = \frac{t_m(1 + k_e^*) - t_o}{t_0} \tag{6}$$

where the velocity factor, k_e^*, describes the contribution of electrophoretic mobility to the separation of a charged species in CEC and is given by:

$$k_e^* = \frac{u_{ep}}{u_{eo}} \tag{7}$$

where u_{eo} is the interstitial electroosmotic velocity of the mobile phase in the CEC column and u_{ep} is the electrophoretic velocity of the charged solutes. For neutral solutes k_e^* is zero and Eq. 6 is reduced back to Eq. 5 which describes the k' found in chromatography. The u_{ep} for charged species can be calculated by running the solutes in CZE mode using the same experimental parameters as in CEC.

Selectivity factor

Selectivity factor, α, is a measure of how well two solutes are separated by a chromatographic system and is determined by the ratio of the retention factors of the specified analytes:

$$\alpha = \frac{t_{m2} - t_o}{t_{m1} - t_o} = \frac{k_2'}{k_1'} \tag{8}$$

where, k_2' is always greater than k_1' and thus, $1 \leq \alpha < \infty$ is a measure of the discriminative power of the separation system of interest. Generally a value of 1.1 is indicative of a good separation.

Separation efficiency

Separation efficiency is a measure of the narrowness of bandwidths produced by a chromatographic column. The height equivalent to a theoretical plate H is used as a measure of efficiency and is defined as the ratio of peak variance (σ_L^2) in unit length to the column effective length (l).

$$H = \frac{\sigma_L^2}{l} \tag{9}$$

The number of theoretical plates per column (N) is a dimensionless unit defined as N=l/H. By substituting H from Eq. 9 and by using migration time instead of column effective length, N can be expressed as:

$$N = \frac{l^2}{\sigma_L^2} = \left(\frac{t_m}{\sigma_t}\right)^2 \tag{10}$$

The migration time t_m and peak standard deviation σ_t are obtained from the electrochromatogram. Since chromatographic peaks are usually approximated as Gaussian distributions, peak variances can be calculated from the peak width at base (W_b), half height (W_h) or at the inflection point (W_i) and are equal to 4σ, 2.354σ, and 2σ, respectively. The inflection point is located at 0.607 of peak height. On substituting for σ into equation (10), N is then defined as:

$$N = 4\left(\frac{t_m}{W_i}\right)^2 = 5.54\left(\frac{t_m}{W_h}\right)^2 = 16\left(\frac{t_m}{W_b}\right)^2 \tag{11}$$

Resolution

Resolution (R_s) measures the extent of separation between 2 adjacent peaks. It is calculated from the chromatogram by the ratio of the difference between the migration times of the 2 adjacent peaks (Δt_m) to the average bandwidth of both peaks at base. Baseline resolution is achieved when R_s=1.5 and a Rs value of 1.0 is considered adequate for most separations. Resolution is a function of selectivity, retention factor and efficiency as shown by equation 12 below [35]:

$$R_s = \left(\frac{\alpha - 1}{\alpha}\right)\left(\frac{k_2'}{1 + k_2'}\right)\left(\frac{\sqrt{N}}{4}\right) \quad (12)$$

where k_2' is the retention factor of the more retained peak. To obtain high resolution, the three terms must be maximized. An increase in *N*, the number of theoretical plates, by lengthening the column leads to an increase in retention time and increased band broadening which may not be desirable. Instead, to increase N, the height equivalent to a theoretical plate can be reduced by reducing the size of the stationary phase particles. It is often found that by controlling the capacity factor, *k'*, separations can be greatly improved. This can be achieved by changing the temperature (in gas chromatography, [GC]) or the composition of the mobile phase (in liquid chromatography [LC] and CEC). The selectivity factor, α, can also be manipulated to improve separations. When α is close to unity, optimizing *k'* and increasing *N* is not sufficient to give good separation in a reasonable time. In these cases, *k'* is optimized first, and then α is increased by either, changing mobile phase composition (LC and CEC), changing column temperature (GC), changing composition of stationary phase or by using special chemical effects (such as incorporating a species which complexes with one of the solutes into the mobile phase).

Band broadening in CEC

The very high separation efficiencies obtained in CEC are known to result from the plug flow profile characteristic of EOF [36-38]. The variance of complex random processes that are not coupled, i.e. are independent, according to statistical theory is given by the summation of the variances generated by the individual processes. For any LC technique, the observed variance is established by the contributions from sample injection (σ^2_{inj}), connections (σ^2_{conn}), detection (σ^2_{det}), and passage of sample through the column (σ^2_{col}). In CEC, connections are not a factor but contribution stemming from heat as a result of the passage of current, or joule heat ($\sigma^2_{joule)}$ becomes an additional consideration. Therefore, the observed variance σ^2, is expressed as:

$$\sigma^2 = \sigma^2_{inj} + \sigma^2_{det} + \sigma^2_{col} + \sigma^2_{joule} \quad (13)$$

Since the plate height H is proportional to the peak variance according to equation (9), it is expected to obey the same additive rule as the variance and can be expressed as:

$$H_{obs} = H_{inj} + H_{det} + H_{col} + H_{joule} \quad (14)$$

Joule heating causes non-uniform temperature gradients and local changes in viscosity that lead to band broadening. This effect however, can be minimized by using low conducting supporting electrolytes in the mobile phase, narrow bore capillaries for efficient heat dissipation, field strengths that are 1000 V/cm or less, and controlled column temperature. The contribution of band broadening in both pressure and electro-driven separations has been thoroughly studied and it has been reported that plate height contributions from H_{inj}, H_{det}, and H_{joule} were all negligible compared to $H_{col,}$ [38].

Therefore, it can be assumed that the observed plate height is determined by the passage of the sample through the column. For LC techniques, factors affecting Hcol include; maldistribution of flow (H_f), longitudinal molecular diffusion (H_{md}) and mass transfer resistance in the pore (H_p). After dropping the negligible terms and substituting these terms for H_{col} equation (14) becomes:

$$H_{obs} = H_f + H_{md} + H_p \tag{15}$$

On substituting the corresponding parameters that define plate height contributions into the equation above, we obtain the van Deemter equation, which is usually represented in a simplified manner by summing up the constants (A, B and C) for a given set of conditions and relates each plate height contributor in terms of mobile phase velocity, as:

$$H = A + \frac{B}{u} + Cu \tag{16}$$

Figure 4 illustrates a typical van Deemter plot and the relative plate height contributions of each term in the van Deemter equation as a function of mobile phase velocity. As shown in Fig. 4, the optimum flow velocity (u_{opt}) produces the minimum plate height (H_{min}). Longitudinal molecular diffusion term, (B/u) depends on the nature of the solute and an increase in the mobile phase flow velocity can minimize this term. The mass transfer resistance in the pores (Cu) increases with increasing mobile phase flow velocity. This diffusion mass transfer resistance is decreased in CEC due to the generated EOF within the flow through pores, which increases the kinetics of the mass transfer [38].

The highest gain in CEC separation efficiency results from decreasing the maldistribution of flow (the A term) observed in pressure driven flow in packed columns,

which is known as “Eddy diffusion” [39]. The plug flow profile in CEC causes the “A” term to become negligible in determining the overall separation efficiency. Once the broadening effects in both the A and C terms of the van Deemter equation are reduced, efficiencies that are 5-10 times better than those obtained in pressure-driven mode under the same conditions are obtained.

Column technologies

In general, columns for CEC can be classified into three categories, namely particle packed columns, continuous-bed or monolithic columns and open-tubular columns. As the name suggests, packed particle columns are filled with finely divided packing materials confined between two retaining frits while in open-tubular columns, the wall contains a bonded stationary phase that can be a coated polymer, bonded molecular monolayer or a synthesized porous network. On the other hand, monolithic columns contain a polymer stationary phase that is formed *in situ* inside the capillary column. A more detailed description of each column category is given in the following sections.

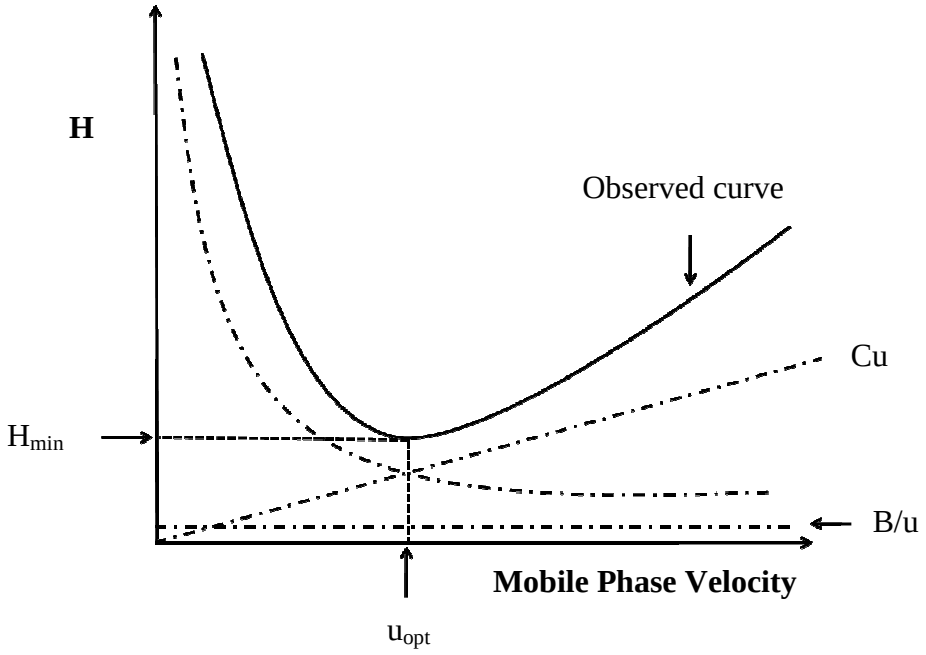

Figure 4. *Illustration of the plate height (H) contribution to each van-Deemter term and the resulting observed plot of H as a function of mobile phase linear velocity.*

Packed columns

In packed columns, frits, which are placed at both the inlet and outlet ends, are necessary to retain the chromatographic bed. The chromatographic bed contains porous small diameter particles with ionizable groups to generate EOF. The use of packed columns for CEC has been reported by various research groups [40-42].

Segmented packed capillaries have also been introduced as a way to tune the EOF [43, 44]. The use of inlet frits in packed columns causes band broadening during sample injection as a result of inhomogeneity in flow through the inlet frit and during elution of the analyte band from the packing into an open section of the capillary before detection [45]. A decrease in sensitivity has also been reported due to the adsorption of the analyte

onto the frit [46]. Whereas column packing is a well established technique for the production of packed columns, repeatability, fragility and bubble formation are major drawbacks in this area of CEC column technology [47].

Open-tubular columns

In open tubular CEC (OT-CEC) a thin porous layer of the retentive stationary phase is attached to the walls of fused silica capillaries (ca. 10 - 25 µm I.D.) either covalently or noncovalently [48]. The development of open tubular columns was facilitated by the simplicity of the column structure and ease of surface functionalization [49]. Open tubular capillary columns are also characterized by smaller plate heights than packed columns as a result of the absence of band broadening effects associated with stationary phase particles and retaining frits [50]. The EOF generated by an open tubular column is higher than in a packed column because higher voltage can be applied due to increased heat dissipation by the narrow columns. Open tubular columns however, suffer from difficult on-column UV detection as a result of short optical path-length resulting from the small column inner diameter and low sample loading capacity due to limited surface area. Etching the inner walls of capillaries has been found to increase the surface area by a factor of up to 1000 as compared to unetched capillaries [51].

Continuous beds or monolithic columns

As a new type of stationary phase for CEC and HPLC, monoliths have been the subjects of intensive studies during the last two decades. While most other chromatographic supports are particulate in nature, monoliths consist of a single piece of highly porous material. Unlike porous particle stationary phases, the pores inside a

monolith are open, forming a highly interconnected network of channels that enhances mass transfer in monoliths than is the case for particle-based stationary phases. As a result, van Deemter plots of plate height against mobile phase flow velocity are shallower which means faster separations can be performed without compromising on separation efficiency. Since the monolith completely fills the column interparticular voids are eliminated and the mobile phase flows through the stationary phase rather than around it, thereby increasing the efficiency by convection. Monoliths possess very unique properties such as high permeability, which means higher flow rates can be tolerated [52], versatility, large surface area, ease of preparation with a wide variety of chemistries available and no retaining frits are required [53].

Monoliths can be classified into two major categories (i) silica- and (ii) rigid organic polymer-based monoliths. Silica-based monoliths are prepared using the sol-gel technology creating a continuous sol-gel network throughout the column [54]. Organic polymer-based monoliths are usually prepared *via* vinyl polymerization and can be acrylamide- [55-58], (meth)acrylate- [59-61] and polystyrene-based [62-65] The analytical potential of monoliths has been demonstrated with separations involving various families of compounds such as environmental pollutants [35, 66, 67] pharmaceuticals [68, 69], biomolecules [16, 48, 70] and chiral molecules [71-73].

Background and progress made in organic polymer monoliths

Although monolithic stationary phases have generated increased attention since their invention two decades ago, there is still room for improvements in terms of their morphology, column efficiency, retention and selectivity [47]. The following section is aimed at providing the reader with an overview of the progress made by various research groups in the development of polymeric monolithic stationary phases. This is followed by the rationale of the investigation in this dissertation and the gap that the dissertation has attempted to fill for furthering the progress of the CEC technique.

Preparation and factors affecting the morphology and porosity of monoliths

Organic polymer-based monoliths are prepared in a single step within the confines of a capillary column by the polymerization of an organic functional monomer in the presence of a crosslinker, initiator and porogens [74]. The functional monomer defines the monolith polarity while the porogens, monomer-to-crosslinker ratio and polymerization temperature control the monoliths morphology [75]. Monoliths are associated with two main types of pores: (i) the flow-through pores and (ii) the mesopores filled with "stagnant" mobile phase in which the solute molecules migrate to access the active adsorption sites. To get large surface area and retention, a significant number of smaller pores should be incorporated into the polymer. Micropores with sizes smaller than 2 nm contribute most significantly to the overall surface area followed by mesopores ranging from 2 to 50 nm [75]. The larger flow-through pores (macropores) are essential to allow liquid to flow through at a reasonably low pressure and contribute very little to the overall surface area [76].

The polymerization can be initiated through the application of heat, UV radiation [77-79], gamma radiation [80, 81] or redox reagents [82, 83]. Once decomposed, the initiator initiates the polymerization and as the polymer chains grow, their solubility in the reaction mixture decreases and the polymer chains precipitate to form nuclei. Thermodynamically, the monomers are better solvents for the formed polymer than the porogens and the nuclei therefore become swollen with monomers. As a result of the monomer concentration in the nuclei being higher than in the surrounding solution, polymerization in the nuclei is kinetically preferred. Further polymerization leads to an increase in the size of the nuclei to microglobules, which then aggregate to form clusters. As the microglobules continue to grow and crosslink to each other the final morphological structure is formed. This process leads to two-phase system consisting of a white colored continuous solid monolith and inert liquid porogens filling the pores. Once the porogens are washed out, the volume occupied by the porogens then corresponds to the volume of the macropores [53].

While varying the monomer-crosslinker ratio or type of initiator can change the composition and rigidity of the monolith, the alteration of the porogen affects only the porous structure of the final polymer. The porogens can either be good or poor solvents for the polymer. The mechanism of pore formation using porogens has been described as follows. At the beginning of the polymerization, the solution is homogeneous until the growing and crosslinked polymer chains precipitates and falls out of the solution. If the porogen is a good solvent for the final polymer, phase separation is delayed and the resultant pores are smaller. Alternatively in the presence of a poor solvent, phase separation occurs early leading to large pores [84]. While there is no standard way of

choosing the right composition of porogens and the right porogen composition has to be based on trial and error, a reduction of monomer/crosslinker ratio represents a straight forward method to increase pore size and decrease pressure drop during operation (in HPLC), this approach however, decreases the homogeneity and rigidity of the macroporous polymer [53].

Traditional approaches used in the fabrication of monoliths with strong EOF

Monoliths with a positive surface. To address the need for a strong EOF in CEC separations, Bedair and El Rassi introduced a novel cationic monolithic stationary phase based on the co-polymerization of pentaerythritol diacrylate monostearate (PEDAS) with a selected quaternary amine acrylic monomer in a ternary porogenic solvent consisting of cyclohexanol, EG and water [85]. While PEDAS functioned as both the ligand provider and the cross-linker, the quaternary amine acrylic monomer in small amount controlled the magnitude of EOF. In an effort to find the optimum monomer for achieving maximum EOF velocity, four different quaternary amine acrylic monomers were investigated. The authors reported that both photo- and thermally initiated polymerization proved effective in producing the cationic C_{17} monolith, and that the best monolith was achieved when [2-(acryloyloxy)ethyl]-trimethylammonium methyl sulfate (AETA) was used as the quaternary amine acrylic monomer. Although the zeta potential of the resulting cationic C_{17} monolith was positive with respect to water, the magnitude and direction of the EOF was markedly affected by the nature of the electrolyte ions in the mobile phase. As a result, anodal, zero or cathodal EOF was observed depending on the nature of the electrolyte ions, and this was attributed to the adsorption of the ionic

components of the electrolyte onto the solid surface of the stationary phase, which is characterized by its amphiphilic nature consisting of C_{17} chains, ester functions, hydroxyl groups and quaternary amine moieties. This early observation triggered El Rassi and co-workers to develop totally neutral monoliths, a research theme that this dissertation has focused on. Optimized PEDAS–AETA monoliths yielded columns with high separation efficiency that allowed rapid separations on a time scale of seconds with short capillaries [85]. In another investigation by Bedair and El Rassi, the PEDAS-AETA monolith [86] was evaluated in the separation of charged species including water-soluble and membrane proteins [86]. The analysis of these proteins necessitated the use of low pH (pH 2.5) to avoid electrostatic interactions between the charged surface and the acidic groups of the proteins.

Along the same lines, and in order to produce monoliths with a relatively strong EOF, Lu *et al* reported the development of a positively charged monolith prepared from the *in situ* copolymerization of iso-butyl methacrylate, ethylene dimethacrylate (EDMA) and N,N-dimethylallylamine (DAMAA) in a binary porogenic solvent consisting of *N*,*N*-dimethylformamide (DMF) and 1,4-butanediol. The scanning electron microscopy (SEM) images of the prepared monolith revealed the pore structure and the effective attachment of the ashes of the organic monolith to the capillary wall [87]. This monolith was characterized in the pCEC of typical homologous such as alkylbenzenes, phenols and anilines. Since these solutes are either neutral (alkylbenzenes and phenols) or weakly basic (anilines) the presence of fixed positive charges on the monolith surface did not cause any significant electrostatic attraction/repulsion. An anodal EOF of 2.45 mm/s was reported when the ACN concentration was increased to 70% [87].

More recently, a polyacrylate-based monolithic column bearing cationic functionalities was recently reported. The monolith was prepared by the photo polymerization of a mixture of hexyl acrylate, butanediol diacrylate, 2-(acryloyloxy) ethyltrimethyl ammonium chloride in a ternary porogenic solvent consisting of acetonitrile, phosphate buffer and ethanol. This monolith afforded an efficiency of 250,000-320,000 plates per meter for the separation of the neutral alkylbenzenes [24]. As expected, due to the presence of positively fixed charges on the monolith surface, the monolith was useful in the separation of peptides at relatively low pH of 2.5, a pH at which the surface and the peptides carry the same charge, a condition that diminishes electrostatic attractions but most likely caused electrostatic repulsion. Electrostatic repulsion is as serious as electrostatic attraction because it lowers retention and in turn separation selectivity.

The preparation of polymeric continuous reversed-phase gradient stationary phases for CEC with a stepwise gradient of hydrophobicity was reported by Maruska *et al* [88]. The columns were prepared from piperazine diacrylamide, N-(hydroxymethyl) acrylamide, diallyldimethyl ammonium chloride. Solutions of the hydrophobic monomers *N*-isopropylacrylamide, hexyl acrylate, and diallyldimethylammoniumchloride were drawn into the capillaries that were marked to prepare columns with a gradient of the reversed-phase stationary phase. For a mixture of alkyl benzoates, the authors reported that efficiency and resolution of the gradient stationary phase was substantially increased than when an isotropic stationary phase was used. Also, it was reported by the authors that inverting the elution direction did not remarkably affect the separation efficiency or resolution of the gradient capillary column.

As revealed from the above overview, only a few monoliths with positively charged surfaces were introduced. This may be due to the fact that such surfaces are not useful for the CEC of acidic compounds carrying negative charges.

Monoliths with a negative surface. Using the same strategy of intentionally introducing fixed charges to the surface of monoliths to generate strong EOF, Bedair and El Rassi replaced AETA in the previously described cationic PEDAS-based monoliths [86] with AMPS to produce columns with cathodic EOF [89]. After trying several macroporogens, such as ACN, methanol, ethanol, 1,5-pentanediol, 1,2-propanediol and ethylene glycol (EG), it was found out that EG gave the best porous solid, the white opaque monolith was confirmed by SEM. Therefore, a ternary porogenic solvent comprising cyclohexanol, EG and water was adopted. This monolithic column retained neutral solutes by a reversed phase retention mechanism and a mixed mode retention mechanism with charged analytes such as amino acids. The EOF generated by this monolith was strong enough to allow the fast separation of small ionizable solutes in a matter of seconds [89].

Another monolith with surface fixed negative charges, namely a poly(styrene-divinylbenzene-vinylbenzenesulfonic acid) monolith was recently developed by Huang *et al* [64] for CEC separations. The monolithic column was made by the copolymerization of styrene, divinylbenzene and vinylsulfonic acid in a ternary porogenic solvent consisting of cyclohexanol, *N*,*N*-dimethyl acetamide and water. The monolith could generate adequate EOF under low pH conditions due to the strong sulfonic acid functionality. In another contribution, the same poly(styrene-divinylbenzene-

vinylbenzenesulfonic acid) monolith was recently produced and evaluated [90] in CEC. SEM images of the resulting monoliths showed a larger diameter when the polymerization time was increased from 3 to 15 h. The monolith was applied to the separation of acidic analytes within 2.2 min with high resolution and theoretical plate counts of >160,000 plates per meter [90]. Very recently, Zhang *et al* [91] reported a poly(styrene-divinylbenzene-methacrylic acid) monolith prepared using microwave irradiation and a binary porogenic solvent consisting of toluene and isooctane. The authors reported a shortening of the polymerization time from 24 h (thermal initiation) to 15 min. Through SEM, the authors noted that by increasing the polarity of the porogenic mixture, i.e., by increasing the toluene volume, monoliths with smaller pores were obtained [91].

By copolymerizing *N,N'*dimethyl-acrylamide (DMAA), methacrylamide (MAA), as functional monomers, piperazine diacrylamide (PDA) as the crosslinker and vinyl sulfonic acid (VSA) as the charged monomer, Freitag compared the chromatographic behavior of the resulting monolith in both CEC and nano-LC modes. The retention of neutral hydroxylated aromatics in both chromatographic modes was found to be the same thereby confirming the assumption that their retention involved primarily hydrophilic interactions. On the other hand, for charged amino acids both electrostatic and hydrophilic interactions contributed to their retention [92].

The preparation of porous polyacrylamide-based monolithic columns *via* vinyl polymerization was reported by Zhang and El Rassi [93]. These monoliths were prepared from aqueous monomer solutions and dispersions, which consisted of an aqueous solution of acrylamide, PDA, VSA and a hydrophobic ligand (stearoyl- or butyl

methacrylate) for chromatographic retention. The authors reported that inclusion of VSA not only supported the EOF but also exhibited hydrophilic interaction with moderately polar compounds such as urea herbicides and carbamate insecticides. Therefore, a mixed-mode (reversed-/normal phase) retention behavior was observed with neutral and moderately polar pesticides. An optimum EOF velocity and adequate chromatographic retention were obtained when 15% VSA was added to the reaction mixture. Very high plate counts reaching greater than 400,000 plates per meter were obtained [93].

By the copolymerization of butyl acrylate (BA), hexyl- or lauryl acrylate and 1,3-butanediol diacrylate as the crosslinker, AMPS as the charged monomer in a casting solvent consisting of ethanol, ACN and phosphate buffer, Bushey and co-workers [94] reported on the behavior of the resulting monoliths using CEC. In their study, a small percentage of butyl acrylate (BA) was replaced with a more hydrophobic polymer such as hexyl- or lauryl acrylate. The authors found out that the substitution of small-branched monomers resulted in a decrease in retention while the substitution with a more hydrophobic monomer led to an increase in the retention factor. A further increase in the percentage of lauryl acrylate lead to lower retention for nonpolar analytes as compared to the polymers made from less hydrophobic monomers. These results were contrary to what was expected and the authors attributed this to non-uniform polymerization of the more hydrophobic monomers [94].

A novel approach to prepare organic polymer-based monoliths by microwave irradiation was recently reported by Ye *et al* [95]. The monoliths were prepared by the copolymerization of styrene, DVB and MAA in a binary porogenic solvent consisting of toluene and isooctane. Through SEM, it was found out that monolithic columns prepared

from a higher content of isooctane generally had bigger pore size and better permeability. The separation of model analytes consisting of neutral aromatic compounds was compared in p-CEC, CEC and low-pressure liquid chromatography.

In another study by Buszewski *et al*. [96], polymeric monolithic columns were prepared from copolymerization of butyl methacrylate (BMA), lauryl methacrylate (LMA), octadecyl methacrylate (OMA), and isobornyl methacylate (IMA) with EDMA and AMPS in a ternary porogen composed of 1,4-butanediol, 1-propanol and water. For polymerization of LMA, OMA and IMA water was excluded and the columns obtained were characterized by a good efficiency of up to 116,000 plates/m. On separation of alkylbenzene homologous series, the highest retention (log *k*') was exhibited by columns made from IMA [96].

Using the same methacrylate-based monolithic columns just described above, Buszewski and Szumski [97] studied the homogeneity and quality of beds using scanning electron microscope (SEM), porosimetry and electrochromatography. To study the bed homogeneity, a 35 cm capillary was filled with the polymerization solution and after polymerization, a detection window was made ca. 8.5 cm from the outlet such that the capillary column consisted of a long (ca. 25 cm) and a short (ca. 8.5 cm) part connected by the detection window. When alkylbenzenes were separated on both parts of the capillary, selectivity and column efficiency were the same, which confirmed the homogeneity of the bed. However, the retention times of the solutes were different for both parts as would be expected [97].

Recently, a highly cross-linked porous monolithic stationary phase having a long alkyl chain ligand (C16) was introduced and evaluated in CEC. The monolithic stationary

phase was prepared by *in situ* copolymerization of 1-hexadecene, TRIM, and AMPS in the presence of ternary porogenic solvent consisting of cyclohexanol, 1,4-butanediol and water. The authors noted that monoliths prepared from TRIM as the crosslinker exhibited a higher permeability than those made from EDMA. These columns were applied to the separation of neutral and charged solutes, e.g., weakly acidic phenols and weakly basic anilines [98]. These solutes would be hardly ionized (i.e., behaving as neutral) when the pH was 3.0 or 11.0 in the case of phenols or anilines, respectively.

Fused silica capillary columns with a porous monolithic stationary phase were prepared form the *in situ* copolymerization of 2-ethylhexyl methacrylate, ethyleneglycol dimethacrylate (EGDMA) and AMPS in the presence of a porogenic mixture containing 1-propanol, 1,4-butanediol and water. The authors reported a decrease in total porosity to a value, which corresponded to a material with very low permeability as the crosslinking agent EGDMA was increased. The resulting columns were successfully applied to the rapid separations of polyphenols, flavones and falavanones-7-O-glycosides in less than 8 min [99].

Lin *et a*l reported a monolithic column for pCEC. The monolith was prepared form the *in situ* copolymerization of octadecyl methacrylate (OMA), 3-sulfopropyl methacrylate (SPMA) and EDMA in a binary porogenic solvent consisting of cyclohexanol and 1,4-butanediol. The OMA ligands offered hydrophobic retentive sites while the SPMA was the charged monomer for generation of EOF. In addition to EOF generation, the SPMA offered hydrophilic/ionic interactions towards polar charged solutes (e.g., nucleic acid bases, nucleosides and nucleotides) in pCEC [100]. Some band broadening was observed for the nucleic acid bases and nucleosides at pH of 3.0 where

SPMA would be negatively charged (due to the strong sulfonic acid of SPMA) and the weak nucleic acid bases and nucleosides would be positively charged. These oppositely charged entities can undergo strong electrostatic attractions causing band broadening via mixed reversed phase/ion exchange retention mechanism.

A method for dead time (t_o) determination in RP-CEC based on homologous series using methacrylate-based stationary phases was recently reported by Ping *et al* [101]. The authors prepared the monolith *via* the *in situ* copolymerization of BMA, EDMA and AMPS. The dead times measured with the homologous series and thiourea, a commonly used EOF marker were compared under various electrochromatographic conditions such as type and concentration of the organic modifier, ionic strength and applied voltage. The results showed that the dead time measured using the homologous series was larger than that determined from thiourea, which seems to behave like a positively charged solute, while under high ionic strength and low applied voltage, the EOF measured by thiourea was close to that obtained by the homologous series.

The effect of various alcohols used as porogens on porous structural properties and chromatographic behaviors of a series of C14 methylacrylamide-based monoliths was investigated [102]. The monoliths were prepared from the copolymerization of methacrylamide, *N*,*N*'-methylenbisacrylamide as the crosslinker, octadecene to increase the hydrophobicity and AMPS as the charged monomer in a binary porogenic solvent consisting of DMF and various alcohols. The SEM of the resulting monolithic columns showed that the pore sizes of the monoliths increased with increasing alcohol alkyl chain length [102].

Recently, an acrylate-based monolith for use in a microfluidic chip for use in RP-CEC was reported by Faure et al [103]. The monolith was prepared from lauryl acrylate, EDMA and acrylamidomethyl-propylsulfonate in a binary porogenic solvent consisting of methanol and 2-propanol. The SEM of the resulting monolith showed a good homogeneity structure with nodules smaller than 1 μm. The monolith was applied to the separation of PAHs affording a theoretical plate count of 85,000 plates per meter [103].

In order to provide a remedy for the possible electrostatic attraction/repulsion between charged solutes and charged monolithic surfaces, shielded stationary phases that prevented/diminished the adsorption of ionizable solutes onto the charged surface were introduced by Hilda *et al*. [104]. A monolithic surface that had been grafted with an "interior" layer of 2-acrylamido-2-methylpropanesulfonic acid (AMPS) was covered by a "top" layer of poly(butyl methacrylate). This monolith provided a method of suppressing the unwanted electrostatic interactions, and consequently allowed the separation of some peptides and proteins at relatively low pH, where the extent of electrostatic interaction may not be significant.

The above overview has provided an insight into another category of charged monoliths, the negatively charged ones. These negatively charged phases although useful for neutral solutes they have limited applicability for CEC of charged solutes, especially those that are polyionic such peptides and proteins.

Monoliths with ampholytic surface. A zwitterionic neutral monolith was prepared by radical polymerization of GMA and EDMA and subsequently reacting the epoxide groups with lysine. The resultant lysine chemically bonded stationary phase could

generate either cathodic or anodic EOF by varying the pH value of the running buffer [105]. This monolith proved useful for neutral solutes and weakly acidic phenols, and weakly basic anilines and pharmaceuticals. The interplay of electrostatic and hydrophobic interactions and electrophoretic migration played a significant role in the separation of ionizable and ionic solutes.

Fu *et al* described a monolithic column possessing an ampholytic character. The monolithic column was prepared by the copolymerization of butyl methacrylate, MAA, 2-(dimethyl amino) ethyl methacrylate (DAMA) and EDMA as the crosslinker in a binary porogenic solvent consisting of 1-propanol and 1,4-butanediol. The MAA provided negative charged functionalities to generate cathodic EOF, whereas DAMA provided positive charged functionalities to promote anodic EOF. Using mercury intrusion porosimetry, the authors found out that the surface area of the stationary phase increased with the polymerization temperature. This monolith was applied to the RP-CEC separations of alkylbenzenes, PAHs, weakly ionizable phenols and anilines [106].

Other monolith formats: Monoliths incorporating single-wall carbon nanotubes and gold nanoparticles. The incorporation of single-wall carbon nanotubes (SWNTs) into a monolithic stationary phase prepared by the copolymerization of vinylbenzyl chloride (VBC) and EDMA to yield a poly(VBC-EDMA-SWNTs) monolith was reported by Li et al. [107]. The fused silica capillary was treated with GPTMS and then flushed with PEI. The primary amino groups on PEI were covalently linked to the GPTMS coating to form an annular positively charged polymer layer in the column for EOF generation. The neutral poly(VBC-EDMA-SWNT) was prepared by the *in situ* copolymerization of VBC

and EDMA in the presence of 2-propanol containing the SWNT and formamide as the porogen. When separation of peptides was compared on poly(VBC-EDMA-SWNTs) and on poly(VBC-EDMA) with annular EOF generation, it was found out that the incorporation of SWNT into the monolith improved peak efficiency and influenced chromatographic retention [107].

Along the same lines of research and involving nanotechnology in the fabrication of monoliths, Connolly *et al* [108] described a method to covalently attach gold nanoparticles direct to the pore surface of a poly(butyl methacrylate-co-ethylene dimethacrylate) onto which poly(4,4-dimethyl-2-vinylazlactone) had been photografted. The resulting azlactone moieities were reacted with either cysteamine or ethylenediamine. Gold nanoparticles were attached to the monolith *via* either the electron lone pair of the nitrogen or the formation of Au-S bond in case of the thiol functionalized monolith. The application of this monolith however was not given in their short communication [108].

The introduction of neutral monolithic columns as the most effective remedy for the elimination of nuisance electrostatic interaction-The research theme of this dissertation

As early as 2003, our research group realized the drawback of generating the EOF by incorporating small amounts of a charged vinyl monomer into the monolith besides the functional monomer. In fact, since the early work of Bedair and El Rassi on the cationic C17 monolith [85], it was noticed that despite the presence of quaternary amine groups on the surface of the cationic C17 monolith, the EOF generated by this column changed direction and magnitude by changing the nature of the electrolyte ions. This led

to the idea that one can substitute the fixed charges on the surface of the monolith by the adsorption of electrolyte ions onto the solid surface of the monolith, which would become the zeta potential determining ions to generate and support a relatively strong EOF. At the same time the electrolyte ions form the ionic cloud around the solutes, thus minimizing electrostatic interactions with the adsorbed ions.

It has to be emphasized that the irreversible adsorption of charged analytes such as proteins and peptides to the fixed charges of the stationary phases that are so functionalized to support and generate EOF has been a major drawback to the application of CEC in the area of protein separations. This adsorption leads to irreproducible retention times, peak tailing and low column efficiencies, a fact that inhibited the growth of CEC and its widespread use in life sciences despite its much potential as a powerful micro-separation technique.

In order to circumvent the above problems, Okanda and El Rassi in our laboratory introduced a neutral C17 acrylate-based monolithic stationary phase that was void of any fixed charges [59] to reduce the undesirable electrostatic interactions but still exhibited a relatively strong EOF. The monolith's ability to adsorb electrolyte ions from the electrolyte imparted it with a zeta potential, thus supporting an EOF. The monolith was prepared by the *in situ* polymerization of PEDAS in a porogenic solvent composed of cyclohexanol, ethylene glycol, and water. The neutral C17 monolith permitted for the first time to the separation of proteins and peptides including the tryptic peptide mapping at neutral pH with separation efficiencies exceeding the 220,000 plates per meter. Also, such column was an important component in a two dimensional platform for proteomics that was introduced by Zhang and El Rassi [109] in 2006, whereby the C17 monolith

produced high separation efficiencies, thus allowing the RP-CEC separation of complex protein mixtures originating from human sera.

To further develop CEC with neutral monoliths, and as a continuation of the above initial study by Okanda and El Rassi, another neutral monolith without any charged monomer and having 'zero" electrostatic interactions was introduced by Karenga and El Rassi [61] (see Chapter II). The neutral monolith was prepared by the *in situ* copolymerization of octadecyl acrylate (ODA) as the functional monomer in the presence of timethylolpropane trimethacrylate (TRIM) as the crosslinker in a ternary porogenic solvent composed of cyclohexanol, EG and water. The monolith thus obtained was referred to as octadecyl acrylate monolith (ODM). The ODM exhibited a relatively strong EOF that allowed the rapid separation of a wide range of neutral and charged solutes. Very recently, Karenga and El Rassi introduced another neutral monolithic stationary phase incorporating naphthyl ligands that provided both hydrophobic and π interactions. The monolith was prepared by the *in situ* polymerization of 2-naphthyl methacrylate (NAPM) as the functional monomer in the presence of TRIM as the crosslinker in a ternary porogenic solvent composed of cyclohexanol, dodecanol and water. This neutral naphthyl methacrylate monolith (NMM) exhibited moderate EOF that allowed the fast separation of aromatic compounds through π interactions [66] (see Chapter IV). In addition, two more neutral monoliths with different functionalities are reported in Chapters III and V. To further develop the field of neutral monoliths in CEC, two hybrid monolithic columns consisting of segmented capillaries and mixed ligand monoliths are described in Chapter VI and VII.

Rationale of the investigation

While CEC has been advancing as a microseparation technique, the development of stationary phases for use in this technique has generated a lot of interest in the recent past. However, the traditional belief that monomers bearing fixed charges must be incorporated onto the stationary phase surface to support a strong EOF has slowed down the application of CEC to the separation of charged solutes especially in the field of proteomics. These incorporated fixed charges interact with oppositely charged solutes electrostatically, leading to irreversible adsorption and band broadening.

The broad objective of this research entailed furthering the development of neutral acrylate/methacrylate-based polymeric stationary phases that are without any fixed charges. The said stationary phases were fabricated from alkyl and aryl ligands exhibiting different retention mechanisms. The fact that these neutral stationary phases supported strong EOF is believed to arise from the adsorption of mobile phase ions to the surface of the monolith. These adsorbed electrolyte ions impart the stationary phase surface with the necessary zeta potential required to generate the EOF. Towards achieving the broader objective, other specific objectives were pursued such as: (i) enhancing the EOF, selectivity and retention of the stationary phase by changing the nature and amount of crosslinker, (ii) introducing segmented monoliths with segments filled with different monolith stationary phases and (iii) developing mixed ligand monolithic stationary phases made from different compositions of different monomers.

The successful application of these stationary phases to the CEC separation of charged solutes has been accomplished where the separation is obtained rapidly and without irreversible adsorption, an area where the potential of CEC has not been fully

exploited. Additionally, the study described in this dissertation has furthered the development of stationary phases that are available for the RP-CEC of a wide range of solutes.

Conclusions

This introductory chapter has (1) outlined the scope of this dissertation, (ii) provided a historical development of CEC and discussed the various formats of CEC in terms of column technologies. Furthermore, the development and applications of organic polymer-based monoliths which form the heart of this dissertation has been emphasized, (iii) summarized the rationale of the investigation, (iv) described some aspects of CEC including its instrumentation, origin of EOF and the performance parameters that will be used in later chapters

References

1. Picó, Y., Rodríguez, R., Mañes, J., *TrAC, Trends Anal. Chem.* **2003**, *22*, 133-151.
2. Klodzinska, E., Moravcova, D., Jandera, P., Buszewski, B., *J. Chromatogr. A.* **2006**, *1109*, 51-59.
3. Lynen, F., Buica, A., Villiers, A. d., Crouch, A., Sandra, P., *J. Sep. Sci.* **2005**, *28*, 1539-1549.
4. Tiselius, A., G. E. Henschen, H. Svensson, *Biochem. J.* **1937**, *31*, 313-317.
5. Strain, H. H., *J. Am. Chem. Soc.* **1939**, *61*, 1292-1293.
6. Mould, D. L., R. L. M. Synge, L. M., *Analyst* **1952**, *77*, 964-969.
7. Mould, D. L. a. S., R. L. M., *Biochem. J.* **1954**, *58*, 571-585.
8. Pretorius, V., Hopkins, B. J., Schieke, J. D., *J. Chromatogr. A.* **1974**, *99*, 23-30.
9. Knox, H. J., Grant, H. I., *Chromatographia* **1987**, *24*, 135-143.
10. Knox, H. J., Grant, H. I., *Chromatographia* **1991**, *32*, 317-328.
11. Steiner, F., Scherer, B., *J. Chromatogr. A.* **2000**, *887*, 55-83.
12. Moring, S. E., Reel, R. T., van Soest, R. E. J., *Anal. Chem.* **1993**, *65*, 3454-3459.
13. Heiger, D. N., *High Performance Capillary Electrophoresis-An introduction.*, Hewlett-Packard Co., France 1**992**.
14. Quigley, W. W. C., Dovichi, N. J., *Anal. Chem.* **2004**, *76*, 4645-4658.
15. Kasicka, V., *Electrophoresis* **2003**, *24*, 4013-4046.
16. El Rassi, Z., *Electrophoresis **2010**, 31*, 174-191.
17. Ye, M., Hu, S., Quigley, W. W. C., Dovichi, N. J., *J. Chromatogr. A* **2004**, *1022*, 201-206.
18. Kasicka, V., *Electrophoresis **2010**, 31*, 122-146.

19. Lamari, F. N., Kuhn, R., Karamanos, N. K., *J. Chromatogr. A* **2003**, *793*, 15-36.

20. Oguri, S., Okuya, Yukie, Yanase, Yukiko, Suzuki, Sayaka, *J. Chromatogr. A* **2008**, *1202*, 96-101.

21. Wall, W., Li, J., El Rassi, Z., *J. Sep. Sci.* **2002**, *25*, 1231-1244.

22. Shediac, R., Ngola, Sarah M., Throckmorton, Daniel J., Anex, Deon S., Shepodd, Timothy J., Singh, Anup K., *J. Chromatogr. A* **2001**, *925*, 251-263.

23. Egelhofer, V., Gobom, Johan, Seitz, Harald, Giavalisco, Patrick, Lehrach, Hans, Nordhoff, Eckhard, *Anal. Chem.* **2002**, *74*, 1760-1771.

24. Augustin, V., Stachowiak, T., Svec, F., Fréchet, J. M. J., *Electrophoresis* **2008**, *29*, 3875-3886.

25. D'Orazio, G., Fanali, S., *J. Chromatogr. A* ***2010***, *1217*, 4079-4086.

26. Que, A. H., Novotny, M.V., *Anal. Bioanal. Chem.* **2003**, *375*, 599-608.

27. Pusecker, K., Schewitz, Jens, Gfrorer, Petra, Tseng, Li-Hong, Albert, Klaus, Bayer, Ernst, *Anal. Chem.* **1998**, *70*, 3280-3285.

28. Erdmann Rapp, A. J., Alexandre Bezerra Schefer, Ernst Bayer and Klaus Albert, *Anal Bioanal Chem* **2003**, *376*, 1053-1061.

29. Klaus Pusecker, J. S., Petra Gfrörer, Li-Hong Tseng, Klaus Albert, Ernst, Bayer, I. D. W., Nigel J. Bailey, Graeme B. Scarfe, Jeremy K. Nicholson and John, Lindon, C., *Anal. Commun.* **1998**, *35*, 213-215.

30. Luong, J. H. T., Bouvrette, P., Liu, Y., Yang, D.-Q., Sacher, E., *J. Chromatogr. A* **2005**, *1074*, 187-194.

31. Cikalo, M. G., Bartle, K. D., Robson, M. M., Myers, P., Euerby, M. R., *Analyst* **1998**, *123*, 87R-102R.

32. Colón, L. A., Reynolds, K. J., Alicea-Maldonado, R., Fermier, A. M., *Electrophoresis* **1997**, *18*, 2162-2174.

33. Rathore, A. S., *Electrophoresis* **2002**, *23*, 3827-3846.

34. Rathore, A. S., Horváth, C., *Electrophoresis* **2002**, *23*, 1211-1216.

35. Dabek-Zlotorzynska, E., Chen, H., Ding, L., *Electrophoresis* **2003**, *24*, 4128-4149.

36. Dittmann, M. M., Wienand, K., Bek, F., Rozing, G. P., *LC-GC* **1995**, *13*, 800-814.

37. Colon, L. A., Guo, Y., Fermier, A., *Anal. Chem.* **1997**, *69*, 461 A-467 A.

38. Wen, E., Asiaie, R., Horváth, C., *J. Chromatogr. A.* **1999**, *855*, 349-366.

39. Giddings, J. C., *Unified Separation Science*, Wiley, New York **1991**.

40. Zhang, M., El Rassi, Z., *Electrophoresis* **1998**, *19*, 2068-2072.

41. Tang, Q., Lee, M. L., *J. High Resolut. Chromatogr.* **2000**, *23*, 73-80.

42. Patel, K. D., Jerkovich, A. D., Link, J. C., Jorgenson, J. W., *Anal. Chem.* **2004**, *76*, 5777-5786.

43. Yang, C., El Rassi, Z., *Electrophoresis* **1999**, *20*, 18-23.

44. Nashabeh, W., El Rassi, Z., *J. Chromatogr. A.* **1993**, *632*, 157-164.

45. Pyell, U., *J. Chromatogr. A.* **2000**, *892*, 257-278.

46. Behnke, B., Johansson, J., Zhang, S., Bayer, E., Nilsson, S., *J. Chromatogr. A.* **1998**, *818*, 257-259.

47. Eeltink, S., Decrop, W. M. C., Rozing, G. P., Schoenmakers, P. J., Kok, W. T., *J. Sep. Sci.* **2004**, *27*, 1431-1440.

48. Li, Y., Xiang, R., Wilkins, J. A., Horváth, C., *Electrophoresis* 2004, *25*, 2242-2256.

49. Pesek, J. J., Matyska, M. T., *J. Chromatogr. A.* **2000**, *887*, 31-41.

50. Simal-Gandara, J., *Crit. Rev. Anal. Chem.* **2004**, *34*, 85-94.

51. Matyska, M. T., Pesek, J. J., Katrekar, A., *Anal. Chem.* **1999**, *71*, 5508-5514.

52. Smith, N. W., Jiang, Z., *J. Chromatogr. A.* **2008**, *1184*, 416-440.

53. Vlakh, E. G., Tennikova, T. B., *J. Sep. Sci.* **2007**, *30*, 2801-2813.

54. Allen, D., El Rassi, Z., *Electrophoresis* **2003**, *24*, 3962-3976.

55. Maruska, A., Rocco, A., Kornysova, O., Fanali, S., *J. Biochem. Biophys. Meth.* **2007**, *70*, 47-55.

56. Hilder, E. F., Svec, F., Fréchet, J. M. J., *J. Chromatogr. A.* **2004**, *1044*, 3-22.

57. Hoegger, D., Freitag, R., *J. Chromatogr. A.* **2001**, *914*, 211-222.

58. Que, A. H., Palm, A., Baker, A. G., Novotny, M. V., *J. Chromatogr. A.* **2000**, *887*, 379-391.

59. Okanda, F. M., El Rassi, Z., *Electrophoresis* **2005**, *26*, 1988-1995.

60. Karenga, S., El Rassi, Z., *Electrophoresis* ***2010***, *31*, 991-1002.

61. Karenga, S., El Rassi, Z., *J. Sep. Sci.* **2008**, *31*, 2677-2685.

62. Jin, W., Fu, H., Huang, X., Xiao, H., Zou, H., *Electrophoresis* **2003**, *24*, 3172-3180.

63. Svec, F., *Electrophoresis* **2009**, *30*, S68-S82.

64. Huang, H.-Y., Lin, H. Y., Lin, S.-P., *Electrophoresis* **2006,** *27*, 4674-4681.

65. Chirica, G. S., Remcho, V. T., *J. Chromatogr. A.* **2001**, *924*, 223-232.

66. Karenga, S., El Rassi, Z., *Electrophoresis* **2010** *31*, 991-1002.

67. Dabek-Zlotorzynska, E., Celo, V., *Electrophoresis* **2006**, *27*, 304-322.

68. Flurer, C. L., *Electrophoresis* 2003, *24*, 4116-4127.

69. Oliver McConnell, A. B. I., Carl Balibar, Neal Byrne, Yanxuan Cai, Guy Carter, Michael Chlenov, Li Di, Kristi Fan, Igor Goljer, Yanan He, Don Herold, Michael Kagan,, Edward Kerns, F. K., Christina Kraml, Vasilios Marathias, Brian Marquez,

Leonard McDonald, Lisa Nogle, Christopher Petucci, Gerhard Schlingmann, Gregory Tawa, Mark Tischler, R. T. W., Alan Sutherland, William Watts, Mairead Young, Mei-Yi Zhang, Yingru Zhang, Dahui Zhou, Douglas Ho, *Chirality* **2007**, *19*, 658-682.

70. Dolník, V., *Electrophoresis* **2008**, *29*, 143-156.
71. Gübitz, G., Schmid, M. G., *Electrophoresis* **2004**, *25*, 3981-3996.
72. Kang, J., Wistuba, D., Schurig, V., *Electrophoresis* **2002**, *23*, 4005-4021.
73. Feng Qin, C. X., Zhiyuan Yu, Liang Kong, Mingliang Ye, Hanfa Zou, *J. Sep. Sci.* **2006,** *29*, 1332-1343.
74. Mojca Merhar, A. P., Miloscaron Barut, Majda, Zcaron, igon, Alescaron Scarontrancar, *J. Sep. Sci.* **2003**, *26*, 322-330.
75. Ji, rcaron, Urban, í., Jandera, P., *J. Sep. Sci.* **2008**, *31*, 2521-2540.
76. Viklund, C., Svec, F., Frechet, J. M. J., Irgum, K., *Chem. Mater.* **1996**, *8*, 744-750.
77. Li, Y., Tolley, H. D., Lee, M. L., *Anal. Chem.* **2009**, *81*, 9416-9424.
78. Rohr, T., Hilder, E. F., Donovan, J. J., Svec, F., Frechet, J. M. J., *Macromolecules* **2003**, *36*, 1677-1684.
79. Tan, A., Benetton, S., Henion, J. D., *Anal. Chem.* **2003**, *75*, 5504-5511.
80. Sáfrány, Á., Beiler, B., László, K., Svec, F., *Polymer* **2005**, *46*, 2862-2871.
81. Beiler, B., Vincze, Á., Svec, F., Sáfrány, Á., *Polymer* **2007**, *48*, 3033-3040.
82. Petra Holdscaronvendová, P. C., Jana Suchánková, Eva Tesa, rcaron,ová, Zuzana Bosáková, *J. Sep. Sci.* **2003**, *26*, 1623-1628.
83. Cantó-Mirapeix, A., Herrero-Martínez, J. M., Mongay-Fernández, C., Simó-Alfonso, E. F., *Electrophoresis* **2008**, *29*, 3858-3865.

84. Peters, E. C., Svec, F., Fréchet, J. M. J., *Advanced Materials* **1999**, *11*, 1169-1181.

85. Bedair, M., El Rassi, Z., *J. Chromatogr. A* **2003**, *1013*, 35-45.

86. Bedair, M., El Rassi, Z., *J. Chromatogr. A* **2003**, *1013*, 47-56.

87. Haixia Lü, J. W., Xiaochun Wang, Xiaoping Wu, Xucong Lin, Zenghong Xie, *J . Sep. Sci.* **2007**, *30*, 2993-2999.

88. Maruska, A., Rocco, A., Kornysova, O., Fanali, S., *J. Biochem. Biophys. Methods* **2007**, *70*, 47-55.

89. Bedair, M., El Rassi, Z., *Electrophoresis* **2002**, *23*, 2938-2948.

90. Huang, H.-Y., Liu, Y.-C., Cheng, Y.-J., *J. Chromatogr. A* **2008**, *1190*, 263-270.

91. Zhang, Y.-P., Ye, Xiong-Wen, Tian, Meng-Kui, Qu, Ling-Bo, Choi, Seong-Ho'Gopalan, Anantha Iyengar, Lee, Kwang-Pill, *J. Chromatogr. A* **2008,** *1188*, 43-49.

92. Freitag, R., *Journal of Chromatography A* **2004**, *1033*, 267-273.

93. Zhang, M., El Rassi, Z., *Electrophoresis* **2001**, *22*, 2593-2599.

94. Waguespack, B. L., Hodges, S. A., Bush, M. E., Sondergeld, L. J., Bushey, M. M., *Journal of Chromatography A* **2005**, *1078*, 171-180.

95. Ye, X. W., Zhang, Yu Ping, Qu, Ling Bo, Fan, Li Qun, Li, Bo, *Chin. Chem. Lett.* **2007,** *18*, 1399-1402.

96. Buszewski, B., Szumski, M., Sus, Sz, *LC-GC* **2002,** *15*, 792-798.

97. Buszewski, B., Szumski, M., *Chromatographia* **2004**, *60*, S261-S267.

98. Minghua Lu, Q. F., Qiaomei Lu, Zongwei Cai, Lan Zhang, Guonan Chen, *Electrophoresis* **2009**, *30*, 3540-3547.

99. Messina, A., Desiderio C., De Rossi A., Bachechi F., Sinibaldi, M, *Chromatographia* **2005**, *62*, 409-416.

100. Lin, J., Wu, X., Lin, X., Xie, Z., *J. Chromatogr. A* **2007**, *1169*, 220-227.

101. Ping, G. C., Zhang, W. B., Zhang, L., Zhang, L. H., Shan, Y. C., Zhang, Y. K., Schmitt-Kopplin, P., Kettrup, A., *Chromatographia* **2003**, *58*, 803-806.

102. Kai Z., Ruyu G., Chao Y., Zhichao Z. and Qinsun W., *Chromatographia* **2005**, *61*, 55-60.

103. Karine Faure, M. A., Vincent Dugas, Gérard Crétier, Rosaria Ferrigno, Pierre Morin, Jean-Louis Rocca, *Electrophoresis* **2008**, *29*, 4948-4955.

104. Hilder, E. F., Svec, F., Frechet, J. M. J., *Anal. Chem.* **2004**, *76*, 3887-3892.

105. Dong, X., Dong, J., Ou, J., Zhu, Y., Zou, H., *Electrophoresis* **2006**, *27*, 2518-2525.

106. Fu, H., Xie, C., Dong, J., Huang, X., Zou, H., *J. Anal. Chem* **2004**, *76*, 4866-4874.

107. Li, Y., Chen, Yuan, Xiang, Rong, Ciuparu, Dragos, Pfefferle, Lisa D., HorvÃ¡th, Csaba, Wilkins, James A., *Anal. Chem.* **2005**, *77*, 1398-1406.

108. Connolly, D., Twamley, B., Paull, B., *Chem. Commun.* **2010**, *46*, 2109-2111.

109. Zhang, M., El Rassi, Z., *J. Proteome Res.* **2006**, *5*, 2001-2008.

CHAPTER II

NEUTRAL OCTADECYL MONOLITH FOR REVERSED PHASE CAPILLARY ELECTROCHROMATOGRAPHY OF A WIDE RANGE OF SOLUTES

Introduction

Capillary electrochromatography (CEC) is emerging as a powerful separation technique combining the best features of two modern liquid phase separation techniques, namely high performance liquid chromatography (HPLC) and capillary electrophoresis (CE). Recent progress in CEC has been well documented in a few review articles [1-6], which reveal the importance of developing new column technology in contributing to the increased applicability of CEC in solving difficult separation problems. The most prominent trend in column technology has been the development of monolithic stationary phases based on silica and organic polymer monoliths. This is not surprising considering the fact that the column is the heart of the separation process.

** The content of this chapter has been published in Journal of Separation Science, **2008**, 31, 2677-2685.*

In CEC, the general trend in the fabrication of monolithic stationary phases has always involved the introduction of small amounts of fixed charges into the monoliths *via* the use of charged monomers in the polymerization process in order to support a relatively strong electroosmotic flow (EOF) for transporting the mobile phase across the column. In the case of reversed phase monolithic columns, the presence of fixed charges on the monolith surface lead to the so-called mixed mode stationary phases, which in addition to the main reversed phase retention mechanism will also superimpose an ion exchange retention mechanism in the case of charged solutes.

Although the presence of a mixed mode retention mechanism can be beneficial for some separations, very often control of the selectivity of the separation can be a tedious process because of the presence of two orthogonal retention mechanisms in the same separation channel. In addition, the prediction of solute retention on mixed mode stationary phases may not be a simple matter.

The above general trend has been changed recently by the work of Okanda and El Rassi [7]. They introduced a C17 acrylate based monolithic stationary phase void of fixed charges, which produced a sufficient EOF to allow for the rapid separation of a wide range of solutes with “zero” electrostatic interactions with the neutral C17 monolith. The produced EOF was attributed to the adsorption of ions (e.g., phosphate ions) to the C17 acrylate based monolith. The C17 monolith was prepared by the *in situ* polymerization of pentaerythritol diacrylate monostearate (PEDAS). The C17 column was very suitable for protein and peptide separations [7-9].

Prior to the above investigation, two attempts were made to produce neutral monoliths [10, 11]. In one attempt, the neutral monolith was made by copolymerizing

butyl methacrylate and ethylene dimethacrylate (EDMA) [11]. Although this neutral monolith did not exhibit any EOF, the separation of small acidic solutes was achieved through their differential electromigration. In the second attempt [10], the inner wall of a fused–silica capillary was grafted with a positively charged polymer layer to support an annular EOF. The neutral monolith was prepared by *in situ* copolymerization of vinylbenzyl chloride and EDMA in a binary porogenic solvent consisting of 1-propanol and formamide. This column separated a mixture of small peptides at a pH of 2.5, to avoid solute-wall interactions.

The present study, which is a continuation of earlier work from our laboratory [7], is aimed at (i) furthering the development of neutral monoliths at moderate EOF devoid of fixed surface charges for RP-CEC of ionic solutes in the absence of electrostatic interactions, (ii) better understanding the behaviors of neutral monoliths in CEC over a wide range of elution conditions, (iii) introducing monoliths with long C18 chains for enhanced retention and selectivity and (iv) enlarging the scope of applications of neutral monoliths in RP-CEC separations.

Experimental

Instrumentation

Two instruments were used in this investigation: a P/ACE 5010 CE system from Beckman (Fullerton, CA, USA) equipped with a fixed wavelength UV detector, and a P/ACE 5510 system, also from Beckman and equipped with a photodiode array detector. All chromatograms were recorded with a personal computer running a Gold P/ACE system. The samples were injected electrokinetically at various applied voltages as stated in the figure captions.

Reagents and materials

Trimethylolpropane trimethacrylate (TRIM), octadecyl acrylate (ODA), 2,2'-azobis(isobutyronitrile) (AIBN), 3-(trimethoxysilyl)propyl methacrylate, alkyl benzenes, alkyl phenyl ketones, polynuclear aromatic hydrocarbons, phenols, anilines, and analytical-grade acetone were from Aldrich (Milwaukee, WI, USA). Cyclohexanol was purchased from J.T. Baker (Phillipsburg, NJ, USA). Ethylene glycol (EG) and HPLC-grade acetonitrile (ACN) were from Fischer Scientific (Fair Lawn, NJ, USA). 1-Naphthol was from Eastman Kodak (Rochester, NY, USA). Pesticides were obtained from ChemService (West Chester, PA, USA). Proteins, peptides and trypsin TPCK from bovine pancreas were purchased from Sigma (St. Louis, MO, USA). Tryptic protein digestion (e.g., chicken white lysozyme and horse heart cytochrome C) was performed after protein reduction and alkylation using the Promega protocol. Buffer solutions were prepared using sodium phosphate monobasic from Mallinckrodt (Paris, KY, USA). Fused silica capillaries with an internal diameter (ID) of 100-µm and outside diameter of 361 µm were from Polymicro Technologies (Phoenix, AZ, USA).

Column pretreatment

The inner wall of the fused-silica capillary was treated with 1.0 M sodium hydroxide for 30 min, flushed with 0.10 M hydrochloric acid for 30 min, and then rinsed with water for 30 min. The capillary inner wall was then allowed to react with a solution of 50% v/v of 3-(trimethoxysilyl)propyl methacrylate in acetone for 6 h at room temperature to vinylize the inner wall of the capillary. Finally, the capillary was rinsed with acetone and then dried with a stream of nitrogen.

In situ polymerization

Polymerization solutions were prepared from 0.24 mmol of ODA as the monomer, 0.48 mmol of TRIM as the crosslinker. The mixtures of monomer and crosslinker were dissolved in a ternary porogenic solvent (1 mL) consisting of cyclohexanol and ethylene glycol in various ratios at constant 3.6% w/w water. AIBN (1.0 wt% with respect to monomers) was added to the solution. The polymerization solution was then sonicated for ~20 min to obtain a clear solution. The sonicating water bath temperature reached ~45 ˚C after ~20 min thus facilitating the dissolution of the ODA and TRIM in the porogenic solvent. A 32 or 42 cm pretreated capillary was filled with the polymerization solution up to 23 or 33 cm, respectively, by immersing the inlet of the capillary in the solution vial and applying vacuum to the outlet to prepare a final column of 27 or 37 cm total length, respectively. The capillary ends were then sealed using a GC septum and the capillary submerged in a 60 °C water bath for 12 h. The resulting monolithic columns were rinsed with an 80:20 v/v acetonitrile:water mixture using an HPLC pump. A detection window was created at 1-2 mm after the end of the polymer bed using a thermal wire stripper. Finally, the column was cut to a total length of 27 or 37 cm with an effective length of 20 or 30 cm, respectively.

Results and discussion

Column fabrication and characterization

Porogens. The ternary porogenic solvent used in this investigation consisted of cyclohexanol, EG and water. This ternary porogen was first introduced by Bedair and El Rassi [12-14] for the fabrication of PEDAS-based monolithic column with either cationic

or anionic sites to support a strong EOF. It consisted of 83.2 wt% cyclohexanol, 13.2 wt% EG and 3.6 wt% water and yielded a column with the highest separation efficiency, strong EOF and high permeability. Water was included to increase the solubility of the charged monomers. More recently, the same ternary porogenic solvent, with slight modification in its composition, proved very useful in the fabrication of a neutral PEDAS column (also referred to as a C17 monolith) reported by Okanda and El Rassi [7]. The ternary porogen was composed of 79.2 wt% cyclohexanol, 17.2 wt% EG and 3.6 wt% water. Although in this case the monolith was void of fixed charges and did not require the addition of water for the solubilization of charged monomers, the exclusion of water yielded a monolith with much lower efficiency than when water was added to the porogenic solvent mixture, an indication that water in small amounts participates in the pore morphology. Obviously, none of the above solvent mixture compositions were found to be suitable for the preparation of an optimal neutral ODM column due to the fact that the monomers used in its preparation are different from those used to prepare monoliths reported by Bedair and El Rassi [12-14] and Okanda and El Rassi [7]. In an attempt to produce an ODM column with acceptable permeability in a pressure driven flow, different mixtures of cyclohexanol and EG were used while keeping the %wt composition of water constant. As expected, an increase in the wt% of the macroporogen (i.e., EG) in the polymerization mixture yielded a monolithic column with a higher permeability in a pressure driven flow. In fact, using a mobile phase of 80:20 v/v ACN:water, the volumetric flow rate increased from ~0.6 µL/min to ~1.5 µL/min when going from a column prepared from a polymerization mixture at 19.7% EG to a column made from a polymerization mixture containing 21.7% EG using a constant pressure drop

of 2000 psi and a column length of 32 cm. Also, the EOF increased by increasing the %EG (see Fig. 1A). The increased mobile phase flow velocity in both pressure and electric driven flow upon increasing the %EG, indicates an increase in the macroporosity of the ODM.

Obviously, as the size of the macroporous channels increases with the amount of macroporogen in the polymerization mixture, the diffusion path length of the solute transfer from the middle to the wall of the channels for adsorption also increases. This will lead to an increased band broadening, and consequently decreased separation efficiency at higher channel diameter. This explains the variation of separation efficiency obtained with eight alkyl benzene test solutes shown in Fig. 1B. The optimum column efficiency and reasonable EOF were obtained with a porogenic mixture composed of cyclohexanol (75.7 wt%), EG (20.7 wt%) and water (3.6 wt%), see Fig. 1A and 1B. This neutral ODM column with the highest efficiency was the one considered further for this study.

It is also worth mentioning here that other porogenic solvent mixtures such as toluene/isooctane, and cyclohexanol/toluene were also tested. These mixtures yielded columns with little or no permeability in a pressure driven flow.

Plate height versus flow velocity-van Deemter plot. The optimal ODM column was further evaluated for its CEC separation efficiency over a wide range of mobile phase flow velocities at 75% v/v ACN in the mobile phase. The results are shown in Fig. 2A by the so-called van Deemter plot using eight alkylbenzenes as the model solutes.

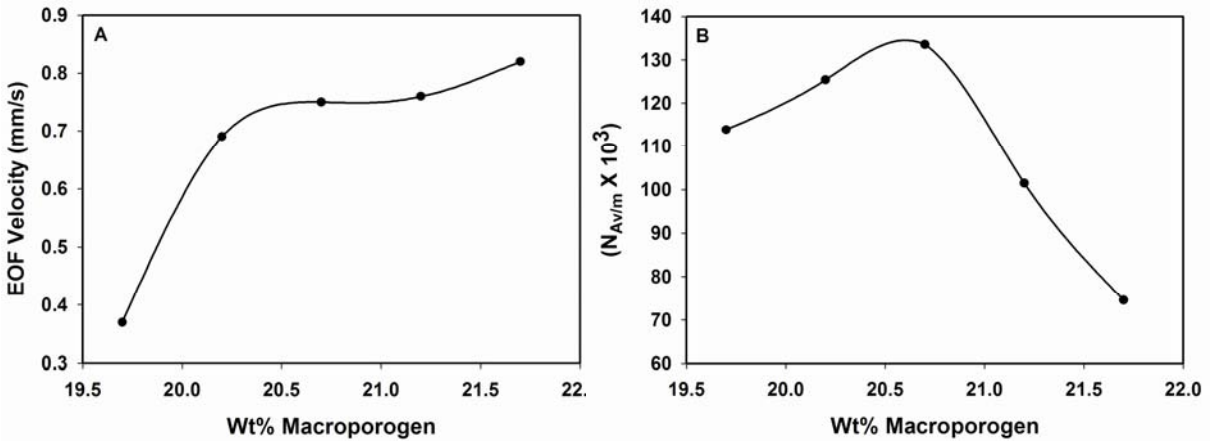

Figure 1. *Effect of wt% EG (macroporogen) in the polymerization solution on the apparent EOF velocity (A) and the average plate number per meter for the alkylbenzene homologous series (B). ODM capillary column, 20 cm effective length, 27 cm total length × 100 μm ID; mobile phase, 1 mM sodium phosphate, pH 7.0, at 65% v/v ACN; running voltage, 10 kV; EOF tracer, uracil; electrokinetic injection for 3 s at 5 kV. Test solutes: benzene, toluene, ethylbenzene, propylbenzene, butylbenzene, pentylbenzene, hexylbenzene, heptylbenzene.*

The apparent EOF velocity was increased by increasing the operating voltage from 8 to 22 kV.

As can be seen in Fig. 2A, H_{min} is obtained at an optimal EOF velocity in the range 0.6–1.0 mm/s. Even if the flow velocity is increased to 1.23 mm/s the loss in separation efficiency is ~12% but with a shortening in the analysis time by about 49% with respect to the analysis time at 0.6 mm/s (13.3 min versus 27.3 min). A typical electrochromatogram of the alkylbenzenes at 1.23 mm/s is shown in Fig. 2B.

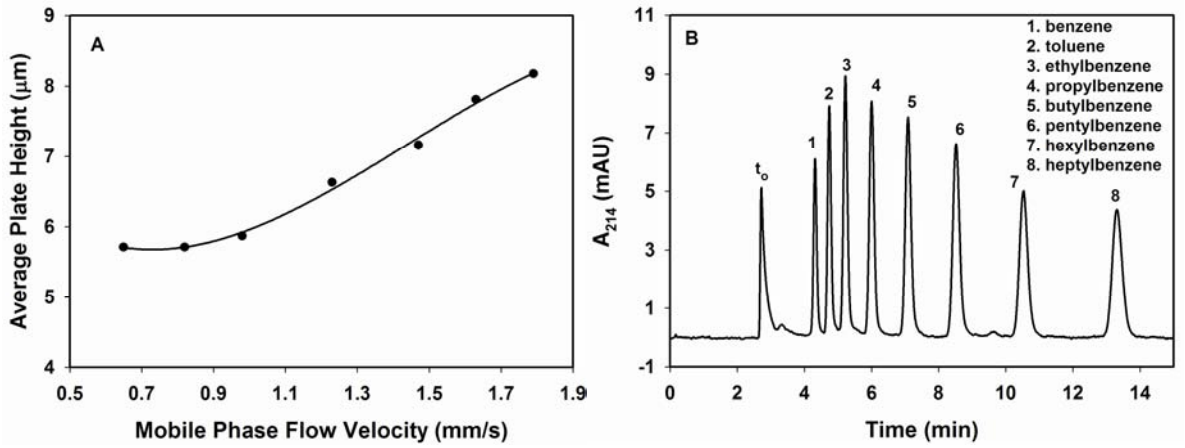

Figure 2. *van Deemter plot showing average plate height as a function of apparent EOF velocity (A) and Electrochromatogram of alkylbenzene homologous series (B) Conditions as in Fig. 1.*

This represents a practical flow velocity range (0.6 to 1.2 mm/s) over which the column can be column can be utilized with virtually little or no variation in the separation efficiency, thus representing an efficient solute mass transfer characteristic within the porous ODM.

Reproducibility of column fabrication. Run-to-run, day-to-day and column-to-column reproducibilities of the optimal ODM column were studied in terms of t_o, the retention factor (k') and the separation efficiency of eight alkyl benzenes using a mobile phase containing 80% v/v ACN in 1 mM sodium phosphate buffer, pH 7. The percent relative standard deviation (% RSD) (n = 3) were 2.67, 4.00 and 12.53, for the EOF velocity (to), k' and separation efficiency, respectively, which are similar to those previously reported in literature [12, 15, 16].

The driving force for EOF. Despite the fact that the ODM column is neutral and void of groups with fixed charges and consequently has no zeta potential with respect to water, the ODM produced a sufficient EOF over a certain pH range as shown in Fig. 3. The presence of polar ester groups in the ODA monomer and the crosslinker TRIM is thought to be significant to the monolith's ability to adsorb enough phosphate ions from the electrolyte solution. This imparts the monolith with the zeta potential necessary to support an EOF. Since the EOF is cathodal, the zeta potential is therefore negative. As can be seen from Fig. 3A, the EOF is somewhat the same in the pH range 4-5 and then increases sharply at pH 5-7. At pH 5-7, the amount of adsorbed phosphate ions carrying a double negative charge increases thus producing the sharp rise in EOF, whereas at pH 3 and 4 most of the phosphate ions have a single negative charge thus explaining the flat

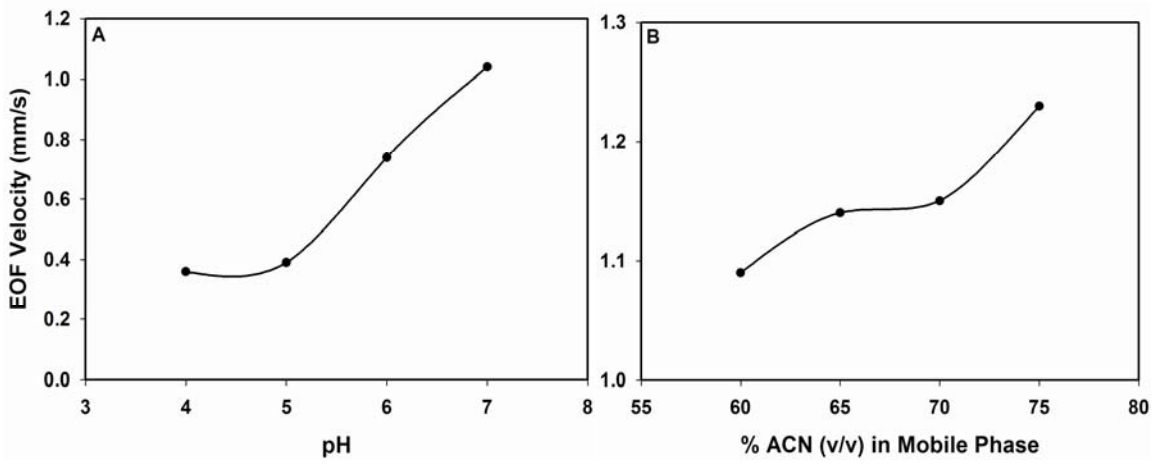

Figure 3. *Plot of the apparent EOF velocity versus (A) the pH of the mobile phase and (B) the % ACN v/v in the mobile phase. ODM capillary column, 20 cm effective length, 27 cm total length × 100 μm ID; mobile phase, 3 mM sodium phosphate at various pH and at 40% v/v ACN in (A) and various % ACN (v/v) at pH 7 in (B); running voltage, 15 kV; EOF tracer, uracil; electrokinetic injection for 3 s at 10 kV.*

part of the curve in Fig. 3A at low pH. This agrees very well with the observation reported earlier by Okanda and El Rassi with a C17 neutral monolith based on the PEDAS monomer [7].

To further gain insight into the origin of the EOF with the neutral ODM, the effect of the ACN content of the mobile phase on the magnitude of the EOF was examined and the results are shown in Fig. 3B. As can be seen in this figure, the magnitude of the EOF increased with the %ACN at varying rate in the range studied 60 to 75% v/v. Although increasing the ACN decreases the dielectric constant of the mobile phase which may diminish the ionization of the adsorbed phosphate ions, the fact that increasing the ACN content decreases the viscosity of the mobile phase and increases the amount of adsorbed phosphate ions to the ODM surface result in increasing the EOF velocity under the given set of running conditions. It is believed that the adsorption of phosphate ions to the solid ODM is of polar nature and the extent of which would increase with the ACN content of the mobile phase. This observation corroborates with that previously reported by Okanda and El Rassi [7] with a different neutral monolith.

Evaluation of Chromatographic Retention

Neutral nonpolar solutes. The performance of the ODM column was investigated with various kinds of neutral solutes spanning a wide range of polarity to gain insight into the retention mechanism. Two homologous series, namely 7 alkylbenzenes (ABs) and 6 alkyl phenyl ketones (APKs) as well as 8 polyaromatic hydrocarbons (PAHs) were used as the model solutes. As expected and using the same mobile phase composition (75% v/v ACN), the heptanophenone (i.e., the APK with the longest alkyl chain used) exhibited a retention time of ~4.3 min at 15 kV which is less than half the retention time of

hexylbenzene (~10.3 min) of the AB series. The most retained solute in the PAHs series (i.e., benzo[ghi]perylene) yielded a retention time of ~23 min, which is nearly twice as much as that of the ABs and ~5.3 fold higher than the APKs. The retention factor values (k') can be readily obtained from Fig. 4, which shows plots of logarithmic k' (log k') versus the %ACN in the mobile phase.

As is evident from the plots, log k' linearly decreases with increasing concentration of ACN, which is an indication that the separation of the ABs, APKs and PAHs on the neutral ODM column is based on a typical reversed phase chromatographic retention mechanism. Furthermore, and as shown in Fig. 4, the magnitude of k' values for APKs, ABs and PAHs were in accordance to their relative hydrophobicity with the least hydrophobic being APKs, medium hydrophobic ABs and most hydrophobic PAHs. This is another indication of a reversed phase separation mechanism. The slopes of the lines in each set of solutes increased with increasing the size of the solute. In other words, the slope increased with increasing the hydrophobic contact area between the solute and the nonpolar ligand (C18 ligand).

Slightly polar solutes. Figure 5 shows the separation of 9 phenols on the ODM column using a mobile phase 30% or 40% v/v ACN, whose aqueous constituent has a pH 7.0. Two of these phenols, namely 2,4-dichlorophenol and 4-cyanophenol with pKas of 7.85 and 7.95, respectively, are very slightly ionized at pH 7.0 (i.e., the pH of the experiment), while all the remaining phenols under investigation with $pK_a \geq 8.5$ are largely undissociated and can be considered as neutral solutes. As can be seen in Fig. 5, increasing the ACN concentration from 30% to 40% v/v decreased the analysis time by

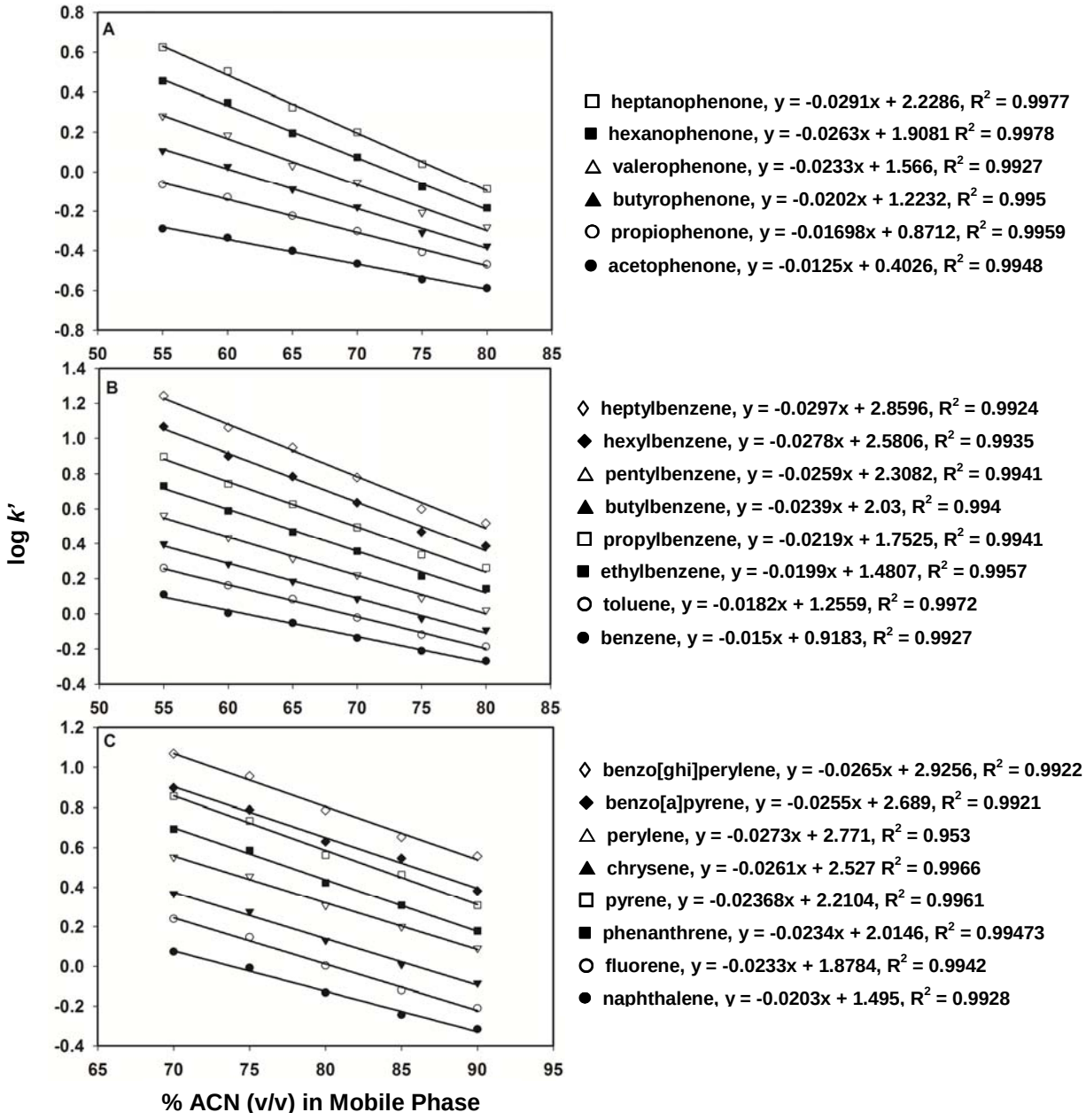

Figure 4. *Plots of log k' for alkyl phenyl ketones (A), alkylbenzenes (B) and polyaromatic hydrocarbons (C) versus % ACN (v/v) in the mobile phase. Solutes in (A): 1, acetophenone; 2, propiophenone; 3, butyrophenone; 4, valerophenone; 5, hexanophenone; 6, heptanophenone; (B): as in Fig.2; (C): 1, naphthalene; 2, fluorene; 3, phenanthrene; 4, pyrene; 5, chrysene; 6, perylene; 7, benzo[a]pyrene; 8, benzo[ghi]perylene. Conditions as in Fig. 3.*

more than 50% and k' too by about 50% in most cases. Also, the log k' of the phenols decreased linearly ($R^2 > 0.992$) by increasing the concentration of ACN in the mobile phase in the 25% to 40% v/v range studied. This is indicative of a hydrophobic interaction that was predominant between the phenols under investigation and the stationary phase despite the fact that two of these solutes are slightly ionized. With only one exception, the phenols investigated eluted in the order of decreasing polarity (see Fig. 6). For instance, phenol and hydroxyphenols (i.e., pyrogallol < catechol < phenol) are less retained than 3-methoxyphenol, which is less retained than monochlorophenols (4-chlorophenol < 3-chlorophenol < 2-chlorophenol) and 2,4-dichlorophenol. Although 4-cyanophenol is more polar than its counterpart 3-methoxyphenol, the former was retained more than the latter, most probably due to its electrophoretic migration in the opposite direction to the EOF.

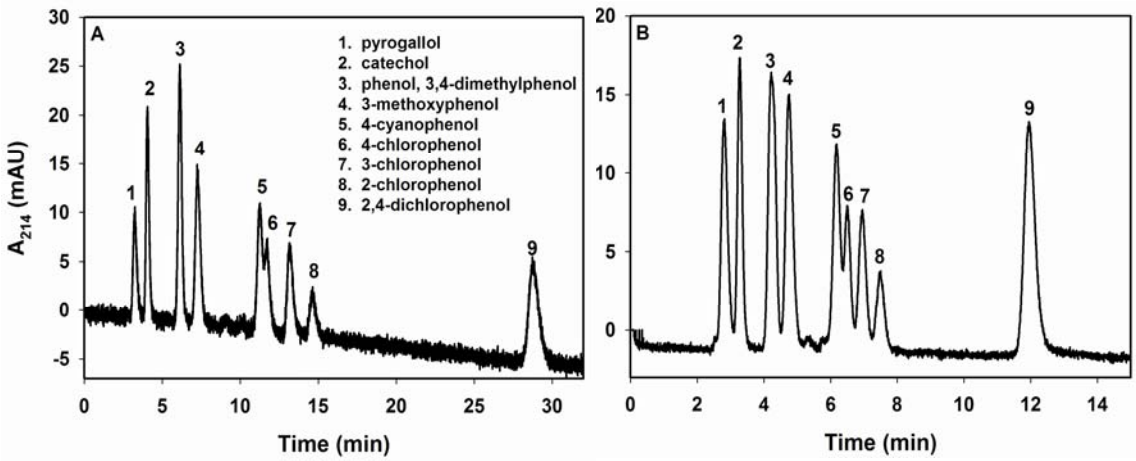

Figure 5. *Electrochromatograms of some phenols. ODM capillary column, 20 cm effective length, 27 cm total length × 100 µm ID; hydro-organic mobile phases, 30% ACN v/v in (A) and 40% ACN v/v in (B), 3mM sodium phosphate monobasic, pH 7.0; voltage, 15 kV, electrokinetic injection, 10 kV for 3 s.*

To evaluate the retention property of ODM with another class of slightly polar solutes, 8 anilines were electrochromatographed at neutral pH (7.0) including aniline (pK_a = 4.70), 3-methylaniline (pK_a = 4.91), *N*-ethylaniline (pK_a = 5.12), 4-isopropylaniline (pK_a = 5.0) 4-chloroaniline (pK_a = 4.06), 4-bromoaniline (pK_a = 3.86), 3-chloro-4-methylaniline (pK_a = 4.05) 3,4-dichloroaniline (pK_a = 3.33). The results are shown in Fig. 6 at 40% and 48% v/v ACN in the mobile phase.

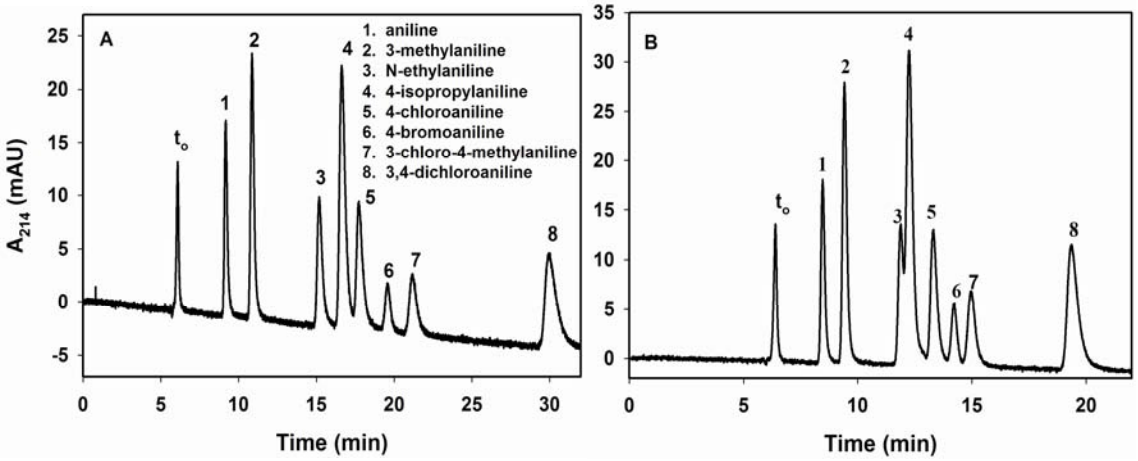

Figure 6. *Electrochromatograms of some anilines. Hydro-organic mobile phases at 40% ACN v/v in (A) and 48% ACN v/v in (B), 1 mM sodium phosphate monobasic, pH 7.0. Other conditions as in Fig. 6. Solutes: 1, aniline; 2, 3-methylaniline; 3, N-ethylaniline; 4, 4-isopropylaniline; 5, 4-chloroaniline; 6, 4-bromoaniline 7, 3-chloro-4-methylaniline; 8, 3,4-dichloroaniline.*

Given the fact that the pK_a values of the anilines under investigation are $\leq$ 5.12, the solutes are uncharged at pH 7.0 and their separation is based on their differences in reversed phase chromatographic partitioning. The eight anilines were baseline separated

in 30 min at 40% ACN and in less than 20 min at 48% ACN affording a theoretical plate count of 107,000 and 104,000 plates/m, respectively (see Fig. 6). The elution order of the anilines on the ODM column is in the order of increasing nonpolar character of the solutes a retention behavior typical for RP-CEC where halogenated anilines are more retained than methyl-substituted anilines and disubstituted anilines are more retained than mono-substituted anilines [17]. The dependence of log *k´* on %ACN in the mobile phase was linear in the range studied (40% to 50% v/v ACN) with an $R^2 > 0.999$. Again, the slope of the lines increased with the increased size of the solute, which is typical of reversed phase CEC.

Effect of ion concentration in the mobile phase: Modulation of surface polarity of the monolith. Eleven different pesticides and metabolites including 3 carbamate pesticides (oxamyl, aldicarb and carbaryl), 1-naphthol, which is the metabolite of carbaryl, and 7 phenyl urea herbicides (monuron, fluometuron, diuron, metobromuron, siduron, linuron and chloroxuron) that differ widely in polarity were taken as model solutes to study the effect of ion concentration in the mobile phase on solute retention. A hydro-organic mobile phase containing 30% v/v ACN, at various sodium phosphate concentrations, pH 7.0, was used as the eluent. As the phosphate ion concentration in the mobile phase was increased, the EOF velocity was decreased due primarily to the decrease in the thickness of the electric double layer at the liquid-solid interface as the ionic strength is increased. In fact, the EOF velocity decreased from 1.75 mm/s at 5 mM sodium phosphate to 1.53 mm/s at 7.5 mM, 1.49 mm/s at 10 mM and to 1.29 mm/s at 12

mM sodium phosphate. However, it was noted that the retention of the solutes decreased, see Fig. 7, which shows the dependence of *k´* on phosphate concentration.

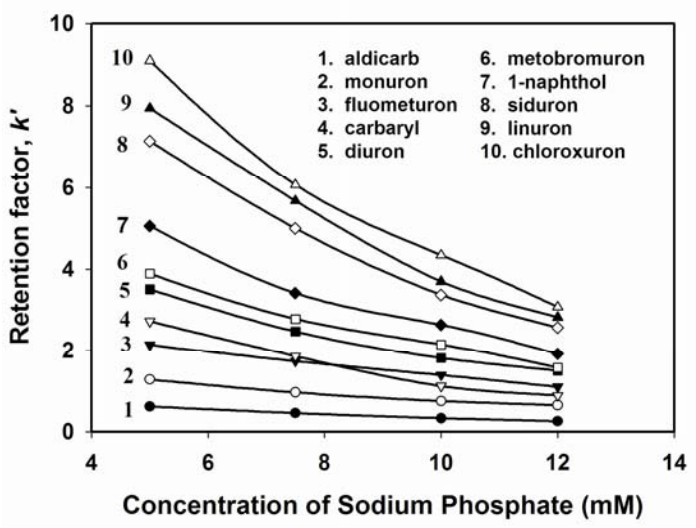

Figure 7. *Plots of retention factor k' of pesticides versus the concentration of sodium phosphate in the mobile phase. Conditions: hydro-organic mobile phase, 30% ACN v/v at various sodium phosphate concentration, pH 7.0. Other conditions as in Fig. 6.*

Figure 8 shows typical separation of the 11 test solutes at 5 mM and 12 mM sodium phosphate where it can be seen that the analysis time decreased by almost 50% when going from 5 to 12 mM sodium phosphate in the mobile phase. Increasing the phosphate ion concentration in the mobile phase increased the ion adsorption to the stationary phase thus increasing the amount of water in the adsorbed layer to the stationary phase surface, which favors solute partitioning in the hydro-organic mobile phase and as a result the solute retention decreases. It should be noted that while fluometuron eluted before carbaryl at 5 and 7 mM, the elution order between these two solutes was interchanged as the salt concentration was increased to 10 and 12mM (see Figs 7 and 8). Also, as the

concentration of phosphate ion in the mobile phase increased, the retention of oxamyl decreased significantly eluting before the EOF tracer.

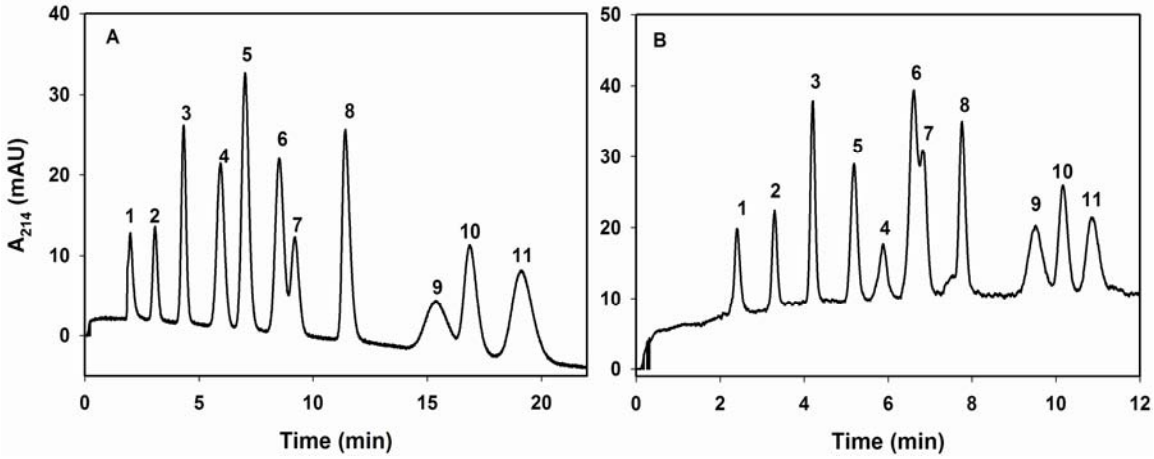

Figure 8. *Electrochromatograms of some pesticides. Hydro-organic mobile phase, 30% ACN v/v, 5 mM in (A) and 12 mM in (B) sodium phosphate monobasic , pH 7.0. Solutes and other conditions as in Fig. 8. Solutes: 1, oxamyl; 2, aldicarb; 3, monuron; 4, fluometuron; 5, carbaryl; 6, diuron; 7, metobromuron; 8, 1-naphthol; 9, siduron; 10, linuron; 11, chloroxuron.*

CEC of Peptides and Proteins. In order to further demonstrate the usefulness of the ODM column in RP-CEC separation of a wide range of species, polyionic solutes such peptides and proteins were electrochromatographed on the column. Obviously in this case, both the electrophoretic mobility and chromatographic partitioning control the migration of the multiply charged peptides and proteins. Figure 9A shows the separation of eleven standard peptides within 17 min with an average separation efficiency of 192,000 plates/m using a mobile phase composed of 40% ACN and 5 mM phosphate, pH 7.0, and a running voltage of 15 kV. For the migration time window of 8-17 min of the

electrochromatogram shown in Fig. 9A, the peak capacity is ~46. This peak capacity corresponds to ~5 peaks/min with a unit resolution. Under the same running conditions but with a slightly shorter ODM column, a mixture of six standard proteins of a widely differing size and charges (i.e., isoelectric points), namely carbonic anhydrase (pI = 6.2), myoglobin (pI = 7.0), β-lactoglobulin B (pI = 5.2), β-lactoglobulin A (pI = 5.1), α-lactalbumin (pI = 4.2 -4.5) and trypsin inhibitor (pI = 4.5) were separated within 14 min with an average separation efficiency of 53 000 plates/m (see Fig. 9B). The observed cathodal EOF under the conditions used in Fig. 9A and B is about 0.8 mm/s. Although this EOF is not very strong the peptides and proteins eluted from the ODM column in a few minutes (see Fig 9) indicating that the chromatographic partitioning contribution to proteins and peptides migration is much less in magnitude than the electrophoretic contribution. In fact, the proteins migrated in the order of decreasing pI values; that is the more acidic protein (trypsin inhibitor) migrated last while the less acidic protein (carbonic anhydrase) migrated first, and those of intermediate pI values in between.

Figure 9A, which offered a peak capacity of 46 for peptides using isocratic elution, suggested that the ODM column would be very useful in tryptic peptide mapping. On this basis, the ODM column was challenged in tryptic peptide mapping of 2 standard proteins cytochrome C and lysozyme, see Fig 10A and B. The tryptic digest of cytochrome C yields 37 peptide fragments while that of lysozyme yields 31 peptide fragments when using the ExPASy program (web page: http://ca.expasy.org/tools/peptide-mass.html) including the peptide fragments with missed cleavages, which amount to 20 and 17 peptide fragments for cytochrome C and lysozyme, respectively.

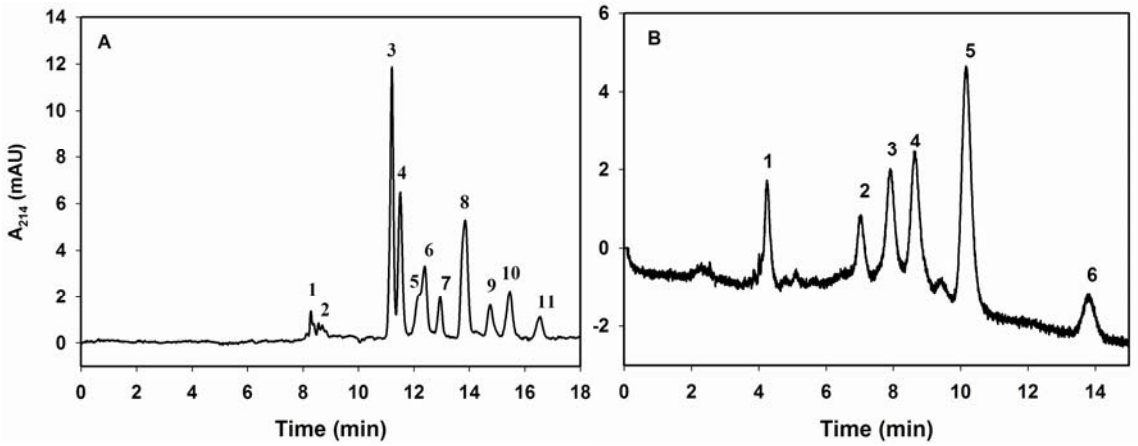

Figure 9. *Electrochromatograms of some standard peptides in (A) and standard proteins in (B). ODM capillary column, 30 cm effective length, 37 cm total length × 100 µm ID in (A) and 20 cm effective length, 27 cm total length × 100 µm ID in (B); hydro-organic mobile phase, 40% v/v ACN, 5 mM sodium phosphate monobasic, pH 7.0; Voltage, 15 kV, electrokinetic injection, 5 kV for 3 s. Solutes in (A): 1, Lys-Cys-Thr-Cys-Cys-Ala acetate; 2, Iva-Val-Val-Sta-Ala-Sta (Pepstatin A); 3, Phe-Gly-Gly-Phe; 4, Ala-Phe; 5, Gly-Gly-Leu; 6, Hist-Leu; 7, Gly-Trp; 8, Gly-Gly-Gly; 9, Arg-Phe-Asp-Ser; 10, Ser-Asp-Gly-Arg-Gly; 11, Gly-Gly-Leu-Pro-Pro-Gly-Pro-Ile-Phe-Pro. Solutes in (B); 1, carbonic anhydrase; 2, myoglobin; 3, β-lactoglobulin B; 4, β-lactoglobulin A; 5, α-lactalbumin; 6, trypsin inhibitor.*

A quick counting of the peaks in Fig. 10A and B including the short and tall peaks as well as the shoulders and assuming that each peak and shoulder correspond to a peptide fragment one can safely say that RP-CEC with an ODM column using isocratic elution is very suitable for peptide mapping. This quality of separation is only reached by the lengthy gradient elution in reversed phase HPLC.

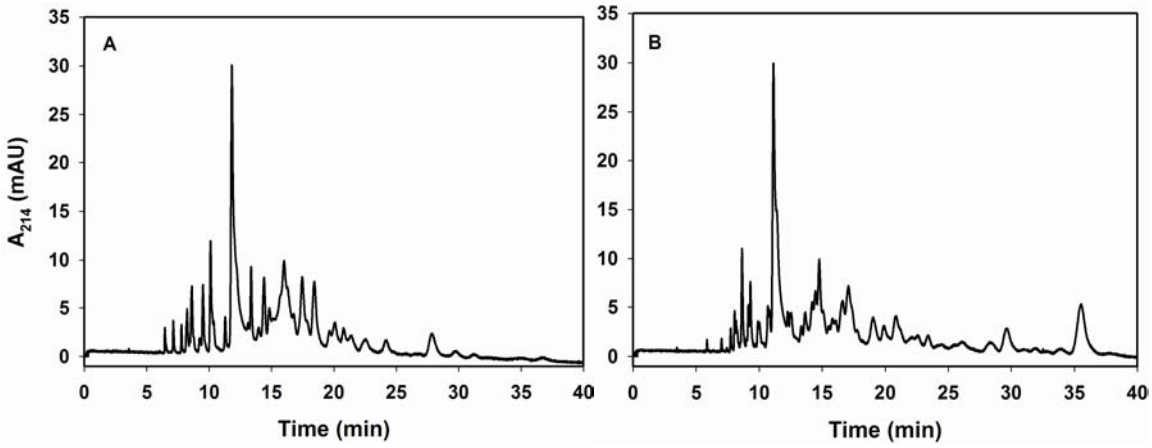

Figure 10. *Electrochromatograms of the tryptic digest of cytochrome C (A) and lysozyme (B). ODM capillary column, 30 cm effective length, 37 cm total length × 100 μm ID; hydro-organic mobile phase, 30 % v/v ACN, 20 mM sodium phosphate, pH 6; voltage, 10 kV; electrokinetic injection, 5 kV, 3s.*

Conclusions

The neutral ODM column offered many useful features for performing RP-CEC separations of a wide range of species of varying polarity. Through ions adsorption to its surface from the mobile phase, the ODM monolith allowed the adjustment of EOF velocity and the modulation of solute retention and separation selectivity. These useful characteristics facilitated the rapid and efficient separation of various species including complex tryptic protein digests by isocratic elution, which would require lengthy gradient elution in HPLC. Furthermore, the superimposition of the electrophoretic mobility on the chromatographic partitioning has made isocratic elution suitable for tryptic peptide mapping of proteins in RP-CEC using the ODM column.

References

1. Eeltink, S., Kok, W. T., *Electrophoresis* **2006**, *27*, 84-96.
2. Eeltink, S., Svec, F., *Electrophoresis* **2007**, *28*, 137-147.
3. Smith, N. W., Jiang, Z., *J. Chromatogr. A* **2008**, *1184*, 416-440.
4. Wu, R., Hu, L., Wang, F., Ye, M., Zou, H., *J. Chromatogr. A* **2008**, *1184*, 369-392.
5. Zhu, G., Zhang, L., Yuan, H., Zhang, W., Zhang, Y., *J. Sep. Sci.* **2007**, *30*, 792-803.
6. Huo, Y., Kok, W. T., *Electrophoresis* **2008**, *29*, 80-93.
7. Okanda, F., El Rassi, Z., *Electrophoresis* **2005**, *26*, 1988-1995.
8. Bedair, M., El Rassi, Z., *J. Chromatogr. A* **2005**, *1079*, 236-245.
9. Zhang, M., El Rassi, Z., *J. Proteome Res.* **2006**, *5*, 2001-2008.
10. Li, Y., Xiang, R., Horváth, C., Wilkins, J. A., *Electrophoresis* **2004**, *25*, 545-553.
11. Zhang, L., Ping, G., Zhang, L., Zhang, W., Zhang, Y., *J. Sep. Sci.* **2003**, *26*, 331-336.
12. Bedair, M., El Rassi, Z., *Electrophopresis* **2002**, *23*, 2938-2948.
13. Bedair, M., El Rassi, Z., *J. Chromatogr. A* **2003**, *1013*, 35-45.
14. Bedair, M., El Rassi, Z., *J. Chromatogr. A* **2003**, *1013*, 47-56.
15. Palm, A., Novotny, M. V., *Anal. Chem.* **1997**, *69*, 4499-4507.
16. Peters, E. C., Lewandowski, K., Petro, M., Svec, F., Frechet, J. M. J., *Anal. Commun.* **1998**, *35*, 83-86.
17. Allen, D., El Rassi, Z., *Analyst* **2003**, *128*, 1249-1256.

CHAPTER III

A NOVEL, NEUTRAL OCTADECYL ACRYLATE MONOLITH WITH FAST ELECTROOSMOTIC FLOW VELOCITY AND ITS APPLICATION TO THE SEPARATION OF VARIOUS SOLUTES INCLUDING PEPTIDES AND PROTEINS IN THE ABSENCE OF ELECTROSTATIC INTERACTIONS

Introduction

In CEC, the stationary phase has two major roles: (i) to provide the desired EOF for mass transport across the column and (ii) to offer sites for chromatographic retention. In order to provide an adequate EOF, moieties with fixed charges are usually incorporated into the monolith. These charged functionalities however, have been known to interact with the charged functionalities in bio-molecules causing band broadening, irreproducible retention times and very often irreversible adsorption of the analytes onto the surface of the monolith. This has limited the potential of CEC in the separation of proteins [1].

** The content of this chapter has been accepted for publication in Electrophoresis.*

In an attempt to reduce electrostatic interactions, a neutral monolith was introduced by Zhang *et al*. [2]. This neutral monolith was made by the copolymerization of butyl methacrylate and ethylene dimethacrylate (EDMA). However, this monolith did not exhibit sufficient EOF, and consequently the separation of acidic components was achieved through their differential electromigration. A second attempt to prepare neutral monoliths was made where the inner wall of a fused silica capillary was grafted with a positively charged polymer for annular generation of EOF. This monolith was made by the *in situ* copolymerization of vinyl benzyl chloride and EDMA in a binary porogenic solvent consisting of 1-propanol and formamide. Finally, the unreacted benzyl chloride groups were hydrolyzed to benzyl alcohol [3]. This monolith separated a mixture of small peptides at pH 2.5, to avoid solute-wall interactions [3]. Another strategy to reduce electrostatic interaction that involved the use of shielded stationary phases containing 2-acrylamido-2-methylpropanesulfonic acid at the monolith surface covered by a top layer of poly(butyl methacrylate) was introduced by Hilder *et al.* [4]. Although the shielding may reduce some weak electrostatic interactions, the electric field of some ions may still have access to the oppositely charged groups on the monolithic surface.

Although the above approaches have alleviated the problems associated with electrostatic interaction, they did not provide monolithic columns that can yield efficient protein separations in CEC. In 2005 and more recently, our laboratory has introduced neutral RP-CEC stationary phases that have been successfully applied to the separation of both neutral and charged solutes [5-7]. These stationary phases, though neutral, afforded adequate EOF that allowed the separation of charged solutes including peptides and proteins at neutral pH in the absence of electrostatic interactions. The EOF resulted from

the adsorption of mobile phase ions to the polar ester sites of the monolith thus imparting the neutral monoliths with the desired zeta potential to generate the EOF [5-7].

In this study, we are introducing an efficient way to enhance the EOF, and modulate selectivity and retention of a previously described neutral octadecyl monolith (ODM) by the proper choice of the crosslinker. Whereas, the previous monolith was prepared using octadecyl acrylate (ODA) as the functional monomer and trimethylolpropane trimethacrylate (TRIM) as the crosslinker [5] (see Chapter II) the present monolith was prepared from the same functional monomer (ODA) using pentaerythritol triacrylate (PETA) as the crosslinker. The use of PETA as a crosslinker has been reported by other authors for the preparation of (i) a methacrylate-based monolithic column with mixed mode hydrophilic/strong cation exchange stationary phase [8] and (ii) a neutral methacrylate-based monolithic column for hydrophilic interaction in pressurized CEC [9]. The presence of a polar OH functional group in PETA offers an additional site for mobile phase ions to bind onto the surface of the monolith increasing its zeta potential (ζ) and consequently the EOF velocity. As will be shown in this report, the resulting octadecyl monolith (referred to as ODM-OH) afforded higher EOF and average plate counts that were more than twice those afforded by the previous neutral ODM. The application of the neutral monolith to the separation of neutral (nonpolar and polar) and charged species such as peptides and proteins is described.

Experimental

Instrumentation

A P/ACE 5010 CE system from Beckman (Fullerton, CA, USA) equipped with a fixed wavelength UV detector was used in this investigation. All electrochromatograms were recorded with a PC running a Gold P/ACE system.

Reagents and materials

Pentaerythritol triacrylate (PETA), trimethylolpropane trimethacrylate (TRIM), octadecyl acrylate (ODA), 2,2' azobis(isobutyronitrile) (AIBN), alkylbenzenes (AB), alkyl phenyl ketones (APK), polycyclic aromatic hydrocarbons (PAH), anilines, phenols and analytical-grade acetone were from Aldrich (Milwaukee, WI, USA). Cyclohexanol was purchased from J.T. Baker (Phillipsburg, NJ, USA). Ethylene glycol (EG) and HPLC-grade acetonitrile (ACN) were from Fischer Scientific (Fair Lawn, NJ, USA). 1-Naphthol was from Eastman Kodak (Rochester, NY, USA). Egg white lysozyme, horse heart cytochrome C, bovine erythrocytes carbonic anhydrase, bovine milk β-lactoglobulin A and B and bovine milk α-lactalbumin, peptides and trypsin TPCK from bovine pancreas were purchased from Sigma (St. Louis, MO, USA). Tryptic protein digestion (e.g., chicken white lysozyme) was performed after protein reduction and alkylation using the Promega protocol. Buffer solutions were prepared using monobasic sodium phosphate from Mallinckrodt (Paris, KY, USA). Fused-silica capillaries with an internal diameter (id) of 100 µm were from Polymicro Technologies (Phoenix, AZ, USA).

Column pretreatment

The inner wall of the fused-silica capillary was treated with 1.0 M sodium hydroxide for 30 min, flushed with 0.10 M hydrochloric acid for 30 min, and then rinsed with water for 30 min. The capillary inner wall was then allowed to react with a solution of 50% v/v of 3-(trimethoxysilyl)propyl methacrylate in acetone for 6 h at room temperature to vinylize the inner walls of the capillary. Finally, the capillary was rinsed with acetone and water and then dried in a stream of nitrogen.

In situ polymerization

For the ODM-OH, polymerization solutions weighing 1.02 g were prepared from 7.6 wt% (0.24 mmol) octadecyl acrylate (ODA) as the monomer, 7.0 wt% (0.24 mmol) PETA as the crosslinker and porogenic solvents cyclohexanol 59.1 wt%, ethylene glycol 22.8 wt% and 3.5 wt% water. AIBN (1.0 wt% with respect to monomers) was added to the solution. The polymerization solution was then sonicated for ~20 min to obtain a clear solution. For the ODM, polymerization solutions weighing 1.03 g were prepared from 7.5 wt% (0.24 mmol) octadecyl acrylate (ODA) as the monomer, 7.9 wt% (0.24 mmol) TRIM as the crosslinker and porogenic solvents cyclohexanol 58.5 wt%, ethylene glycol 22.6 wt% and 3.5 wt% water. AIBN (1.0 wt% with respect to monomers) was added to the solution. The sonicating water bath temperature reached ~45 ˚C after ~20 min thus facilitating the dissolution of the ODA and TRIM/PETA in the porogenic solvent. A 30cm pretreated capillary was filled with the polymerization solution up to 21 cm by immersing the inlet of the capillary in the solution vial and applying vacuum to the outlet to prepare a final column of 21 cm. The capillary ends were then sealed using a

GC septum and the capillary submerged in a 60 °C water bath for 12 h. The resulting monolithic columns were rinsed with a 80:20 v/v acetonitrile:water mixture using a HPLC pump. A detection window was created at 1-2 mm after the end of the polymer bed using a thermal wire stripper. Finally, the column was cut to a total length of 27 cm with an effective length of 20 cm.

In this study, the composition of monomers used for preparing the ODM were chosen to be the same as the optimal composition of monomers used to prepare the ODM-OH in order to provide a direct comparison between ODM and ODM-OH. The ODM prepared in this study is different from the one reported earlier [5] (see Chapter II) in the sense that the composition of monomers is not the one that gives the monolith with the best CEC performance since it is not possible to prepare an ODM-OH that would have good permeability in pressure driven flow with the same composition of monomers as for the optimal ODM reported earlier [5] (see Chapter II).

CEC procedures

Before running the monolithic column on the instrument each day, it was equilibrated with the running buffer using a syringe pump for 30 min. Thereafter, the column was placed in the CEC instrument and equilibrated with the mobile phase by applying a stepwise increase in voltage up to 25 kV. The column was further equilibrated at the running voltage until a stable current and baseline were observed. Separations were performed at 25 °C at several voltages as stated in the figure captions. Mobile phases were prepared by adjusting the pH of the aqueous before the ACN was added and degassed by sonicating for 40 min. Stock solutions were prepared in ACN except for

peptides and proteins that were prepared in water and thereafter diluted with the running buffer. The samples were injected electrokinetically at various applied voltages as stated in the figure captions.

Results and discussion

EOF and electrochromatographic characterization

Effect of nature and concentration of crosslinker on EOF and retention. In order to understand the effect of PETA (see structure **I**) on the EOF, thiourea the EOF marker was injected at 75% ACN, 1 mM sodium phosphate monobasic, pH 7 at 10 kV on the ODM and on ODM-OH. On the ODM, the EOF was 0.81 mm/s whereas for the ODM-OH, the EOF was 1.09 mm/s. This represents a ~35% increase in EOF velocity under otherwise the same electrochromatographic conditions on changing the crosslinker from TRIM (see structure **II**) to PETA at the same monomer (ODA) concentration and same porogenic solvent composition. For a mixture of 8 ABs using the same electrochromatographic conditions above, the analysis time on ODM was 18 min whereas the analysis time on ODM-OH was 9 min, which represents a 50% reduction of analysis time. The fact that the PETA structure contains an OH functional group that is not on TRIM increases the number of available sites to which the electrolyte ions can adsorb onto the surface of the neutral monolith thus increasing the ζ and consequently the EOF. As a consequence, retention time also decreases.

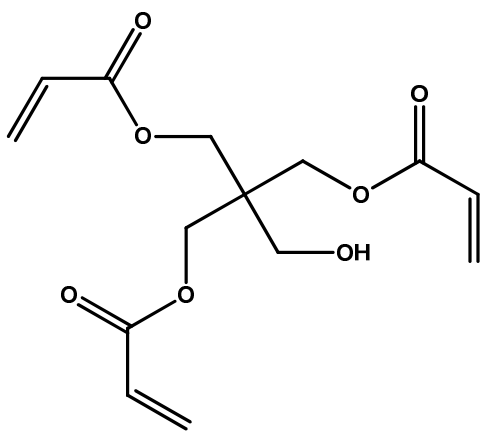

PETA **(I)**

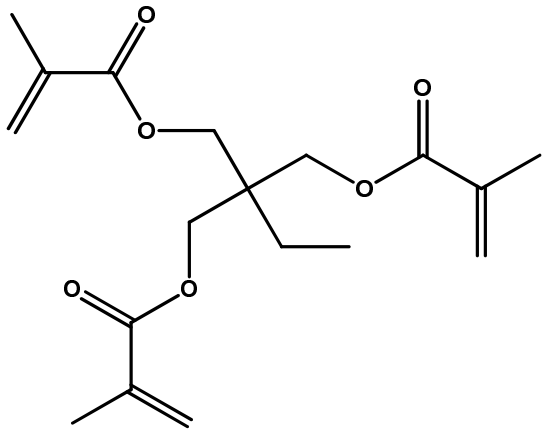

TRIM **(II)**

The retention factors k' of the 8 ABs obtained on the two monoliths ODM and ODM-OH, prepared using the same proportion of functional monomer and crosslinker, revealed that the values are higher on the former than on the latter monolith. The k' values were 0.34, 0.46, 0.58, 0.84, 1.15, 1.58, 2.25 and 3.33 for benzene, toluene, ethylbenzene, propylbenzene, butylbenzene, pentylbenzene, hexylbenzene and heptylbenzene, respectively, on the ODM column as opposed to the k' values of 0.22, 0.31, 0.39, 0.54, 0.76, 1.06, 1.49 and 2.13 for the same solutes on the ODM-OH column. The k' values on ODM are at least one and a half times higher than on the ODM-OH. The differences in retention can be attributed to a higher ligand density on the ODM surface, prepared by *in situ* polymerization of ODA and TRIM as compared to ODM-OH, which is prepared by *in situ* polymerization of ODA and PETA. In other words, the reactivity ratio of ODA with TRIM is higher than that with PETA. Also, the presence of OH in the crosslinker will impart a more polar character to the monolith surface of the ODM-OH. However, in terms of separation efficiency the ODM-OH offered on average ~17 fold higher plate counts (354,000 plates/m) than ODM (21,000 plates/m). Thus,

despite its lower retentivity, the ODM-OH should be beneficial for rapid separation at higher resolution.

It should be mentioned that when the ODM-OH was prepared using the same monomer proportion as the optimal ODM [5] (see Chapter II), the resulting monolith did not give any noticeable pressure driven flow. The ODM column prepared using the optimal monomer composition and reported earlier [5] (see Chapter II) exhibited k' values of 0.60, 0.76, 0.94, 1.23, 1.64, 2.17, 2.92 and 3.96 for benzene, toluene, ethylbenzene, propylbenzene, butylbenzene, pentylbenzene, hexylbenzene and heptylbenzene, respectively. These k' values are at least two times higher than those obtained on the optimal ODM-OH. On the other hand, the separation efficiency obtained on the optimal ODM column was half that obtained on the optimal ODM-OH column (172,000 plates/m compared to 354,000 plates/m) under otherwise the same CEC conditions.

In another investigation, the amount of octadecyl acrylate monomer (i.e., the ligand provider) and cross-linking monomer (PETA) were varied while maintaining the total ligand and crosslinker amount to be 0.48 mmol. The effect of this variation on the EOF and the average theoretical plate count for a mixture of 8 ABs homologous series was studied and represented in a plot of EOF and average theoretical plate count ($N_{Av/m}$) versus the amount (mmol) of the crosslinker in Fig. 1A and 1B, respectively. As can be seen in Fig. 1A, when the amount of crosslinker was increased from 0.12 mmol to 0.18 mmol (i.e., from 0.25 to 0.375 mole fraction), the EOF decreased from 1.32 to 1.06 mm/s. A further increase of the crosslinker amount to 0.24 mmol (i.e., to 0.5 mole fraction) increased the EOF slightly to 1.09 mm/s which translates to a ~3% increase in

EOF. When the crosslinker weight was further increased to 0.30 mmol (i.e., 0.625 mole fraction) the EOF velocity dropped from 1.09 to 0.81 mm/s, which translates to ~35% decrease in EOF. The general trend discussed above shows a decrease in EOF velocity as the amount of crosslinker is increased the amount of ligand is decreased. Increasing the amount of crosslinker in the polymerization solution decreases the average pore size of the final monolith as a result of an early formation of highly cross-linked globules with a reduced tendency to coalesce [10-14].

The effect of varying the amount of crosslinker on the average plate count for a mixture of an 8 AB homologous series is represented in the form of a plot of $N_{av/m}$ against the amount of the crosslinker (mmol) in Fig. 1B. When the amount of crosslinker was increased from 0.12 mmol to 0.18 mmol (or from 0.25 to 0.375 in mole fraction), the $N_{av/m}$ increased from 265,000 to 320,000 plates/m. A further increase in the crosslinker amount to 0.24 mmol (or 0.5 mole fraction) increased the $N_{av/m}$ to 350,000 plates/m, which translates to a ~9% increase in $N_{av/m}$. When the crosslinker amount was further increased to 0.30 mmol (or 0.625 mole fraction), the $N_{av/m}$ dropped from 350,000 plates/m to 170,000 plates/m, which translates to a decrease in $N_{av/m}$ by more than half. In order to obtain a monolithic column with a low flow resistance and a large surface area, the monolith should contain both flow-through pores and mesopores. Monoliths made from 0.18 and 0.24 mmol of PETA offered theoretical plate counts of 320,000 and 350,000 plates/m, respectively. These two monoliths additionally had reasonable flow indicating that at these two PETA compositions, a good compromise between flow and efficiency had been achieved.

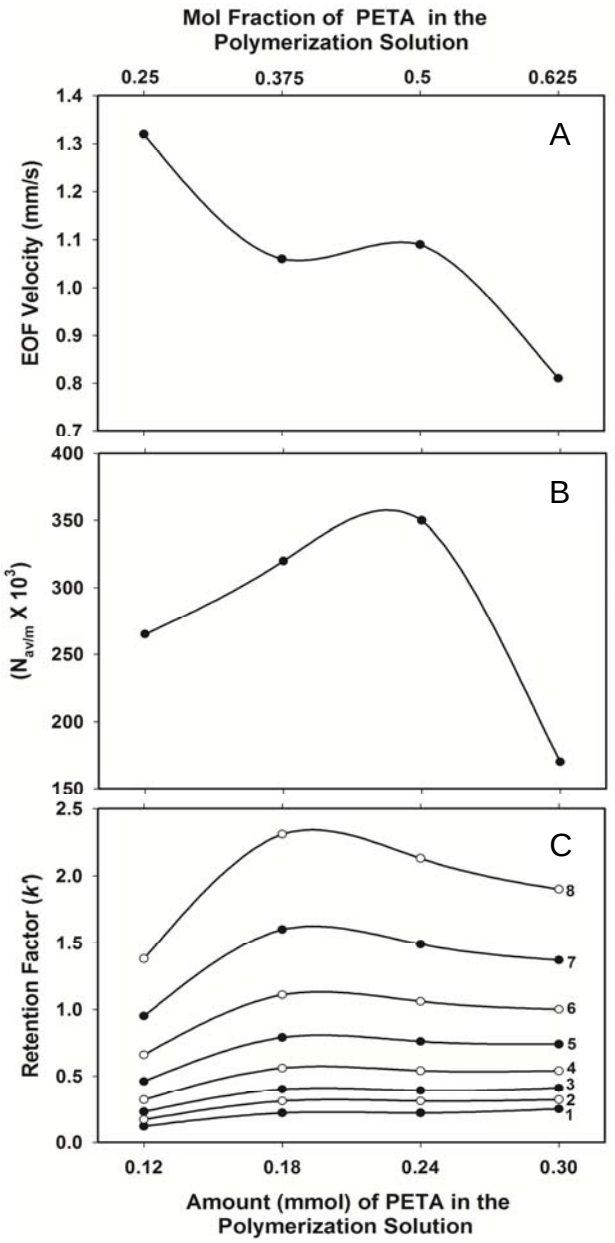

Figure 1. *Effect of amount of PETA (mmol) in the polymerization solution on the EOF velocity (A), the average plate number per meter (B) and k' (C). ODM-OH capillary column, 20 cm effective length, 27 cm total length × 100 μm ID; mobile phase, 1 mM sodium phosphate, pH 7.0, at 75% v/v ACN; running voltages 10 kV; EOF tracer, uracil; electrokinetic injection for 3 s at 5 kV. Solutes: 1, benzene; 2, toluene; 3, ethylbenzene; 4, propylbenzene; 5, butylbenzene 6, pentylbenzene; 7, hexylbenzene; 8, heptylbenzene.*

Additionally, the effect of varying the amount of crosslinker on the retention factor (k') for a mixture of an 8 AB homologous series is represented in the form of a plot of k' against the amount of crosslinker (mmol) in Fig. 1C. The general trend that can be observed in Fig. 1C is that for the combination of 0.18 mmol ODA and 0.30 mmol PETA, the ODM-OH exhibits the highest surface octadecyl ligand density as manifested by the maximum in k' values. On the other hand, it is also apparent from the plot that a monolith column made from a 1:3 ODA:PETA ratio (0.12 mmol crosslinker PETA:0.36 mmol ODA) has the least retention and selectivity for the 8 ABs. Since this monolith has three times more of the monomer than the crosslinker, the surface does not contain a good surface coverage for hydrophobic chromatographic partitioning due to a lack of crosslinked polymer chains. At the other end, with the ratio of ODA:PETA at 0.18 mmol:0.30 mmol, the resulting ODM-OH monolith is highly corsslinked, a fact that may be responsible for the significant decrease in efficiency, most likely due to the generation of narrow pores that would give rise to strong mass transfer resistance in and out of the small pores.

The above results showed that a monolith made from a 0.18 mmol or 0.24 mmol of PETA had a morphology structure that is more balanced between sufficient flow-through pores and mesopores. This yielded monoliths that represented good compromise for satisfactory permeability in pressure driven flow and an acceptable EOF velocity as well as optimal retention and column efficiency. These two monoliths were considered for further study with the monolith made from 0.18 mmol of PETA being used in the analysis of charged solutes such as peptides and proteins as will be discussed in a later section of this chapter.

Plate height against flow velocity–van Deemter plot. The optimal ODM-OH column in terms of separation efficiency (i.e., obtained using 0.24 mmol of PETA) was further evaluated for its CEC separation efficiency over a wide range of flow velocities using 75% v/v ACN in the mobile phase. The results are shown in Fig. 2A by the so-called van Deemter plot using 8 ABs as the model solutes. The EOF velocity was increased by increasing the operating voltage from 8 to 25 kV. As can be seen in Fig. 2A, H_{min} is obtained at an optimal EOF velocity in the range 1.09 – 1.36 mm/s. Even if the flow velocity is increased to 1.73 mm/s, the loss in separation efficiency is ~ 21 % but with a shortening in the analysis time by about 60% with respect to the analysis time at 1.09 mm/s (5.8 min versus 9.6 min). Figures 2B and 2C show typical electrochromatograms of ABs and APKs respectively, at the optimal EOF velocity of 1.09 mm/s. Under the same mobile phase composition and applied voltage, the APKs eluted much faster than the ABs (by a factor of 1.9) due to the fact that they are less hydrophobic solutes than the ABs.

Reproducibility of column fabrication. The reproducibility of column preparation was assessed through the percent relative standard deviation (% RSD) for the EOF velocity, solute retention and separation efficiency using a homologous series of ABs as model solutes. Typically, the observed % RSD for the monolith made from 0.24 mmol PETA from batch to batch (n = 3) was 5%, 9% and 12% for the retention factor, k' for toluene, EOF velocity and average separation efficiency, respectively. These reproducibility data are in close agreement with those recently reported in the literature [5, 6, 15].

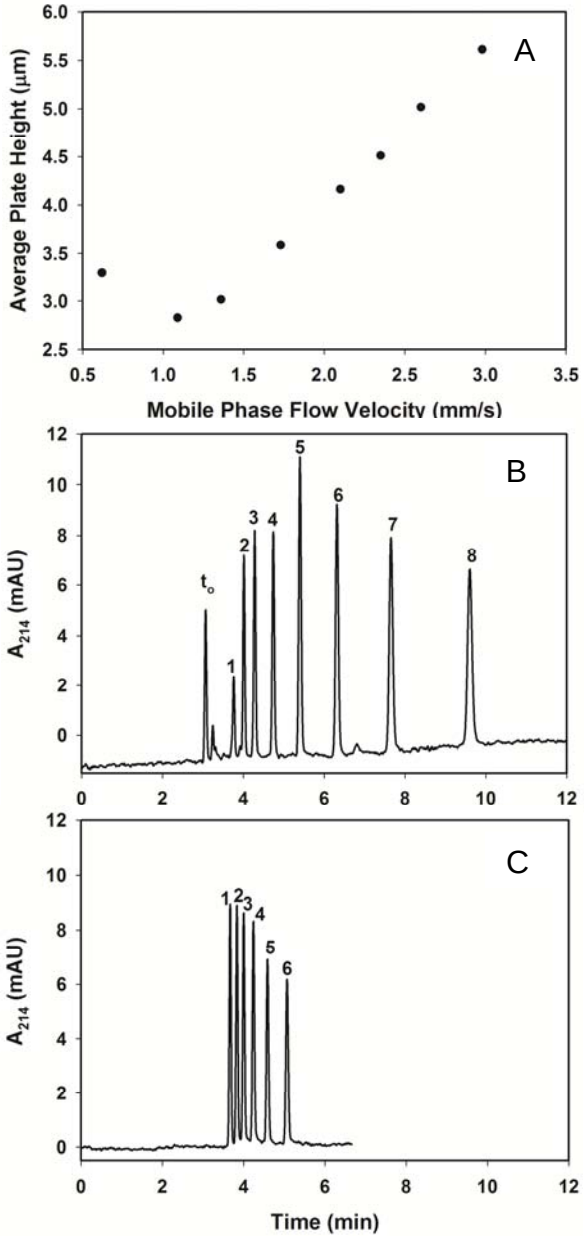

Figure 2. *van Deemter plot showing average plate height as a function of EOF velocity (A) and electrochromatograms of AB (B) and APK (C) homologous series. ODM-OH capillary column, 20 cm effective length, 27 cm total length × 100 μm ID. Conditions as in Figure 1 except various running voltages in (A).*

Evaluation of chromatographic retention

Nonpolar solutes: polycyclic aromatic hydrocarbons (PAHs). A mixture of 11 selected PAHs with different polarities was electrochromatographed on the ODM-OH using 70% ACN and 5 mM sodium phosphate monobasic, at pH 7. As shown in Fig. 3, the neutral monolith was able to separate all the 11 PAHs in 8 min affording a theoretical plate count of 250,000 plates/m. For the migration time window of 2-8 min of the electrochromatogram in Fig. 3, the peak capacity is ~70. This peak capacity corresponds to ~14 peaks/min with a unit resolution. This value demonstrates the high resolving power of this monolithic column.

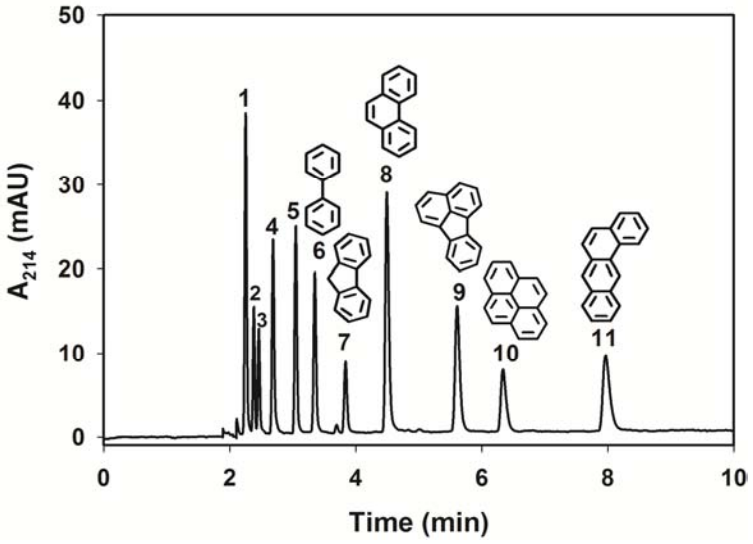

Figure 3. *Electrochromatograms of some selected PAHs. ODM-OH capillary column, 20 cm effective length, 27 cm total length × 100 μm ID; mobile phase, 5 mM sodium phosphate, pH 7.0, using 70% v/v ACN; running voltage, 20 kV; electrokinetic injection for 3s at 10 kV. Solutes: 1, 1-naphthol; 2, benzene; 3, 1-cyanonaphthalene; 4, 1-nitronaphthalene; 5, naphthalene; 6, biphenyl; 7, fluorene; 8, phenanthrene; 9, fluoranthene; 10, pyrene; 11, benz[a]anthracene.*

Considering 1-naphthol, 1-cyanonaphthalene, 1-nitronaphthalene with –OH, -CN, $-NO_2$ substituents respectively, the solutes are eluted according to the increasing hydrophobicity of the substituent, i.e. OH<CN<NO_2. The other 7 solutes namely; naphthalene, biphenyl, fluorene, phenanthrene, fluoranthene, pyrene and benz[a]anthracene are eluted with k' values of 0.61, 0.81, 1.08, 1.43, 2.03, 2.42 and 3.30, respectively, which is consistent with the increasing nonpolar character of the solute.

Slightly polar solutes. The usefulness of the neutral ODM-OH monolith was further evaluated in separating a class of slightly polar basic solutes, the anilines. A mixture of six anilines with different substituents was electrochromatographed on this neutral monolith at pH 7.0. The order of elution of the aniline mixture was *m*-methylaniline, *p*-nitroaniline, aniline, 4-methoxy-2-nitroaniline, 4-methyl-2-nitroaniline and 3,4-dichloroaniline and the six basic solutes were baseline separated in about 11 min affording a theoretical plate count of 250,000 plates per meter (see Fig. 4A). Generally, the order of elution was consistent with increasing hydrophobicity of the solute and is typical for RP-CEC where halogenated anilines are more retained than methyl substituted anilines. The effect of a polar $–NO_2$ group on *p*-nitroaniline made it elute before aniline, which has a more exposed non-polar aromatic ring in contact with the hydrophobic alkyl chain ligand of the stationary phase. Additionally, the effect of a polar $–OCH_3$ group on 4-methoxy-2-nitroaniline caused it to elute before 4-methyl-2-nitroaniline with a non-polar $–CH_3$ group.

To evaluate the retention property of the ODM-OH monolith with another class of slightly polar solutes, 8 phenols were electrochromatographed under the same

electrochromatographic conditions. These phenols with a $pK_a \geq 8.5$ are largely undissociated and can be considered neutral at pH 7.0. As shown in Fig. 4B, the phenol derivatives investigated were retained in order of decreasing polarity. For instance phenol and hydroxyphenols (i.e., hydroquinone < resorcinol < catechol < phenol) are less retained than 3,4-dimethylphenol, which is less retained than 2-chlorophenol. The last two solutes 1-naphthol and 2-naphthol with two aromatic rings are slower to elute than the phenols with a single aromatic ring as a result of increased hydrophobic contact area with the non-polar alkyl ligands of the ODM-OH.

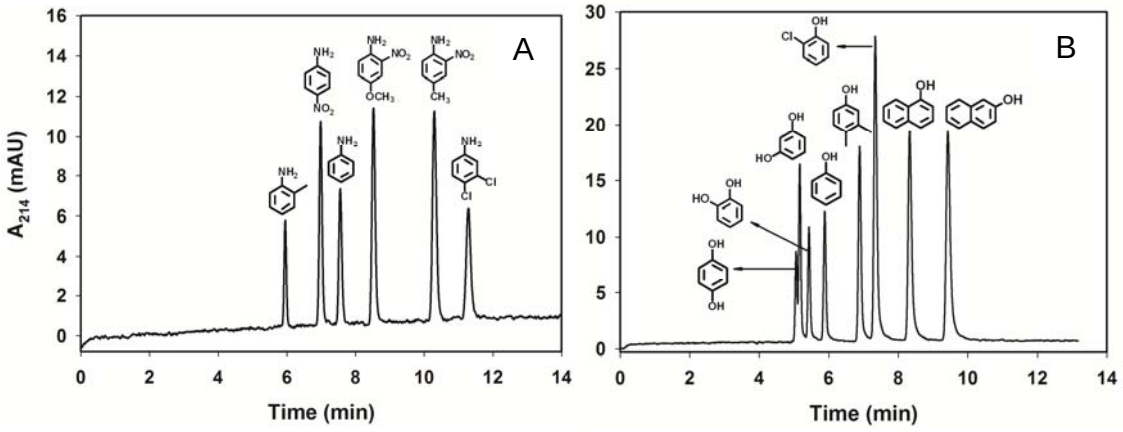

Figure 4. *Electrochromatograms of some selected aniline (A) and phenol (B) derivatives. ODM-OH capillary column, 20 cm effective length, 27 cm total length × 100 μm ID; mobile phase, 10 mM sodium phosphate, pH 7.0, at 45% v/v ACN; running voltage, 10 kV; electrokinetic injection for 3 s at 5 kV. Solutes are as shown on the electrochromatograms.*

CEC of charged solutes: peptides and proteins. Two ODM-OH columns prepared from 0.18 and 0.24 mmol PETA were evaluated in the separation of polyionic solutes such as peptides and proteins. Figure 5 shows the simultaneous separation of 6 peptides, namely Ala-Phe, Gly-Trp, Gly-Phe, Gly-Gly-Leu, Gly-Gly-Ala, and Phe-Pro on these two neutral ODM-OH columns. Although at pH 6.0 these peptides with pI values of ~6.0 are believed to be nearly neutral in aqueous media, an interplay between the electrophoretic mobility and chromatographic partitioning control the migration of these peptides since the mobile phase is a hydro-organic medium which may cause shift in the dissociation of the peptides. While it took the 6 peptides 21 min to elute on the column made from 0.24 mmol of PETA, it took only6.2 min for the same elution to be completed on a column made from 0.18 mmol of PETA.

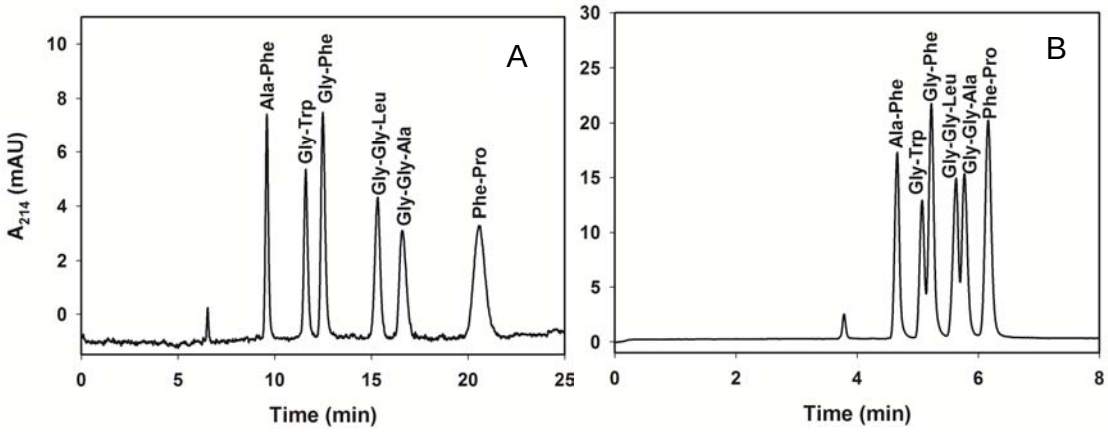

Figure 5. *Electrochromatograms of some standard peptides on columns made from 0.24 mmol PETA in (A) and 0.18 mmol in (B). ODM-OH capillary column, 20 cm effective length, 27 cm total length × 100 µm ID; hydro-organic mobile phase, 45% v/v ACN, 10 mM sodium phosphate monobasic, pH 6.0; voltage, 12 kV, electrokinetic injection, 10 kV for 3 s.*

In another experiment and using 50% ACN, 10 mM phosphate, pH 7.0 and 12 kV, a mixture of six standard proteins was separated on ODM-OH columns containing 0.24 and 0.18 mmol of PETA as shown in Fig. 6A and Fig. 6B, respectively. The six proteins

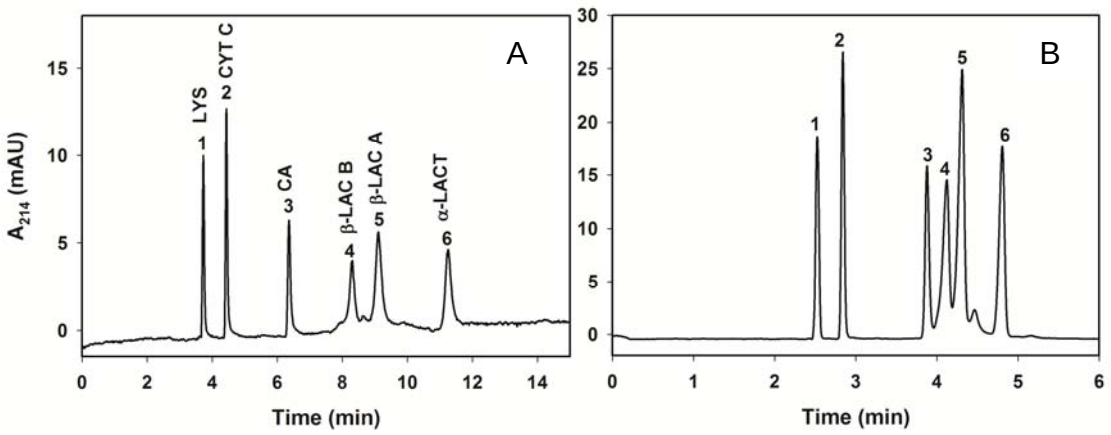

Figure 6. *Electrochromatograms of some standard proteins on columns made from 0.24 mmol PETA in (A) and 0.18 mmol in (B). ODM-OH capillary column, 20 cm effective length, 27 cm total length × 100 µm ID; hydro-organic mobile phase, 50% v/v ACN, 10 mM sodium phosphate monobasic, pH 7.0; Voltage, 12 kV, electrokinetic injection, 10 kV for 3 s. Solutes; 1, lysozyme; 2, cytochrome C; 3, carbonic anhydrase; 4, β-lactoglobulin B; 5, β-lactoglobulin A; 6, α-lactalbumin.*

in the mixture were lysozyme (pI = 11.1), cytochrome C (pI = 10.2), carbonic anydrase (pI = 6.2), β-lactoglobulin B (pI = 5.2), β-lactoglobulin A (pI = 5.1) and α-lactalbumin (pI = 4.2-4.5). The six proteins migrated in the order listed above which is in accordance to their decreasing pI values with the most acidic protein, α-lactalbumin eluting last while the most basic protein, lysozyme eluted first. On the monolithic column made from 0.18 mmol of PETA, the six proteins eluted in less than 5 min with an average theoretical

plate count of 207,000 plates per meter, while on the monolithic column made from 0.24 mmol of PETA, the six proteins were eluted in 11.5 min with an average theoretical plate count of 201,000 plates per meter. The EOF was 1.31 and 1.00 mm/s on the column made of 0.18 and 0.24 mmol of PETA, respectively. Although there was little difference in terms of the separation efficiency between the two monolithic columns, a significant difference was recorded in terms of the elution time where the column made of 0.18 mmol of PETA completed the separation analysis in a time that is less than half (compare 11.5 min to 5 min) the time taken to complete the same analysis for a column made of 0.24 mmol.

Having found that the column could successfully separate a mixture of simple peptides, the ODM-OH column was challenged with a complex peptide mixture originating from a tryptic digest of chicken egg white lysozyme. Figure 7 shows the electrochromatogram obtained from a lysozyme tryptic map under the same electrochromatographic conditions as in Fig. 5 on columns prepared from 0.18 and 0.24 mmol of PETA. The separation was completed in 35 and 12 min on columns made from 0.24 and 0.18 mmol, respectively. Despite the longer analysis time for the monolith with 0.24 mmol PETA, this monolith provided better separation for early eluting peptide fragments, see insert in Fig. 7A. By considering the chromatogram shown in Fig. 7, one can safely conclude that RP-CEC with this ODM-OH column using isocratic elution is very applicable for peptide mapping. This quality of separation is only reached by the lengthy gradient elution in reversed phase HPLC.

The separation experiments discussed above show that although the ODM-OH column made from 0.18 mmol of PETA had afforded a slightly lower theoretical plate

count on separating a mixture of ABs (see section3.2.1), it could still be applied to the separation of charged solutes successfully and in fact with shorter analysis times than an ODM-OH column made from 0.24 mmol of PETA.

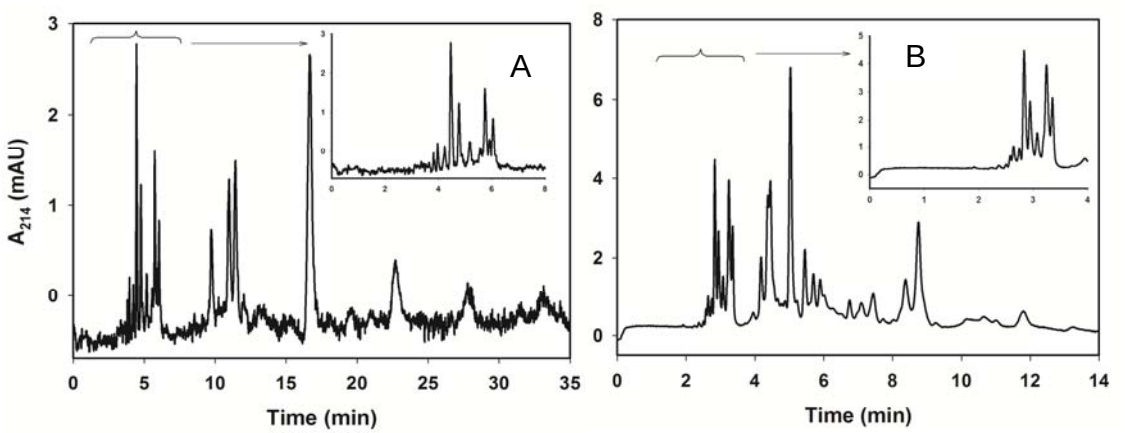

Figure 7. *Electrochromatograms of tryptic peptide map of chicken egg white lysozyme on columns made from 0.24 mmol of PETA in (A) and 0.18 mmol in (B). Other conditions as in Fig. 5.*

Conclusions

This investigation has demonstrated how the EOF of a neutral monolith can be enhanced by the choice of monomer and in this case the crosslinker. The neutral ODM-OH column offered many useful features for performing RP-CEC separations of a wide range of species of varying polarity. Through ions adsorption to its surface from the mobile phase, the ODM-OH monolith allowed the adjustment of EOF velocity as well as the modulation of solute retention and separation selectivity. These useful characteristics facilitated the rapid and efficient separation of various species including a complex tryptic protein digest by isocratic elution, which would otherwise require a lengthy gradient elution in HPLC.

References

1. El Rassi, Z., *Electrophoresis* ***2*****010**, *31*, 174-191.
2. Zhang, L., Ping, G., Zhang, L., Zhang, W., Zhang, Y., *J. Sep. Sci.* **2003**, *26*, 331-336.
3. Li, Y., Xiang, R., Horváth, C., Wilkins, J. A., *Electrophoresis* **2004**, *25*, 545-553.
4. Hilder, E. F., Svec, F., Fréchet, J. M. J., *Anal. Chem*. **2004**, *76*, 3887-3892.
5. Karenga, S., El Rassi, Z., *J. Sep. Sci.* **2008**, *31*, 2677-2685.
6. Karenga, S., El Rassi, Z., *Electrophoresis* **2010**, *31*, 991-1002.
7. Okanda, F., El Rassi, Z., *Electrophoresis* **2005**, *26*, 1988-1995.
8. Lin, J., Huang, G., Lin, X., Xie, Z., *Electrophoresis* **2008**, *29*, 4055-4065.
9. Wang, X., Lin, X., Xie, Z., Giesy, J. P., *J. Chromatogr. A* **2009**, *1216*, 4611-4617.
10. Li, Y., Tolley, H. D., Lee, M. L., *Anal. Chem.* **2009**, *81*, 4406-4413.
11. Urban, J., Jandera, P., *J. Sep. Sc.* **2008**, *31*, 2521-2540.
12. Viklund, C., Svec, F., Frechet, J. M. J., Irgum, K., *Chem. Mater.* **1996**, *8*, 744-750.
13. Vlakh, E. G., Tennikova, T. B., *J. Sep. Sci*. **2007**, *30*, 2801-2813.
14. Zhang, K., Yan, C., Yang, J., Zhang, Z., Wang, Q., Gao, R., *J. Sep. Sci.* **2005**, *28*, 217-224.
15. Bedair, M., El Rassi, Z., *Electrophopresis* **2002**, *23*, 2938-2948.

CHAPTER IV

NAPHTHYL METHACRYLATE-BASED MONOLITHIC COLUMN FOR REVERSED-PHASE CAPILLARY ELECTROCHROMATOGRAPHY *VIA* HYDROPHOBIC AND π INTERACTIONS

Introduction

Thus far, and with only a few exceptions, e.g., poly(styrene-co-divinylbenzene-co-methacrylic acid) monolith [1], most nonpolar polymer-based monolithic stationary phases developed for reversed-phase capillary electrochromatography (RP-CEC) have been those bearing n-alkyl chains on their surface. Typical examples are monoliths based on butyl methacrylate [2], hexyl methacrylate [3], octyl methacrylate [4], lauryl methacrylate [5], butyl-, hexyl- and lauryl-acrylate [6], stearyl-acrylate monolithic columns [7-9], and recently octadecyl acrylate [10] (see chapter II). Although these monolithic columns have proved useful in a number of RP-CEC separations (for recent reviews, see [11, 12]), the solution to many separation problems are still awaiting the introduction of novel nonpolar ligands that can afford the required selectivity.

The content of this chapter has been published in Electrophoresis, **2010, 31, 991-1002.*

The main approach to the fabrication of most of the above nonpolar monolithic stationary phases involved the intentional introduction of fixed charges to the monolith by the inclusion of small amounts of charged monomers to support a strong electroosmotic flow (EOF) that transports the mobile phase through the column [1, 2, 6-8, 13]. This represents a drawback as far as the application of these charged nonpolar monoliths (i.e., mixed-mode monoliths) to the separations of charged species are concerned, due to the strong electrostatic interactions between the charged analytes and the surface fixed charges on the monolith, causing band broadening and/or irreversible adsorption of analytes.

Recently, neutral nonpolar monoliths that are void of fixed charges were introduced and evaluated in our laboratories. The first neutral monolith was reported by Okanda and El Rassi [9] while another one was reported by Karenga and El Rassi [10] (see chapter II). The former neutral monolith was a stearyl (C17) acrylate based monolithic stationary phase, while the latter was an octadecyl acrylate based monolith (ODM). Although both these neutral monoliths were void of fixed charges, they exhibited sufficient EOF that allowed the rapid separation of a wide range of neutral and charged solutes including peptides and proteins in the absence of nuisance electrostatic interactions. The observed EOF was attributed to the adsorption of ions from the mobile phase to the surface of the C17 and ODM stationary phases.

In an effort to further develop the concept of neutral nonpolar monoliths for RP-CEC in the absence of surface fixed charges and to introduce other nonpolar ligands than the traditionally used alkyl chains, a reversed-phase monolith bearing surface naphthyl ligands is described and evaluated in this report. This novel neutral monolith was

prepared by *in situ* polymerization of naphthyl methacrylate monomer with Trimethylolpropane trimethacrylate crosslinker in the presence of an appropriate porogenic solvent. The resulting naphthyl methacrylate monolith (NMM) possesses 10 π-electrons per each naphthyl ligand, which can function as a π-electron donor vis-à-vis a π-electron deficient solute and vice versa, thus leading to a π-π interaction mechanism in addition to its nonpolar character. When this happens the π-electron donor acts a soft Lewis base while the π-electron acceptor acts as a soft Lewis acid [14], which can lead to a π-donor/π-acceptor complex whose stability is determined by the energy levels of the Highest Occupied Molecular Orbital (HOMO) and the Lowest Unoccupied Molecular Orbital (LUMO) of the donor and acceptor, respectively [15].

Prior to and after the advent of CEC, a variety of HPLC stationary phases containing various aromatic ligands have been reported. Typical recent silica bonded stationary phases bearing surface aromatic ligands include silica particles with surface bound phenyl [16], 3-[(pentabromobenzyl)oxy]propylsilyl [17], fluorenyl [15], naphthalimide [18] and anthracenyl groups [19]. Furthermore, a novel silica-based stationary phase having surface bound sulfonated naphthylamido ligands was recently introduced for CEC [20]. The sulfonic acid groups contributed to the generation of an EOF and constituted cation-exchanger sites. The sulfonated naphthylamido-silica exhibited a rather complex mixed mode retention mechanism involving hydrophobic, electrostatic and π-π interactions in the separation of barbiturates and benzodiazepines. The prediction of solute retention and optimum mobile phase composition on such mixed-mode columns are not usually very obvious.

The aim of this research project is to describe the preparation and characterization of a neutral naphthyl methacrylate monolithic (NMM) stationary phase for RP-CEC with moderate EOF possessing a retention mechanism based on both π-π and hydrophobic interactions. As will be shown, the NMM column offered improved separation of aromatic compounds such as polycyclic aromatic hydrocarbons (PAHs) and positional isomers that are hard to separate using conventional alkyl bonded stationary phases.

Experimental

Instrumentation

A P/ACE 5010 CE system from Beckman (Fullerton, CA, USA) equipped with a fixed wavelength UV detector and a P/ACE 5510 system, also from Beckman but equipped with a photodiode array detector, were used in this investigation. All electrochromatograms were recorded with a PC running a Gold P/ACE system. The samples were injected electrokinetically at various applied voltages as stated in the figure captions.

Reagents and materials

Trimethylolpropane trimethacrylate (TRIM), naphthyl methacrylate (NAPM), 1-dodecanol, 2,2' azobis(isobutyronitrile) (AIBN), 3-(trimethoxysilyl)propyl methacrylate, alkylbenzenes (ABs), alkyl phenyl ketones (APKs), polycyclic aromatic hydrocarbons (PAHs), anilines, and analytical-grade acetone were from Aldrich (Milwaukee, WI, USA). Cyclohexanol was purchased from J.T. Baker (Phillipsburg, NJ, USA). Ethylene glycol (EG), dodecanol, HPLC-grade methanol (MeOH) and acetonitrile (ACN) were from Fischer Scientific (Fair Lawn, NJ, USA). 1-Naphthol was from Eastman Kodak

(Rochester, NY, USA). Buffer solutions were prepared using monobasic sodium phosphate from Mallinckrodt (Paris, KY, USA). Fused-silica capillaries with an internal diameter (ID) of 100 µm were from Polymicro Technologies (Phoenix, AZ, USA).

Column pretreatment

The inner wall of the fused-silica capillary was treated with 1.0 M sodium hydroxide for 30 min, flushed with 0.10 M hydrochloric acid for 30 min, and then rinsed with water for 30 min. The capillary inner wall was then allowed to react with a solution of 50% v/v of 3-(trimethoxysilyl)propyl methacrylate in acetone for 6 h at room temperature to vinylize the inner wall of the capillary. Finally, the capillary was rinsed with acetone and water and then dried with a stream of nitrogen.

In situ polymerization

Polymerization solutions weighing 0.125 g each were prepared from 15% NAPM as the monomer, 15% TRIM as the crosslinker and porogenic solvents in the ratios of 30:70 w/w monomers/porogenic solvents. The mixtures of monomer and crosslinker were dissolved in a ternary porogenic solvent consisting of cyclohexanol and dodecanol in various ratios at constant 2.5% water. 2,2' azobis(isobutyronitrile) (1.0 wt% with respect to monomers) was added to the solution. The octadecyl monolithic (ODM) columns were fabricated using a previously described method [10] (see chapter II). In brief, polymerization solutions weighing 0.80 g each were prepared from 9.7% octadecyl acrylate (ODA) as the monomer, 20.5% TRIM as the crosslinker and porogenic solvents cyclohexanol 52.3%, ethylene glycol 15% and 2.5% water. AIBN (1.0 wt% with respect to monomers) was added to the solution. The polymerization solution was warmed in a

water bath at 40 °C for ~1 min to facilitate the dissolution of the NAPM/ODA and TRIM in the porogenic solvent. The polymerization solution was then purged with nitrogen for 10 min. A 32 cm pretreated capillary was filled with the polymerization solution up to 22 cm by immersing the inlet of the capillary into the solution vial and applying vacuum to the outlet to prepare a final column of 32 total length. The capillary ends were then sealed using a GC septum and the capillary submerged in a 60 °C water bath for 12 h. The resulting monolithic column was washed with an 80:20 v/v acetonitrile:water mixture using an HPLC pump. A detection window was created at 1-2 mm after the end of the polymer bed using a thermal wire stripper. Finally, the column was cut to a total length of 27 with an effective length of 20 cm.

Results and discussion

Column fabrication and electrochromatographic characterization

Porogens and monomers composition. Two porogens differing in nature and composition were examined in order to find the most suitable porogen for the preparation of the NMM monolith under investigation. First, a porogenic mixture composed of cyclohexanol (75.7 wt%), EG (20.7 wt%) and water (3.6 wt%) that was previously used successfully with other monoliths was tested in this study [10] (see chapter II). The monomer to crosslinker ratio was kept at 60:40. In another set of porogens, the EG macroporogen was replaced by the less polar macroporogen, dodecanol. The column performance (20 cm effective length, 27 cm total length x 100 µm ID) was evaluated with a test mixture consisting of six APKs using a mobile phase composed of 1 mM monobasic sodium phosphate monobasic, pH 7.0, at 55% v/v ACN and a running voltage of 15 kV. The column made in the presence of EG exhibited a higher permeability and

the solutes eluted in 39 min with an efficiency of 124,000 plates/m. On the other hand, the six APKs eluted in 46 min under the same conditions on the column made in the presence of dodecanol with an average separation efficiency of 142,000 plates/m. Since dodecanol yielded a monolith with higher separation efficiency than EG, it was concluded that dodecanol was a better macroporogen than EG and it was used in fabricating further columns throughout the study.

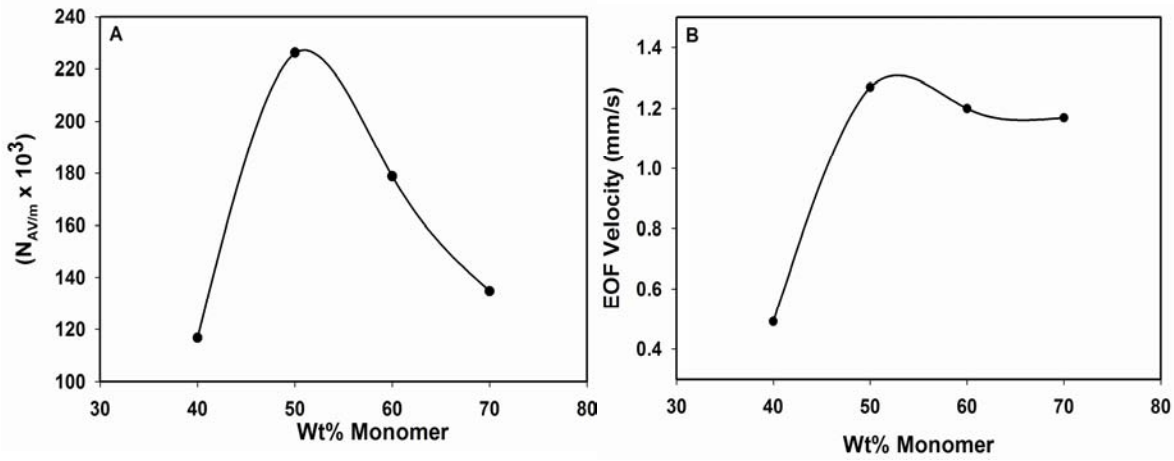

Figure 1. *Effect of wt% monomer in the polymerization solution on (A) the separation efficiency and (B) the EOF velocity. NMM capillary column, 20 cm effective length, 27 cm total length × 100 μm ID; mobile phase, 1 mM sodium phosphate, pH 7.0, at 80% v/v ACN; running voltage, 15 kV; electrokinetic injection for 3 s at 10 kV. Test solutes: benzene, toluene, ethylbenzene, propylbenzene, butylbenzene, pentylbenzene, hexylbenzene, heptylbenzene.*

In an attempt to produce an NMM column with acceptable permeability in a pressure driven flow, different mixtures of the monomer NAPM, and the crosslinker TRIM were used while keeping the % composition of porogenic solvents constant. The

columns performances were evaluated using a test mixture of 8 alkylbenzenes (ABs) using 80% v/v ACN. As can be seen from Fig. 1A, an increase in the wt% of the NAPM monomer from 40% to 50% increased the separation efficiency from ~120,000 to 220,000 plates/m and the EOF increased from 0.49 mm/s to 1.27 mm/s (Fig. 1B).

A further increase of the monomer to 60% and 70% yielded a drop in separation efficiency to 180,000 and 130,000 plates/m, respectively, while the EOF more or less remained the same at 1.20 and 1.17 mm/s at 60 and 70 wt% monomer, respectively, Fig. 1B. The optimum wt% NAPM monomer from Fig. 1A was 50% and this was used in fabricating the columns used in this study.

Plate height *versus* flow velocity–van Deemter plot. The optimal NMM column was further evaluated for its CEC separation efficiency over a wide range of mobile phase flow velocity using 75% v/v ACN in the mobile phase. The results are shown in Fig. 2A by the van Deemter plot using 8 ABs as the model solutes. The apparent EOF velocity was varied by increasing the operating voltage from 8 to 25 kV.

As can be seen in Fig. 2, H_{min} is obtained at an optimal EOF velocity in the range 0.55–0.70 mm/s. When the flow velocity is increased to 0.84 mm/s the loss in separation efficiency is ~4% but with a shortening in the analysis time by about half with respect to the analysis time at 0.55 mm/s (35 min compared to 18 min). A typical electrochromatogram of the alkylbenzenes at 0.66 mm/s is shown in Fig. 2B. This represents a practical flow velocity range (0.55 to 0.84 mm/s) over which the column can be utilized with virtually little or no variation in the separation efficiency, thus representing an efficient solute mass transfer characteristic within the porous NMM.

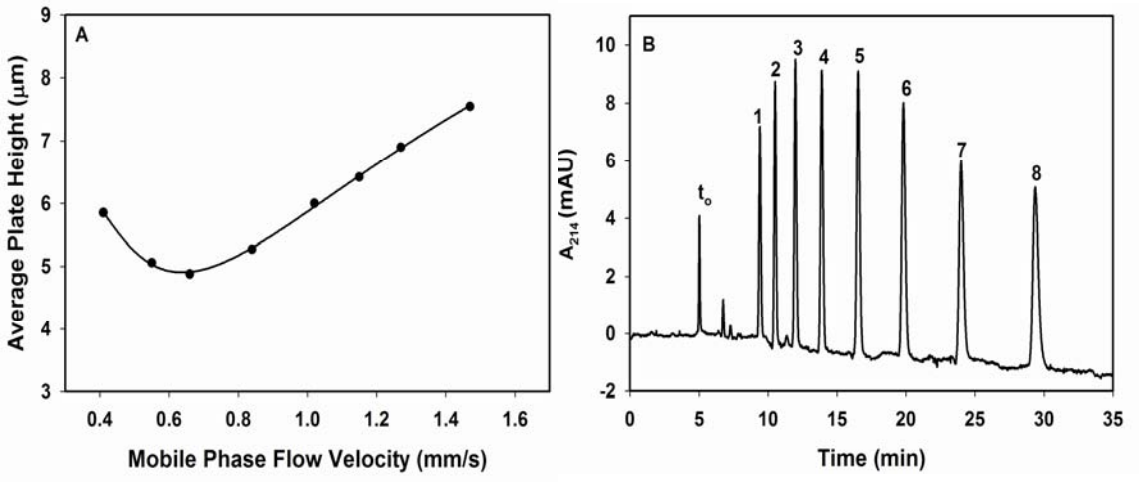

Figure 2*. (A), van Deemter plot showing average plate height as a function of EOF velocity and (B), electrochromatogram of alkylbenzene homologous series at optimal EOF velocity. In (A) the plate height is the average taken for the first eight alkylbenzene homologous series. In (A) and (B), mobile phase, 1 mM sodium phosphate, pH 7.0, using 75% v/v ACN; electrokinetic injection for 3 s at 10 kV; in (A), running voltage, various kV; in (B), running voltage, 12 kV. Solutes in (B): 1, benzene; 2, toluene; 3, ethylbenzene; 4, propylbenzene; 5, butylbenzene; 6, pentylbenzene; 7, hexylbenzene;and 8, heptylbenzene. Monolith and column dimensions are the same as in Fig. 1.*

Reproducibility of column fabrication. Run-to-run, day-to-day and column-to-column reproducibilities of the optimal NMM column were studied in terms of EOF velocity (t_o), retention factor (*k'*) and separation efficiency of eight ABs using a mobile phase containing 80% v/v ACN in 1 mM sodium phosphate monobasic buffer, pH 7. The overall percent relative standard deviation (% RSD) (n=3) were 2.24, 5.63 and 2.70, for the EOF velocity (t_o), *k'* and separation efficiency, respectively, which are similar to those previously reported in literature [2, 6, 7].

EOF. The neutral NMM column which is void of groups with fixed charges and consequently has no zeta potential with respect to water, produced sufficient EOF over a pH range of 5-8 as shown in Fig. 3A. The presence of polar ester groups in the NAPM monomer and the crosslinker TRIM is thought to be significant to the monolith's ability to adsorb enough phosphate ions from the mobile phase. This imparts the monolith with the zeta potential necessary to support the EOF. Since the EOF is cathodal, the zeta potential is therefore negative. As seen from Fig. 3A, the EOF is somewhat the same in the pH range 4-5 and then increases sharply at pH 5-8. At pH 5-8, the amount of adsorbed phosphate ions carrying a double negative charge increases thus producing the sharp rise in EOF, whereas at pH 4 most of the phosphate ions have a single negative charge, thus explaining the plateau on the curve in Fig. 3A at low pH. This agrees very well with the observation reported earlier with a C17 and C18 neutral monoliths based on pentaerythritol diacrylate monostearate **(**PEDAS) and octadecyl acrylate (ODA) monomers, respectively [9, 10].

Additionally, the effect of the ACN content of the mobile phase on the magnitude of the EOF was examined and the results are shown in Fig. 3B. As can be seen from the figure, the magnitude of the EOF increased with the %ACN at varying rate in the range studied 55 to 80% v/v. Although increasing the ACN decreases the dielectric constant of the mobile phase which may diminish the ionization of the adsorbed phosphate ions, the fact that increasing the ACN content decreases the viscosity of the mobile phase and increases the amount of adsorbed phosphate ions at the NMM surface results in an increase of the EOF velocity under the given set of running conditions. It is believed that the adsorption of phosphate ions to the NMM surface is of a polar nature and would

increase with the ACN content of the mobile phase. This observation corroborates with that previously reported from our laboratory [9, 10, 21] using different neutral monoliths.

Evidence of π-π interactions with the NMM column

Case of alkylbenzenes homologous series The performance of the NMM column was examined with a homologous series of ABs and the results were compared to those obtained on an ODM column. Plots of log *k*' for the ABs versus %ACN (v/v) in the mobile phase on both NMM and ODM columns linearly decreased with increasing %ACN, an indication that the separation of alkylbenzenes on these two different monolithic columns is based on a typical reversed phase chromatographic retention mechanism. In both cases, the slopes of the lines increased with the size of the solute, which corresponds to increasing the hydrophobic contact area between the solute and the non-polar ligand of the stationary phase.

To further understand the difference in the separation mechanism for both types of monolithic columns, the slopes of the lines (from the log k´ vs. %ACN in the mobile phase) were plotted against the number of carbons in the alkyl chain of the homologous ABs for both NMM and ODM columns. As can be seen in Fig. 4, the slope increases linearly with increasing number of carbons in the ABs studied for the ODM column, which is not the case for the NMM column. In addition, the slope is higher on the NMM column than on the ODM column, which reveals the presence of a second separation mechanism involving π-π interaction on the NMM column *via* the benzene ring of the ABs. However, as the number of carbons in the alkyl chains of the homologous series

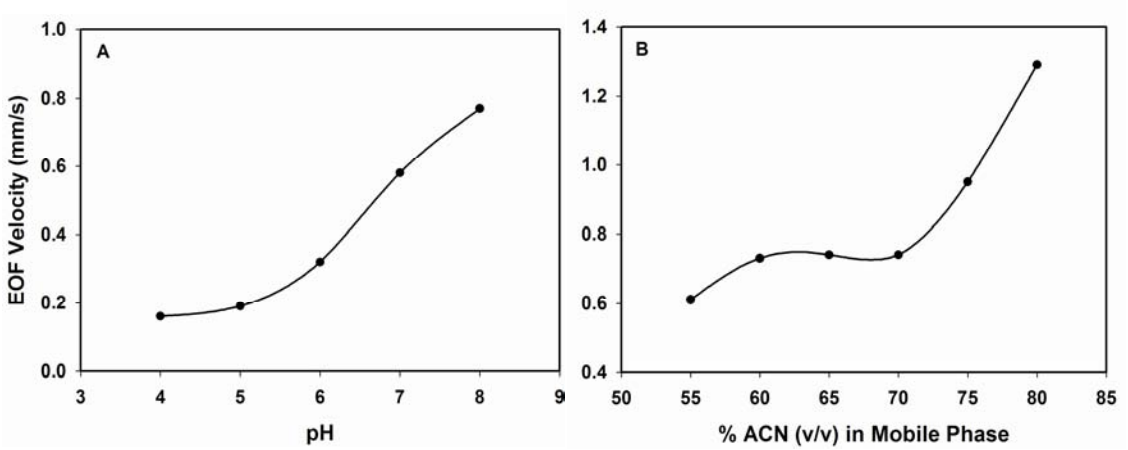

Figure 3. *Plots of EOF velocity versus the pH of the mobile phase (A) and the % ACN v/v in the mobile phase (B). Mobile phase, 1 mM sodium phosphate at various pH and at 80% v/v ACN in (A) and various % ACN (v/v) at pH 7 in (B); running voltage, 15 kV; EOF tracer, thiourea; electrokinetic injection for 3 s at 5 kV. Monolith and column dimensions are the same as in Fig. 1.*

increases to more than four, the slope on the NMM column tapers off and by the time the number of carbon atoms is seven, the slope on NMM and ODM columns are nearly the same. At this alkyl chain length, the participating separation mechanisms consisting of hydrophobic and π-π interactions for the *n*-heptylbenzene with the NMM column seems to add up in magnitude to equate the hydrophobic interaction of this solute with the ODM column. The tapering off of the curve for the NMM column may indicate that the π-π interaction of the benzene moiety of the ABs with the naphthyl ligands has reached its maximum strength at an alkyl chain length consisting of four carbon atoms (i.e., *n*-butyl) and the hydrophobic contact area (i.e., hydrophobic interactions) of the ABs with the small naphthyl ligands did not increase significantly after a chain length of *n*-butyl.

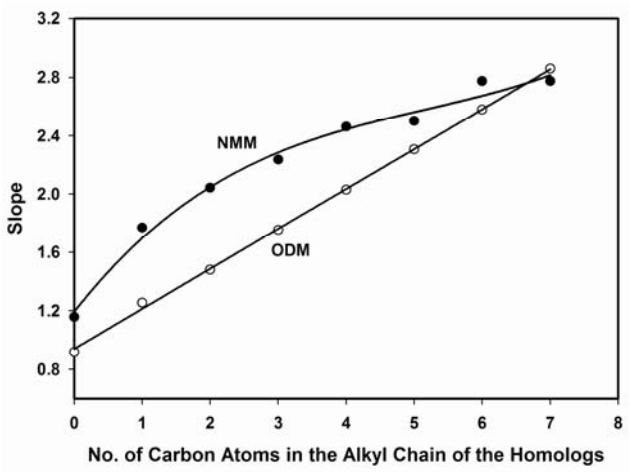

Figure 4. *Plots of slopes of the lines of log k' vs. %ACN in the mobile phase obtained for alkylbenzenes vs. the number of carbon atoms in the homologous on the NMM and ODM columns. Capillary column, 20 cm effective length, 27 cm total length × 100 μm ID; mobile phase, 1 mM sodium phosphate, pH 7.0, at various %ACN; running voltage, 15 kV; electrokinetic injection for 3 s at 10 kV. Solutes as in Fig. 2.*

Case of aromatic compounds with varying electron-donating/electron-withdrawing functional groups. In order to illustrate the presence of a dual retention mechanism consisting of hydrophobic and π-π interactions with the NMM stationary phase, three test mixtures consisting of aromatic solutes with different electron donating/electron withdrawing functional groups were separated on both the NMM and ODM columns under the same chromatographic conditions.

Electron-donating substituents on a benzene ring make the ring more π-donating than benzene itself and are called activating groups [22]. Oppositely, electron-withdrawing substituents on a benzene ring make the ring more π-accepting than benzene itself and are considered as deactivating groups. Typical examples of (i) strongly

activating groups are $–NH_2$, $–NHR$, $–NR_2$, $–OH$ and O^-; (ii) moderately activating substituents are $–NHCOCH_3$, $–NHCOR$, $–OCH_3$ and $–OR$; (iii) weakly activating substituents are $–CH_3$, $–C_2H_5$, $–R$ and $–C_6H_5$. Examples of (i*) weakly deactivating groups are –F, –Cl, –Br and –I; (ii*) moderately deactivating substituents are –CN, $–SO_3H$, –COOH, –COOR, –CHO, and –COR; (iii*) strongly deactivating groups are $–NO_2$, $–NR_3^+$, $–CF_3$ and $–CCl_3$ [22].

First, *p*-toluidine, *p*-tolualdehyde, *p*-tolunitrile, toluene and *p*-nitrotoluene were used as the model solutes. On the NMM column, the elution order was as listed in the preceding sentence with retention factors (*k'*) of 0.59, 0.94, 1.06, 1.47, and 1.71, respectively, Fig. 5A. When the same test mixture was separated on the ODM column, the elution order was *p*-toluidine, *p*-tolualdehyde, *p*-tolunitrile, *p*-nitrotoluene and toluene with *k'* of 0.26, 0.35, 0.38, 0.59, and 0.83, respectively, Fig. 5B. Here, the elution order of the first three solutes was found to be the same on both columns. On the other hand, *p*-nitrotoluene eluted before toluene on the ODM column, whereas it eluted later than toluene on the NMM column. Comparatively, the solutes were more retained on the NMM column than they were on the ODM column.

Considering hydrophobicity, nitrotoluene with a nitro group is less hydrophobic than toluene and therefore elutes before toluene on the ODM column where the participating retention mechanism is based purely on the hydrophobicity of the solute.

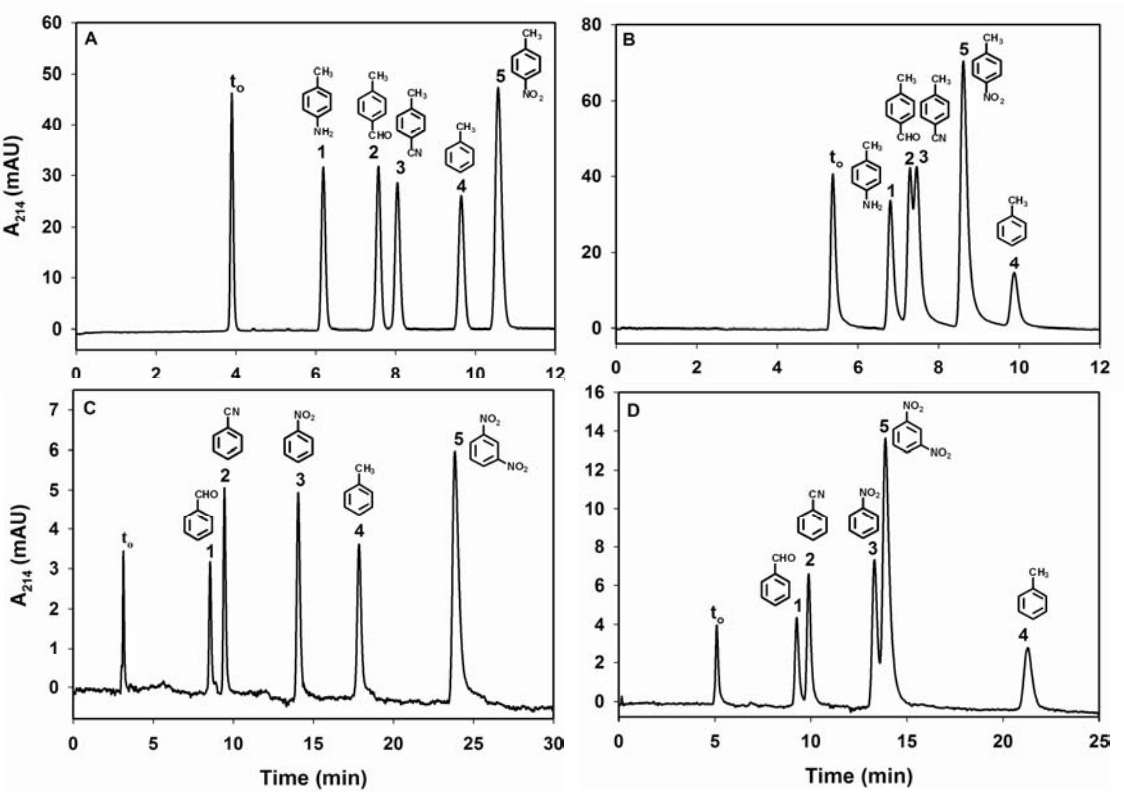

Figure 5. *Upper panel: electrochromatograms of some toluene derivatives on (A) NMM and (B) ODM columns; lower panel: electrochromatogram of some benzene derivatives on (C) NMM and (D) ODM columns. Capillary column, 20 cm effective length, 27 cm total length × 100 μm ID; mobile phase, 1 mM sodium phosphate, pH 7.0, at 70% v/v ACN in upper panel and 50% v/v ACN in lower panel; running voltage, 15 kV (upper panel) and 20 kV (lower panel); electrokinetic injection for 3 s at 10 kV. Solutes in (A) and (B): 1, p-aminotoluene; 2, p-tolualdehyde; 3, p-tolunitrile; 4, toluene and 5; p-nitrotoluene; Solutes in (C) and (D): 1, benzaldehyde; 2, benzonitrile; 3, nitrobenzene; 4, toluene and 5; m-dinitrobenzene.*

When it comes to the NMM column, the strong electron-withdrawing nitro group on nitrotoluene decreases the π-electron density on the aromatic ring, making it a soft Lewis

acid that can accept π-electrons from the π-electron rich naphthyl ligand of NMM stationary phase [15]. This kind of interaction causes nitrotoluene to be more strongly retained on the NMM column than on the ODM column. Since the first three eluting solutes, i.e., *p*-toluidine, *p*-tolualdehyde, and *p*-tolunitrile differ only slightly in their hydrophobic character they elute in a narrow time window (~1 min) and do not resolve completely from each other on the ODM column. In contrast on the NMM column, the various substituents modulate the electron accepting/donating capability of the solutes, and in turn their retention and selectivity. In fact, the electron-donating ability of *p*-toluidine is the compounded effect of the weakly activating methyl group and the strongly activating amino group. This makes *p*-toluidine differ significantly from *p*-tolualdehyde and *p*-tolunitrile since these two solutes carry both a weakly activating methyl group and moderately deactivating aldehyde and nitrile groups. It is clear from the two chromatograms in Fig. 5 that the second participating mechanism of π-π interaction not only enhances retention of the solutes but also modulates the selectivity.

The retention behavior of other solute probes including nitrobenzene, *m*-dinitrobenzene, toluene, benzonitrile and benzaldehyde was studied on both monolithic columns under the same chromatographic conditions. On the NMM column, the elution order was benzaldehyde, benzonitrile, nitrobenzene, toluene and *m*-dinitrobenzene, with *k'* values of 1.72, 2.02, 3.49, 4.70, and 6.62, respectively, Fig 5C. The elution order on the column ODM was as follows: benzaldehyde, benzonitrile, nitrobenzene, *m*-dinitrobenzene and toluene, with *k*' values of 0.82, 0.94, 1.61, 1.72 and 3.17, respectively, Fig. 5D. On both columns, the elution order is consistent with the expected retention mechanism. With the exception of toluene which has a weakly activating

methyl group, all other solutes have deactivating substituents with the strongest being the nitro group followed by the moderate nitrile and then the aldehyde. On the NMM column, one can see the effect of the electron-withdrawing nitro group on the benzene ring, which results in the retention of the solute by the π-electron rich naphthyl ligand of the NMM stationary phase. As discussed earlier the nitro-substituted benzene ring possesses a low π-electron density (can accept π-electrons) while the naphthyl groups of the stationary phase possess a higher π-electron density (can donate π-electrons). The result is a π-π interaction that leads to π-donor-π-acceptor complexes. The higher the number of nitro substituents on the benzene ring, the lower its π-electron density, and the stronger the π-π interaction with the π-electron rich donor which is the stationary phase ligand [15], compare *m*-dinitrobenzene to nitrobenzne. Thus, *m*-dinitrobenzene with two nitro substituents is retained the most on the NMM column, which has two retention mechanisms namely hydrophobic and π-π interaction. Oppositely, on the ODM column it was observed that toluene being more hydrophobic than both nitrobenzene and *m*-dinitrobenzene elutes last, which conforms to the fact that the separation mechanism on the ODM is purely dependent on the hydrophobicity of the solute.

The π-π interactions with the NMM column were studied once more with a mixture containing eight anilines, a class of slightly polar solutes. The order of elution on the NMM column was aniline, 3-methylaniniline, 4-nitroaniline, 3-chloro-4-methyl aniline, 3-nitroaniline, 4-methoxy-2-nitroaniline, 3,4-dichloroaniline and 4-methyl-2-nitroaniline, with *k'* values of 1.07, 1.54, 1.77, 2.12, 2.24, 2.90, 3.72 and 4.09, respectively, Fig. 6A. The 8 anilines were baseline separated within 16 min using 50% (v/v) ACN in the mobile phase. The elution order of the anilines on the NMM column is

in the order of increasing nonpolar character of the solutes, a retention behavior typical for RP-CEC where halogenated anilines are more retained than methyl-substituted anilines. In addition, the effect of a nitro group on retention can be readily noticed as a result of low π-electron density and therefore more interaction with the stationary phase. The same test mixture was separated on the ODM column under the same chromatographic conditions. Since the operating retention mechanism on the ODM column is based on the hydrophobicity of the solute, a switch in the elution order compared to that on NMM was observed and some solutes coeluted. The order of elution was, aniline, 3-methylaniniline co eluted with 4-nitroaniline, 3-chloro-4-methyl aniline coeluted with 3-nitroaniline and 4-methoxy-2-nitroaniline, 4-methyl-2-

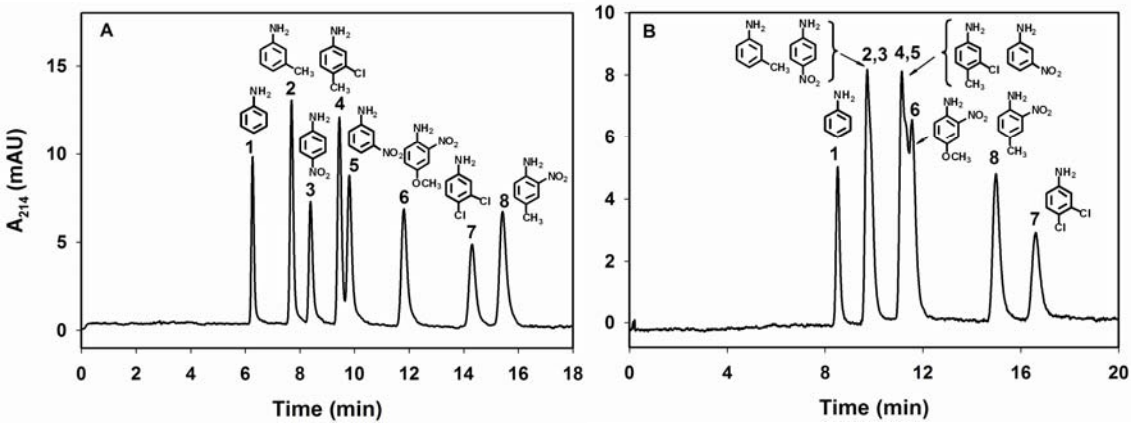

Figure 6. *Electrochromatogram of some anilines on (A) NMM and (B) ODM columns. Conditions as in Fig. 5C and D. Solutes: 1, aniline; 2, 3-methylaniline; 3, 4-nitroaniline; 4, 3-chloro-4-methylaniline; 5, 3-nitroaniline; 6, 4-methoxy-2-nitroaniline; 7, 3,4-dichloroaniline and 8; 4-methyl-2-nitroaniline.*

nitroaniline and 3,4-dichloroaniline with *k'* values of 0.55, 0.77, 1.03, 1.10, 1.72, and 2.02, respectively Fig. 6B. The presence of a less hydrophobic nitro group in 4-methyl-2-nitroaniline made it elute before 3,4-dichloroaniline on the ODM column while it eluted after 3,4-dichloroaniline on the NMM column. This once again demonstrates the fact that both hydrophobicity and π-π interactions play a major role in separation for the NMM monolith while hydrophobicity is the major separation mechanism on ODM column.

Case of polycyclic aromatic hydrocarbons (PAHs). Besides their chemical, industrial and environmental importance, polycyclic aromatic hydrocarbons (PAHs) are also suitable model solutes to evaluate the extent of π-π interactions with the NMM column. First, six PAH solutes including benzene, naphthalene, phenanthrene, pyrene, benzo[e]pyrene and benzo[ghi]perylene were electrochromatographed on the NMM column as well as on the ODM monolith under otherwise the same chromatographic conditions.

The results are shown in Fig. 7 in terms of plots of k´ versus the number of aromatic rings in the solutes. As can be seen in this figure the k´ on the NMM column increased exponentially with an increase in the number of aromatic rings as compared to a much shallower increase on the ODM column. This behavior is a reflection of the π-π interactions of PAHs solutes with the NMM column.

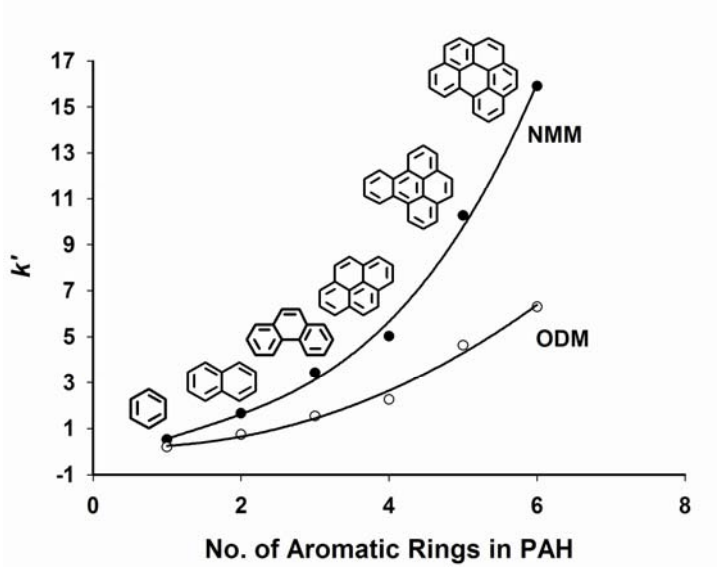

Figure 7. *Plots of k' versus number of aromatic rings of some PAHs. NMM and ODM capillary columns, 20 cm effective length, 27 cm total length × 100 μm ID; mobile phase, 1 mM sodium phosphate, pH 7.0, at 75% v/v ACN, running voltage, 15 kV; electrokinetic injection for 3 s at 10 kV.*

In a second set of experiments, a mixture of 16 selected PAHs was electrochromatographed using the same running conditions on both the NMM and ODM columns, and the results are shown in Fig. 8A and 8B. As can be seen in Fig. 8 A, the NMM column was able to separate all the 16 PAHs within 34 min. On the other hand, the same PAHs were less retained on the ODM column and some of the solutes coeluted while the elution order for others was switched from what was observed on the NMM column, Fig. 8B. This kind of behavior is further evidence that the NMM column has a second separation mechanism involving π-π interactions that enhance retention as well as selectivity.

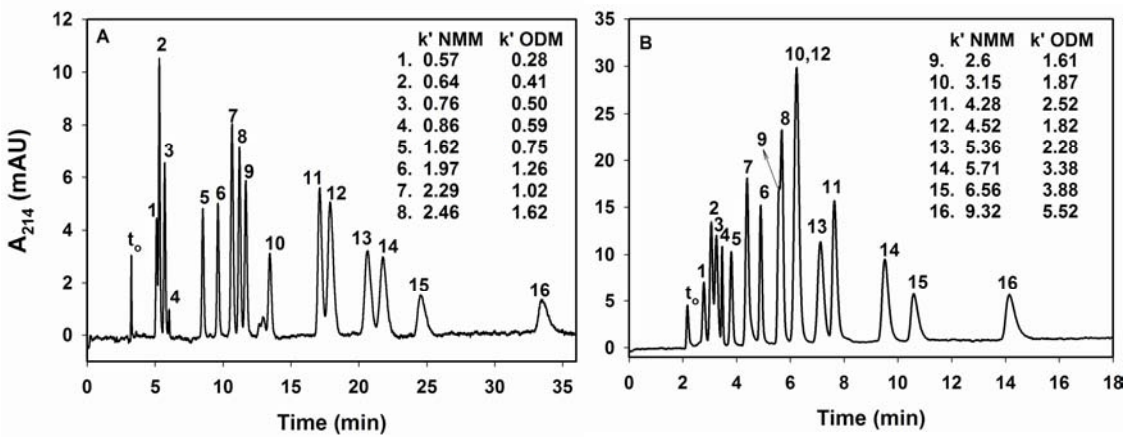

Figure 8. *Electrochromatograms of some polycyclic aromatic hydrocarbons on (A) NMM column and (B) ODM column with inserts of k´ values on NMM and ODM columns. Capillary column, 20 cm effective length, 27 cm total length × 100 μm ID; mobile phase, 5 mM sodium phosphate, pH 7.0, at 70% v/v ACN; running voltage, 20 kV; electrokinetic injection for 3 s at 10 kV. Solutes: 1, naphthaleneethanol,; 2,2-naphthol; 3, 1-naphthol; 4, benzene; 5, 1-cyanonaphthalene; 6, naphthalene; 7, 1-nitronaphthalene; 8, 2-methylnaphthalene; 9, biphenyl; 10, fluorene; 11, phenanthrene; 12, 9-anthracenecarbonitrile; 13, 9-nitroanthracene; 14, fluoranthene; 15, pyrene; 16; benz[a]anthracene.*

As can be seen in Fig. 8 (see also the k´ values in the inserts in Fig. 8), while the first 5 PAHs are eluted in the same order on both columns, the next pair (i.e., naphthalene and 1-nitronaphthalene) are eluted in the opposite order on the two columns. That is, 1-nitronaphthalene, which is more polar is eluted before naphthalene on the ODM column, and after naphthalene on the NMM column. This is due to the fact that the $–NO_2$ group is a strong deactivating group (i.e., electron-withdrawing substituent), thus allowing 1-nitronaphthalene to interact strongly with the naphthyl ligand of the NMM column. The

next two solutes, 2-methylnaphthalene and biphenyl (nos. 8 and 9) are very well resolved on the NMM column but almost co-eluting on the ODM column. This enhanced selectivity for the two solutes on the NMM column is due to the fact that the biphenyl possesses 2 π electrons extra than 2-methylnaphthalene (12 π electrons for biphenyl compared to 10 π electrons for 2-methylnaphthalene). For the subsequent 4 solutes (nos. 10, 11, 12 and 13) there is a total unparallel elution order between NMM and ODM column. As expected, phenanthrene with 14 π electrons is more retained than fluorene with 2 fewer π electrons on the NMM column. Also, 9-anthracenecarbonitrile and 9-nitroanthracene having the same number of π-electrons than that of phenanthrene but with a nitrile and a nitro substituent, respectively, should be more retarded on the NMM column than the preceding two PAHs. A nitro group, which is a much stronger electron withdrawing group than nitrile (i.e., more deactivating) favors stronger π-π interactions with the naphthyl ligand of the NMM column. That is, 9-nitroanthracene should be more retained than 9-anthracencarbonitrile. These four solutes, i.e., fluorene, phenanthrene, 9-anthacenecarbonitrile, and 9-nitroanthacene elute on the ODM column in the order of their nonpolar character. A nitrile group confers more polar character to the solute than a nitro group thus making 9-anthracenecarbonitrile to be less retained than 9-nitroanthracene, and both solutes are less retained (more polar) than phenanthrene. The elution of the last 3 PAHs (nos. 14, 15 and 16) parallels each other on both columns with a difference in that they are more retained (by more than two folds) on the NMM column than on the ODM column. Solute no. 16 (i.e., benz[a]anthracene) has 18 π electrons whereas the PAH isomers nos. 14 and 15 have 16 π electrons each. This would explain the higher retention of benz[a]anthracene on both columns whereby for the NMM

column, an extra pair of π electrons would lead to more π-π interactions whereas for the ODM column an additional two carbon atoms brings more hydrophobic interaction. For the two PAH isomers, fluoranthene and pyrene, the length-to-breadth (L/B) ratio increases from 1.22 to 1.27, respectively, thus favoring better nonpolar interactions as well as π-π interactions for pyrene over fluoranthene with the octadecyl and naphthyl ligands, respectively. These findings agree with previous observations on octadecyl silica (ODS) stationary phase and on a 3-(4-amino-1,8-naphthalimido)propyl modified silyl silica gel utilizing π-π interaction in HPLC [14].

It is clear from the above discussion that although the reversed-phase mode of retention is pronounced on both columns, the NMM column realized more selectivity for the separation of the PAHs as compared to the ODM column, which is attributed to the strong π-π interaction between the PAH solutes and the naphthyl ligand.

Effect of organic modifier on π-π interactions. Two different organic modifiers, namely ACN and methanol (MeOH) were examined and compared for their effect on π-π interactions. In this regard, three phthalonitrile positional isomers and benzene were electrochromatographed on the NMM column using a mobile phase containing either ACN or MeOH as the organic modifier under otherwise the same CEC conditions. In the presence of ACN, the three phthalonitrile isomers could not be resolved, Fig. 9A. In the presence of MeOH as the organic modifier, the three pthalonitrile positional isomers and benzene were separated in 34 min. The order of elution was benzene, *o*-phthalonitrile, *p*-phthalonitrile and *m*-phthalonitrile with *k'* of 3.06, 5.00, 5.82 and 6.41, respectively, Fig. 9B. In the absence of ACN, π-π interactions between the solutes and the stationary

phase, are stronger and the phthalonitrile positional isomers are separated on the basis of their π-electron density. This agrees with previous findings on an HPLC phenyl silica column [23] in that ACN impedes the selective π-π interactions between the analyte molecules and the bonded phenyl groups on the stationary phase surface. This suppression of π-π interactions by ACN is reported to arise from the interaction of its triple bond, with the aromatic stationary phase [23].

It has to be mentioned that a change of organic modifier from ACN to MeOH in the hydro-organic mobile phase leads to an increase in the viscosity of the mobile phase, which causes a decrease in the EOF velocity in CEC [24]. As a result, and for the same mobile phase composition, the analysis time is much longer with MeOH than with ACN, compare Fig. 9B to 9A.

To further understand the effect of the nature of the organic modifier on π-π interactions, a mixture containing benzonitrile, benzaldehyde, nitrobenzene and toluene was electrochromatographed on the NMM column using either ACN or MeOH. In the presence of ACN, the order of elution was benzaldehyde, benzonitrile, nitrobenzene and toluene with *k'* of 0.73, 0.73, 1.15 and 1.36, respectively, Fig. 9C. It can also be seen from Fig. 9C that benzaldehyde coeluted with benzonitrile. When the same mixture was separated with a mobile phase containing MeOH, the order of elution changed to benzaldehyde, benzonitrlie, toluene and nitrobenzene with *k'* of 2.38, 2.57, 4.33 and 6.02, respectively Fig. 9D. The cyano group in benzonitrile is a stronger π-electron withdrawing group than the carbonyl group in benzaldehyde and this means that

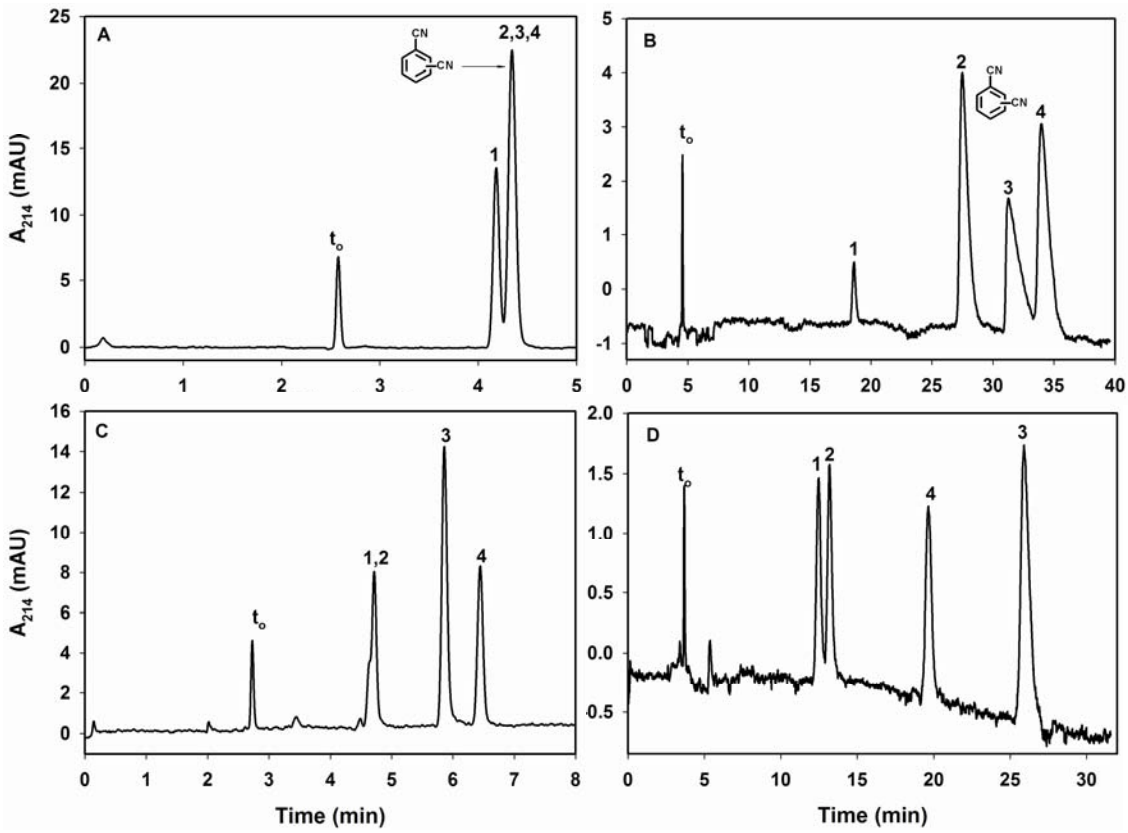

Figure 9. *Upper panel: electrochromatograms of benzene and phthalonitrile positional isomers on NMM column with ACN (A) and MeOH (B); lower panel: electrochromatograms of benzene derivatives on NMM column with ACN (C) and MeOH (D). Capillary column, 20 cm effective length, 27 cm total length × 100 μm ID; mobile phase, 1 mM sodium phosphate, pH 7.0 in 70% v/v ACN in (A) and (C) and 70% v/v MeOH in (B) and (D), running voltage, 20 kV; electrokinetic injection for 3 s at 10 kV. Solutes in upper panel: 1, benzene; 2, o-phthalonitrile; 3, p-phthalonitrile; 4, m-phthalonitrile. Solutes in lower panel: 1, benzaldehyde; 2, benzonitrile; 3, nitrobenzene; 4, toluene.*

benzonitrile has less π-electron density and therefore it can accept more π-electrons from the π-electron rich naphthyl group of the NMM column, thus making it more retained than benzaldehyde in the presence of MeOH in the mobile phase, which enhances π-π interactions. Taking into consideration that ACN suppresses π-π interactions, both benzaldehyde and benzonitrile coeluted under the same chromatographic conditions. Also, with MeOH nitrobenzene was found to be more retained than toluene on the NMM column whereas the inverse occurred with ACN (compare Fig. 9D to 9.C). MeOH enhanced π-π interactions that were otherwise suppressed when ACN was used as the organic modifier in the mobile phase.

Although MeOH was found to enhance π-π interactions, as discussed above the EOF velocity was significantly reduced, and as a result the analysis time was substantially increased, see Fig. 9B and D. Also, the columns were more readily equilibrated with the ACN- than with the MeOH-based mobile phase, and the baseline with MeOH was found to be very unstable, see Fig. 9. This observation agrees with what has previously been reported in CEC on an octadecyl silica (ODS) column [25-27]. For this reason, it is advised to use ACN in the mobile phase at lower concentration to allow sufficient π-π interactions between solute and stationary phase for achieving an acceptable selectivity and separation. On this basis, and throughout the present study, the mobile phases used contained ACN at moderate concentrations and/or as adequately needed for achieving a given separation.

Illustrative separation of positional isomers

The usefulness of the strong π-π interactions with the NMM column was demonstrated in the separation of different positional isomers and the resulting electrochromatograms were compared to those obtained on the ODM column under otherwise the same electrochromatographic conditions. It is well established that a pure RPC retention mechanism usually does not afford sufficient selectivity towards positional isomers, and synthetic organic chemists have found normal phase or adsorption chromatography on bare silica or alumina to be more selective and effective for such applications than RPC [28]. As will be shown below, a NMM stationary phase that offers π-π interactions as well as nonpolar interactions is a more effective approach for separating positional isomers than the RPC mode.

Three toluidine positional isomers were used as solute probes for evaluating the effectiveness of the NMM column in such an application. As can be seen in Fig. 10A, the three isomers were baseline separated on the NMM within 7 min. The order of elution was *o*-, *p*-, and *m*-isomer on the NMM column with *k'* values of 0.33, 1.14, and 1.29, respectively, Fig 10A. The order of elution for the three toluidine positional isomers on the ODM column was the same (Fig. 10B) but with *k'* values of 0.17, 0.63, and 0.72, respectively, that are ~50% of those obtained on the NMM column. It is evident from the electrochromatograms in Fig 10A that the effect of π-electron localization (especially on *p*-isomers) allowed a noticeable baseline separation of *m*- and *p*-isomers on the NMM column that could not similarly be achieved on the ODM column.

Under the same chromatographic conditions used in the preceding example, the separation of tolunitrile isomers was compared on both NMM and ODM columns. The

order of elution on NMM was *o*-, *p*-, and *m*-isomer with *k'* values of 3.78, 3.99, and 4.26, respectively, Fig. 10C and the three isomers were baseline separated within 18 min. On the other hand, the ODM column was unable to achieve baseline separation of the three positional isomers with both *o*-, *p*-isomers co-eluting, Fig. 10D. The order of elution however, was similar to that observed on the NMM column.

Nitrotoluene positional isomers were also separated on both NMM and ODM columns. The order of elution on NMM was *o*-, *p*-, and *m*-isomer with *k'* values of 5.00, 5.48, and 5.72, respectively, (Fig. 11A). The three positional isomers were baseline separated within 24 min. On the ODM column, the order of elution switched from *o*-, *p*-, and *m*-isomer to *o*-, *m*-, and *p*-isomer and the *o*- and *m*-isomers coeluted, Fig. 11B.

Three nitro xylenes, that are another set of positional isomers, were electrochromatographed on both NMM and ODM columns. The presence of two methyl groups combined with the presence of a nitro group would increase the retention of the solutes on the NMM column compared to any other positional isomers studied so far and mentioned above. The three positional isomers studied were 4-nitro-*o*-xylene, 2-nitro-*m*-xylene, and 4-nitro-*m*-xylene and the order of elution on the NMM column was observed to be 2-nitro-*m*-xylene, 4-nitro-*o*-xylene, and 4-nitro-m-xylene with *k'* values of 7.56, 9.15, and 10.10, respectively, Fig. 11C. When the same mixture was separated on the ODM column, the order of elution switched to 4-nitro-*o*-xylene, 4-nitro-*m*-xylene, and 2-nitro-*m*-xylene with *k'*, 3.21, 3.42, and 3.58, respectively, Fig. 11D.

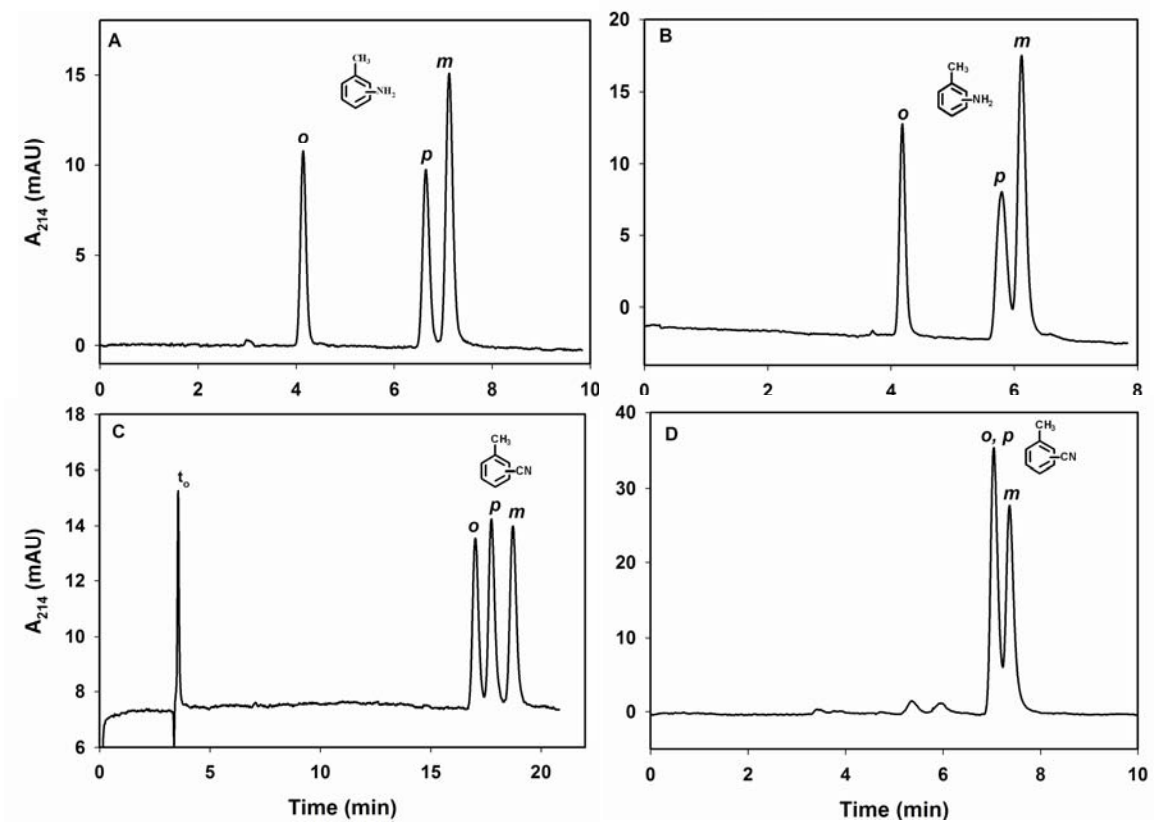

Figure 10. *Upper panel: electrochromatograms of toluidine positional isomers on (A) NMM and (B) ODM columns; lower panel: electrochromatograms of tolunitrile positional isomers on (A) NMM and (B) ODM columns. Capillary column, 20 cm effective length, 27 cm total length × 100 μm ID; mobile phase, 1 mM sodium phosphate, pH 7.0, at 50% v/v ACN; running voltage, 20 kV; electrokinetic injection for 3 s at 10 kV.*

As shown in Fig 11C and D, the retention of the three positional isomers on ODM is lower and the selectivity is poorer in comparison to their retention and selectivity on the NMM column. The presence of a nitro group decreases the hydrophobic character of the solute making the solutes less retained on ODM, while at the same time it increases

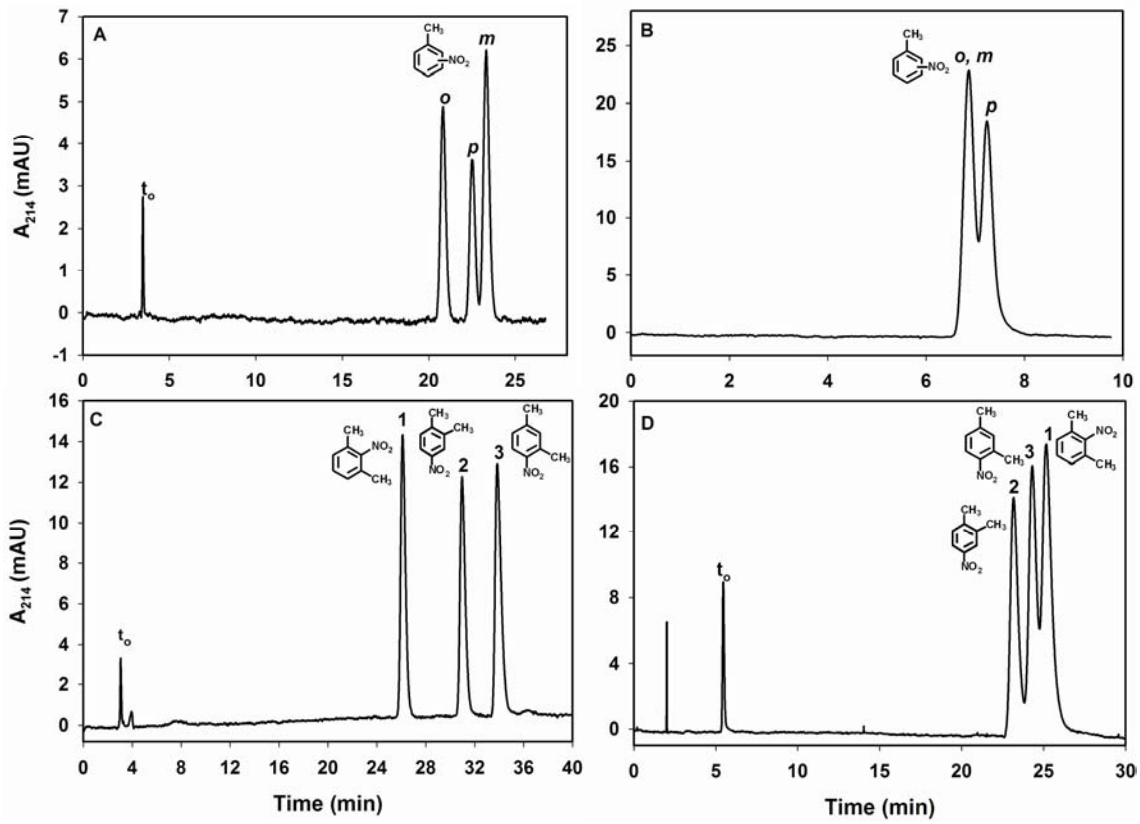

Figure 11. *Upper panel: electrochromatograms of nitrotoluene positional isomers on (A) NMM and (B) ODM columns; lower panel: electrochromatograms of nitroxylene positional isomers on (A) NMM and (B) ODM columns. Capillary column, 20 cm effective length, 27 cm total length × 100 μm ID; mobile phase, 1 mM sodium phosphate, pH 7.0, at 50% v/v ACN; running voltage, 20 kV; electrokinetic injection for 3 s at 10 kV.*

the π-π interaction between the π-electron poor solute and the π-electron rich stationary phase that enhances retention as well as selectivity on the NMM column.

Conclusions

The NMM column has proved useful in RP-CEC separations of a wide range of aromatic compounds such as PAHs, benzene derivatives, toluene derivatives, anilines and positional isomers. When compared to a nonpolar monolithic column bearing *n*-octadecyl functional ligands (e.g., ODM column), the selectivity offered by the NMM column is superior due to both hydrophobic and π-π interactions. In view of the importance and the large number of aromatic compounds and compounds with π electrons both synthetic and natural, the NMM column can be regarded as an important addition to the field of CEC column technology for solving many separation problems in the life sciences.

References

1 Jin, W., Fu, H., Huang, X., Xiao, H., Zou, H., *Electrophoresis* **2003**, *24*, 3172-3180.

2. Peters, E. C., Petro, M., Svec, F., Frechet, J. M. J., *Anal. Chem.* **1998**, *70*, 2288-2295.

3. Umemra, T., Ueki, Y., Tsunoda, K., Katakai, A., Tamada, M., Haraguchi, H., *Anal. Bioanal. Chem.* **2006**, *386*, 566.

4. Huang, X., Wang, Q., Yan, H., Huang, Y., Huang, B., *J. Chromatogr. A* **2005**, *1062*, 183.

5. Dong, J., Xie, C., Tian, R., Wu, R., Hu, J., Zou, H., *Electrophoresis* **2005**, *26*, 3452.

6. Palm, A., Novotny, M. V., *Anal. Chem.* **1997**, *69*, 4499-4507.

7. Bedair, M., El Rassi, Z., *Electrophopresis* **2002**, *23*, 2938-2948.

8. Bedair, M., El Rassi, Z., *J. Chromatogr. A* **2003**, *1013*, 35-45.

9. Okanda, F., El Rassi, Z., *Electrophoresis* **2005**, *26*, 1988-1995.

10. Karenga, S., El Rassi, Z., *J. Sep. Sci.* **2008**, *31*, 2677-2685.

11. Huo, Y., Kok, W. T., *Electrophoresis* **2008**, *29*, 80-93.

12. Wu, R., Hu, L., Wang, F., Ye, M., Zou, H., *J. Chromatogr. A* **2008**, *1184*, 369-392.

13. Zhang, M., El Rassi, Z., *Electrophoresis* **2001**, *22*, 2593-2599.

14. Reubsaet, J. L. E., Vieskar, R., *J. Chromatogr. A* **1999**, *841*, 147-154.

15. Brindle, R., Klaus, A., *J. Chromatogr. A* **1997**, *757*, 3-20.

16. Goss, J. D., *J. Chromatogr. A* **1998**, *828*, 267-271.

17. Kimata, K., Hirose, T., Moriuchi, K., Hosoya, K., Araki, T., Tanaka, N., *Anal. Chem.* **1995**, *67*, 2556-2561.

18. Horak, J., Maier, N. M., Lindner, W., *J. Chromatogr. A* **2004**, *1045*, 43-58.

19. Grosserhode, C., Kicinski, H. G., Kettrup, A., *Chromatographia* **1990**, *29*, 489-494.

20. Ohyama, K., Shirasawa, Y., Wada, M., Kishikawa, N., Ohba, Y., Nakashima, K., Kuroda, N., *J. Chromatogr. A* **2004**, *1042*, 189-195.

21. Zhong, H., El Rassi, Z., *J. Sep. Sci.* **2009**, *32*, 10-20.

22. Graham Solomons, T. W., Fryhle, C. B., *Organic Chemistry*, John Wiley & Sons, Inc **2008**, pp. 650 - 653.

23. Yang, M., Fazio, S., Munch, D., Drumm, P., *J. Chromatogr. A* **2005**, *1097*, 124-129.

24. Dittmann, M. M., Rozing, G. P., *J. Microcol. Sep.* **1997**, *9*, 399-408.

25. Euerby, M. R., Johnson, C. M., Smyth, S. F., Gillort, N., Barrett, D. A., Shaw, P. N., *J. Microcol. Sep.* **1999**, *11*, 305-311.

26. Newton, K. A., Zhou, L. L., Johnson, B. D., Thompson, R., Ellison, D., Wyvratt, J. M., *J. Liq. Chrom. & Rel. Technol.* **2001**, *24*, 755-771.

27. Yan, C., Dadoo, R., Zhao, H., Zare, R. N., *Anal. Chem.* **1995**, *67*, 2026-2029.

28. Snyder, L. R., Kirkland, J. J., *Introduction to Modern Liquid Chromatography*, Wiley, New York **1979**, pp. 355-356.

CHAPTER V

NAPHTHYL METHACRYLATE-PHENYLENE DIACRYLATE BASED MONOLITHIC COLUMN FOR REVERSED-PHASE CAPILLARY ELECTROCHROMATOGRAPHY *VIA* HYDROPHOBIC AND π-INTERACTIONS

Introduction

Polymeric monolithic columns have witnessed increased interest and developments in recent years as stationary phases for CEC. Unlike their counterparts the packed columns, monolithic columns require no retaining frits and have relatively high permeability and stability not to mention the ease in their method of preparation. Towards this end, various monomers and crosslinkers are available for their synthesis. For recent reviews see [1].

Polymeric stationary phases made from styrene as the functional monomer and divinyl benzene as the crosslinker constitute an important class of organic polymeric

** The content of this chapter has been accepted for publication in Electrophoresis.*

stationary phases. Whereas polystyrene-based monoliths have been popular in HPLC [2-4], their use in CEC has been limited as noted previously [5-7]. This limitation has been attributed to unfavorable reactivity ratios characterizing copolymerization of hydrophobic aromatic monomers possessing ionizable functionalities needed to generate EOF [7]. Additionally, methacrylic acid used as the charge bearing monomer only generates EOF at pH higher than 7 [5, 7]. For this reason, Huang *et al*., introduced a poly(styrene-divinylbenzene-vinylsulfonic acid) monolith using vinylsulfonic acid as the charge bearing monomer and studied the effects of process parameters such as polymerization mixture composition and reaction time [6].

Very recently, we introduced a neutral hydrophobic naphthyl methacrylate-based monolith made from the *in situ* copolymerization of 2-naphthyl methacrylate (NAPM) as the functional monomer and trimethylolpropane trimethacrylate (TRIM) as the crosslinker. This monolith that exhibited π-π and hydrophobic interactions was successfully applied to the separation of aromatic analytes and isomers [8] (see Chapter IV). In the present study, the crosslinker TRIM was replaced with 1,4-phenylene diacrylate (PDA) to make a neutral monolith that would offer the chromatographic retention mechanism of polystyrene divinyl benzene (PSDVB) without possessing the limitations of PSDVB mentioned above, and still exhibit sufficient EOF for realizing differential migration. In fact, and as shown in this report the NPM exhibited a higher EOF than the previous monolith made from TRIM as the crosslinker. It is believed that being a diacrylate, PDA does not crosslink as extensively as TRIM, which is a trimethacrylate. Therefore, using TRIM as a crosslinker leads to a more rigid monolith with less permeability than when PDA is used as the crosslinker. Previously, EOF

generation in a styrene based monolith void of any ionizable monomer and possessing no polar functionalities for mobile phase adsorption was reported [9]. The use of PDA as a crosslinker for stationary phases used in HPLC has been reported previously [10, 11].

The NPM monolith reported in this study is similar to previously described PSDVB monoliths whose chromatographic surfaces are covered with aromatic phenyl rings but differs significantly from the PSDVB monoliths since it has no ionizable groups on its surface. The NPM is rich in ester functionalities through which the monolith surface can adsorb ions from the electrolyte solution imparting it with the needed zeta potential to generate an adequate EOF [8, 12, 13]. As will be shown in this study, the neutral NPM also exhibited both π-π and hydrophobic interactions towards various solutes, both neutral (e.g. alkylbenzenes, anilines, polycyclic aromatic hydrocarbons) and charged biomolecules (e.g. peptides, proteins). This monolith was also employed to the separation of peptide maps resulting from tryptic digests of standard proteins such as, lysozyme, cytochrome C and β-casein under isocratic elution conditions.

Experimental

Instrumentation

A P/ACE 5010 CE system from Beckman (Fullerton, CA, USA) equipped with a fixed wavelength UV detector was used in this investigation. All electrochromatograms were recorded with a PC running a Gold P/ACE system.

Reagents and materials

2-Naphthyl methacrylate (NAPM), 1-dodecanol, 2,2'-azobis(isobutyronitrile) (AIBN), 3-(trimethoxysilyl)propyl methacrylate, alkylbenzenes (ABs), nitroalkanes (NAs), polycyclic aromatic hydrocarbons (PAHs), anilines, and analytical-grade acetone were from Aldrich (Milwaukee, WI, USA). Egg white lysozyme, horse heart cytochrome C, bovine erythrocytes carbonic anhydrase, bovine milk β-lactoglobulin A and B and bovine milk α-lactalbumin, peptides and trypsin TPCK from bovine pancreas were purchased from Sigma (St. Louis, MO, USA). Tryptic protein digestion (e.g., chicken white lysozyme, horse heart cytochrome C and bovine milk β-casein) was performed after protein reduction and alkylation using the Promega protocol. Cyclohexanol was purchased from J.T. Baker (Phillipsburg, NJ, USA). HPLC-grade acetonitrile (ACN) were from Fischer Scientific (Fair Lawn, NJ, USA). Buffer solutions were prepared using monobasic sodium phosphate from Mallinckrodt (Paris, KY, USA). Fused-silica capillaries with an internal diameter (id) of 100 μm were from Polymicro Technologies (Phoenix, AZ, USA).

Crosslinker synthesis

The procedure for the synthesis of the crosslinker, 1,4-phenylene diacrylate (PDA, for structure see **I**), was obtained from the literature [10, 14] and modified as follows: 4.62 g (42 mmol) of hydroquinone was dissolved in 80 mL dried THF with 7.7 mL (94.8 mmol) triethylamine at room temperature under nitrogen. After stirring the reaction under nitrogen for 20 min, 7.7 mL (94.8 mmol) of acryloyl chloride was added slowly from a dropping funnel for a period of 15 min. The reaction was continuously

stirred and the reaction progress was monitored by TLC using a hexane:ethylacetate (9:1 mixture). On achieving a 100% conversion of reactants to product as indicated by the TLC, the residue was dissolved in ether. The ether solution was washed twice with a 5% solution of acetic acid followed by a saturated $NaHCO_3$ wash. It was finally washed with distilled water after which it was dried over anhydrous $MgSO_4$. Diethyl ether was removed by rotary evaporation and the crude product purified by recrystallization from cold $MeOH/H_2O$ mixture yielding 6.45 g (70% yield from a theoretical yield of 9.16 g) of 1,4-phenylene diacrylate as white shiny plates with a melting point of 86-87 ˚C. The purity of the product was checked and confirmed by ^1H- and ^{13}C-NMR spectroscopic techniques. ^1H NMR ($CDCl_3$), δ = 7.17 (s, 4H), 6.63, 6.59 (dd; ^3J = 17.2 Hz, 2H), 6.33, 6.31 (dd; ^3J = 10.4 Hz, ^3J = 17.2 Hz, 2H), 6.04, 6.01 (dd; ^3J = 10.4 Hz, 2H). ^{13}C NMR ($CDCl_3$) δ = 164.3, 147.9, 132.8, 127.7, 122.4 ppm.

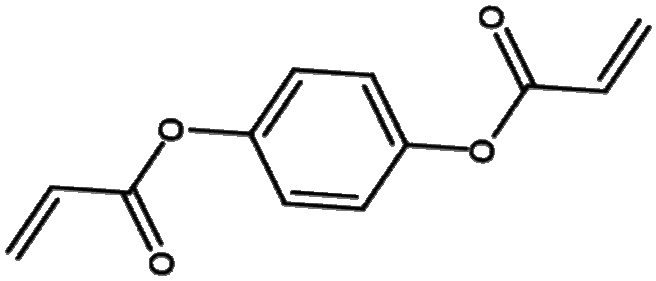

PDA (**I**)

Column pretreatment

The inner wall of the fused-silica capillary was treated with 1.0 M sodium hydroxide for 30 min, flushed with 0.10 M hydrochloric acid for 30 min, and then rinsed with water for 30 min. The capillary inner wall was then allowed to react with a solution of 50% v/v of 3-(trimethoxysilyl)propyl methacrylate in acetone for 6 h at room temperature to vinylize the inner wall of the capillary. Finally, the capillary was rinsed with acetone and water and then dried with a stream of nitrogen.

In situ polymerization

Polymerization solutions weighing 0.5 g each were prepared from 15% NAPM as the monomer, 15% 1,4-PDA as the crosslinker and porogenic solvents cyclohexanol 53%, dodecanol 14.5% and 2.5% water. AIBN (1.0 wt% with respect to monomers) was added to the solution. The polymerization solution was warmed in a water bath at 40 °C for ~10 min to facilitate the dissolution of the NAPM and PDA in the porogenic solvent. Pretreated capillary columns were warmed in the oven to avoid precipitation of the crosslinker [10]. Thereafter the capillary was filled with the polymerization solution up to 21 cm by immersing the inlet of the capillary into the solution vial and applying vacuum to the outlet to prepare a final column of 30 cm total length. The capillary ends were then sealed using a GC septum and the capillary submerged in a 60 °C water bath for 12 h. The resulting monolithic column was washed with an 80:20 v/v acetonitrile:water mixture using an HPLC pump. A detection window was created at 1-2 mm after the end of the polymer bed using a thermal wire stripper. Finally, the column was cut to a total length of 27 cm with an effective length of 20 cm.

CEC procedures

Before running the monolithic column on the instrument each day, it was equilibrated with the running buffer using a syringe pump for 30 min. Thereafter, the column was placed in the CEC instrument and equilibrated with the mobile phase by applying a stepwise increase in voltage up to 25 kV. The column was further equilibrated at the running voltage until a stable current and baseline were observed. Separations were performed at 25 °C at several voltages as stated in the figure captions. Mobile phases were prepared by adjusting the pH of the aqueous solution before the ACN was added. The samples were injected electrokinetically at various applied voltages as stated in the figure captions.

Results and discussion

EOF and electrochromatographic characterization

EOF velocity. In order to understand the effect of PDA on the EOF, thiourea, the EOF marker was injected at 70% ACN, 5 mM sodium phosphate monobasic, pH 7, at 20 kV on a column made from TRIM [12] (see Chapter II) and one made from PDA as the crosslinker. On the neutral monolithic column made from TRIM, the EOF was 0.88 mm/s whereas for the column made from PDA, the EOF was 1.96 mm/s. This represents a doubling of the EOF under otherwise the same electrochromatographic conditions on changing the crosslinker from TRIM to PDA at the same 2-naphthyl methacrylate monomer amount and same porogenic solvent. The analysis time for some alkyl benzenes on the column made from TRIM was 23 min. On the other hand, the analysis time of the same mixture on the column made from PDA was 7 min, which represents a

reduction of analysis time by a factor of three. The fact that PDA is an acrylate and TRIM a methacrylate might explain the higher EOF generated by NPM. It is believed that the acrylate-based monolith NPM adsorbs more ions from the mobile phase than the methacrylate-based one NMM.

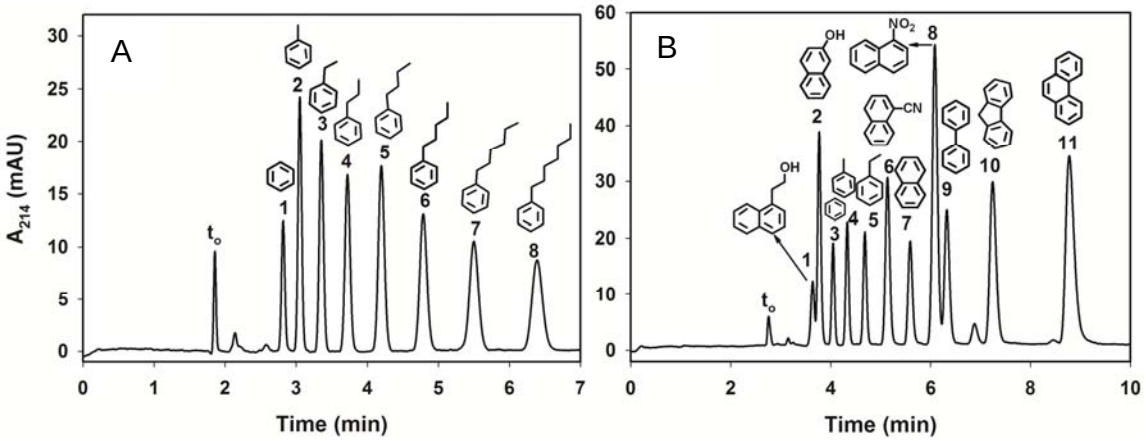

Figure 1. *Electrochromatograms showing the separation of alkylbenzenes in (A) and polycyclic aromatic hydrocarbons in (B). 20 cm effective length, 27 cm total length × 100 μm id. Mobile phase: 5 mM sodium phosphate, pH 7.0, at 70% v/v ACN; running voltage, 20 kV in (A) and 15 kV in (B); electrokinetic injection for 3 s at 10 kV. Solutes: (A) 1, benzene; 2, toluene; 3, ethylbenzene; 4, propylbenzene; 5, butylbenzene; 6, pentylbenzene; 7, hexylbenzene; 8, heptylbenzene, (B) 1, naphthaleneethanol; 2, 2-naphthol; 3, benzene; 4, toluene, 5, ethylbenzene; 6, 1-cyanonaphthalene, 7, naphthalene, 8, 1-nitroanthracene; 9, biphenyl; 10, fluorene and 11, phenanthrene. EOF tracer: thiourea.*

Evaluation of Chromatographic retention

Neutral non-polar solutes. A mixture of 8 alkylbenzenes (ABs) was electrochromatographed on the NPM column under study at 70% ACN, 1 mM phosphate at pH 7. Being neutral solutes possessing a benzene ring moiety, the retention of the ABs was governed by a combination of π-π and hydrophobic interactions between the solute and the non-polar π-electron rich naphthyl ligands and the phenyl rich backbone of the NPM. Under these electrochromatographic conditions, the 8 homologous ABs were separated in less than 7 min as can be seen in Fig. 1A.

In another set of experiments, a mixture containing 11 polycyclic aromatic hydrocarbons (PAHs) was electrochromatographed on the neutral NPM column using a hydro-organic mobile phase containing 75% ACN, 5 mM phosphate, pH 7, at 15 kV. The 11 PAHs were baseline separated in 9 min affording an average theoretical plate count of 140,000 per meter (Fig. 1B). The 11 solutes are largely separated based on their π- interactions with the non-polar π-electron rich benzene-based monolith and naphthyl ligands of the stationary phase, as well as hydrophobic interactions. Because a nitro substituent is a relatively polar group, 1-nitronaphthalene would be expected to be less retained than naphthalene in RP-CEC. However, 1-nitronaphthalene was more retained due to the fact that the presence of a nitro group leads to more pronounced π-interactions with the non-polar ligands [8] (see Chapter IV). On the other hand, 1-cyanonaphthalene with a moderately deactivating cyano group is less retained than 1-nitronaphthalene with a stronger deactivating nitro group [16]. On this basis the 1-nitronaphalene should establish stronger π-π interaction than the 1-cyanonaphthalene with the π-rich surface of the NPM.

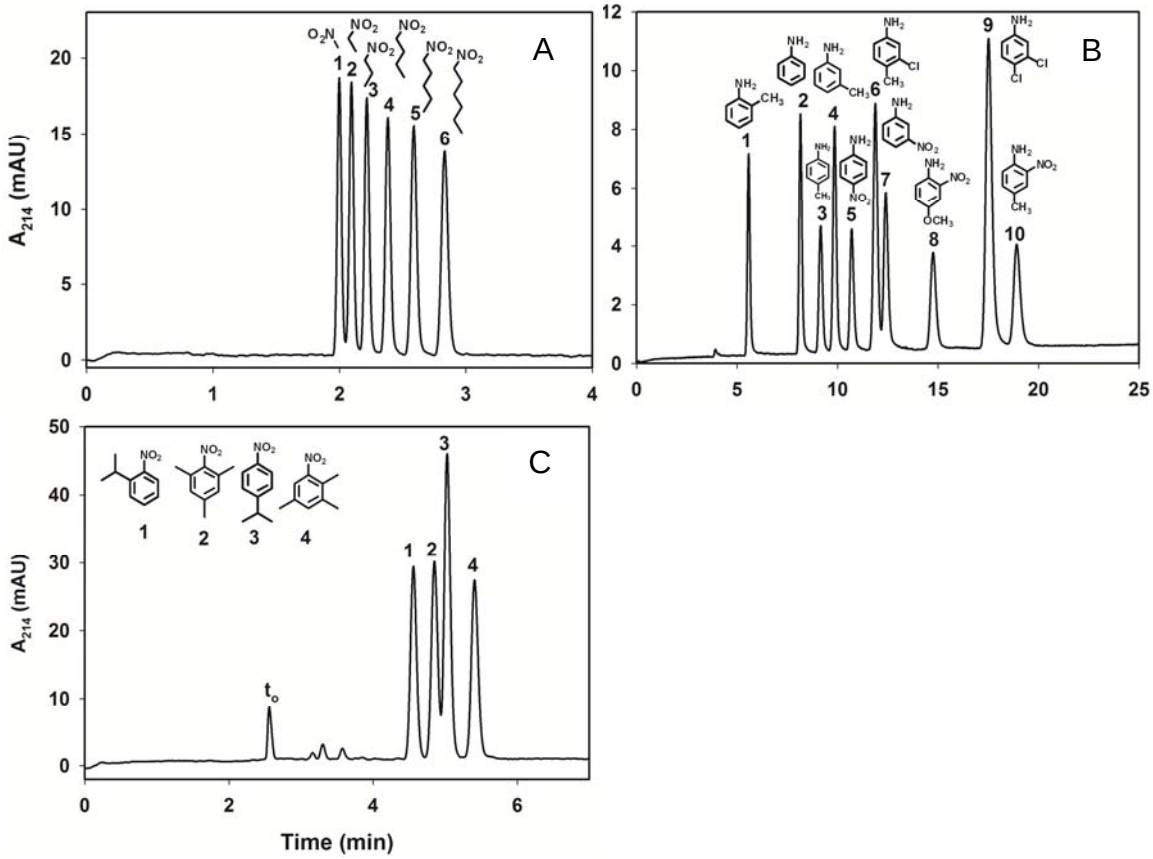

Figure 2. *Electrochromatograms showing the separation of nitroalkanes in (A), anilines in (B) and some structural isomers in (C). Capillary column: 20 cm effective length, 27 cm total length × 100 μm id. Mobile phase: 5 mM in (A) and (C), 1 mM in (B) sodium phosphate, pH 7.0, at 70% in (A) and (C), 50% in (B); running voltage, 20 kV in (A) and (C), 10 kV in (B); electrokinetic injection for 3 s at 10 kV. Solutes: in (A) 1, nitromethane; 2, nitroethane; 3, nitropropane; 4, nitrobutane; 5, nitropentane and 6, nitrohexane, in (B) 1, 2-methylaniline; 2, aniline; 3, 4-methylaniline; 4, 3-methylaniline; 5, 4-nitroaniline; 6, 3-chloro-4-methylaniline; 7, 3-nitroaniline; 8, 4-methoxy-2-nitroaniline; 9, 3, 4-dichloroaniline and 10; 4-methyl-2-nitroaniline, (C) 1, 1-isopropyl-2-nitrobenzene; 2, 1,3,5-trimethyl-2-nitrobenzene; 3, 1-isopropyl-4-nitrobenzene and 4, 1,2,5-trimethyl-3-nitrobenzene.*

Neutral polar solutes. In a second set of experiments and under the same electrochromatographic conditions as for the ABs above, a mixture containing six nitroalkanes of different sizes and hydrophobicity were electrochromatographed on the NPM column. Nitroalkanes possess a polar nitro group that has less π-electron density (2 π electrons) than the benzene moiety of ABs that has more π-electron density (6 π electrons). The retention of the slightly polar NAs arising from a lower π-electron density contribution and less hydrophobicity is therefore lower than the retention of ABs arising from a higher π-electron density and hydrophobicity of the benzene ring moiety. Consequently, while the NAs are eluted in less than 3 min, the elution time of the ABs is twice that of the NAs (Compare Fig. 2A to Fig. 1A).

The separation of basic solutes in CEC can be problematic because of peak tailing caused by the undesirable interactions between these solutes and the fixed charges that are usually incorporated into the stationary phase to support the EOF. Figure 2B shows the separation of a mixture containing 10 aniline derivatives on the neutral NPM with 50/50 v/v ACN/phosphate buffer (pH 7) at a field strength of 500 V/cm (10 kV). The 10 anilines in the mixture were: 2-methylaniline (pKa = 4.44), aniline (pKa = 4.70), 4-methylaniniline (pKa = 4.58) 3-methylaniniline (pKa = 4.73), 4-nitroaniline (pKa = 1.02), 3-chloro-4-methyl aniline (pKa = 4.05), 3-nitroaniline (pKa = 2.50), 4-methoxy-2-nitroaniline (pKa = 0.96), 3,4-dichloroaniline (pKa = 3.33) and 4-methyl-2-nitroaniline (pKa = 0.43). The baseline separation of the 10 aniline derivatives was achieved in 18 min with an average theoretical plate count of 81,000 plates/m with no observable obvious peak tailing. Since the pKa values of these anilines are ≤ 4.73, the solutes are uncharged at pH 7 and their separation is based on their differences in RP

chromatographic partitioning resulting from a combination of hydrophobic and π-interaction. The effect of π-interaction with the aryl rings on the stationary phase was evident by considering the retention of 4-methylaniline and 4-nitroaniline, for example. Possessing a non-polar methyl group at the para position, 4-methylaniline would be expected to elute after 4-nitroaniline, which has a polar nitro group rendering it more polar. On the other hand, however, the nitro group in 4-nitroaniline withdraws electrons from the aromatic ring by resonance and inductive effects lowering the π-electron density of the aromatic ring [16]. The ring therefore becomes a soft Lewis acid that can accept π-electrons from the π-electron rich aryl ligands on the stationary phase which acts as a soft Lewis acid [17], creating a π-π-interaction that preferentially leads to 4-nitroaniline being more retained than 4-methylaniline. Other solutes that are retained more by this kind of π-interaction are 3-chloro-4-methyl aniline and 3-nitroaniline.

In a third set of experiments, a mixture containing four structural isomers of molecular formula $C_9H_{11}NO_2$ namely: 1-isopropyl-2-nitrobenzene, 1,3,5-trimethyl-2-nitrobenzene, 1-isopropyl-4-nitrobenzene and 1,2,5-trimethyl-3-nitrobenzene was separated on the NPM at 70 % ACN, 5 mM phosphate pH 7 at 15 kV. As shown in Fig. 2C, the order of elution was as listed above. This rapid resolution of structural isomers is believed to arise from the presence of an additional π-interaction mechanism offered by the aromatic backbone of the stationary phase in addition to a hydrophobic interaction retention mechanism.

Charged solutes: peptides and proteins. Unlike neutral solutes whose retention is solely based on chromatographic partitioning between the stationary and mobile phase,

multiply charged species such as peptides and proteins are retained on the basis of a combination of their electrophoretic migration and chromatographic partitioning. Before the NPM could be applied to the separation of a complex peptide mixture, its performance was evaluated with a mixture of seven standard peptides namely Ala-Phe, Gly-Trp, Gly-Phe, Gly-Gly-Leu, Gly-Gly-Ala, Phe-Pro and Leu-Phe, Figure 3A shows the separation of the seven standard peptides, with an average separation efficiency of 121,000 plates /m.

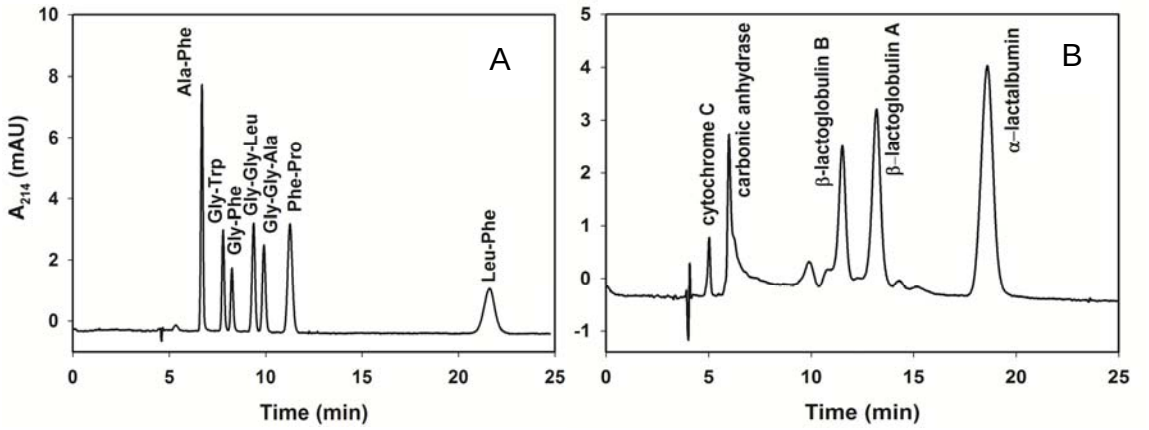

Figure 3. *Electrochromatograms of some standard peptides in (A) and some standard proteins in (B). Capillary columns, 20 cm effective length, 27 cm total length × 100 μm ID; mobile phase, 10 mM sodium phosphate, pH 6.0 in (A) and 7.0 in (B), at 45% in (A) and 50% in (B) v/v ACN; running voltage, 12 kV; electrokinetic injection for 3 s at 10 kV.*

In a second set of experiments, a mixture of five standard proteins namely: cytochrome C (pI = 10.2), carbonic anhydrase (pI = 6.2), β-lactoglobulin B (pI = 5.2), β-lactoglobulin A (pI = 5.1), α-lactalbumin (pI = 4.2-4.5) were separated and eluted in 19

min. As can be seen from Fig. 3B, the five proteins migrated in the order of decreasing pI values with the more acidic α-lactalbumin eluting last while the less acidic cytochrome C eluted first. The unique selectivity of this monolithic column is evident from its ability to afford a complete baseline resolution between β-lactoglobulin B and its polymorph β-lactoglobulin A with only a 0.1 difference in pI value and despite the very small difference in the amino acid sequence of the two β-lactoglobulins. In fact, the bovine β lactoglobulin A variant differs from the β-lactoglobulin B variant by only two amino acids: aspartate-64 (Asp) and valine-118 (Val). These amino acids are substituted by glycine (Gly) and alanine (Ala) in the B variant [18].

Using the same CEC conditions as with the standard peptides, the NPM was successfully applied to the separation of complex peptide mixtures originating from the tryptic digests of the standard proteins lysozyme, cytochrome C and β-casein as shown by Fig. 4A, 4B and 4C, respectively. These results are indicative of the usefulness of NPM in tryptic peptide mapping.

Conclusions

This study has advanced the use of polystyrene-like monoliths for use in RP-CEC. The described monolith bearing polar ester functional groups allowed the monolith's surface to adsorb mobile phase ions imparting the NPM with the desired zeta potential to generate an adequate EOF velocity. The NPM was successfully applied to the separation of a wide range of solutes differing in polarity, size and charge

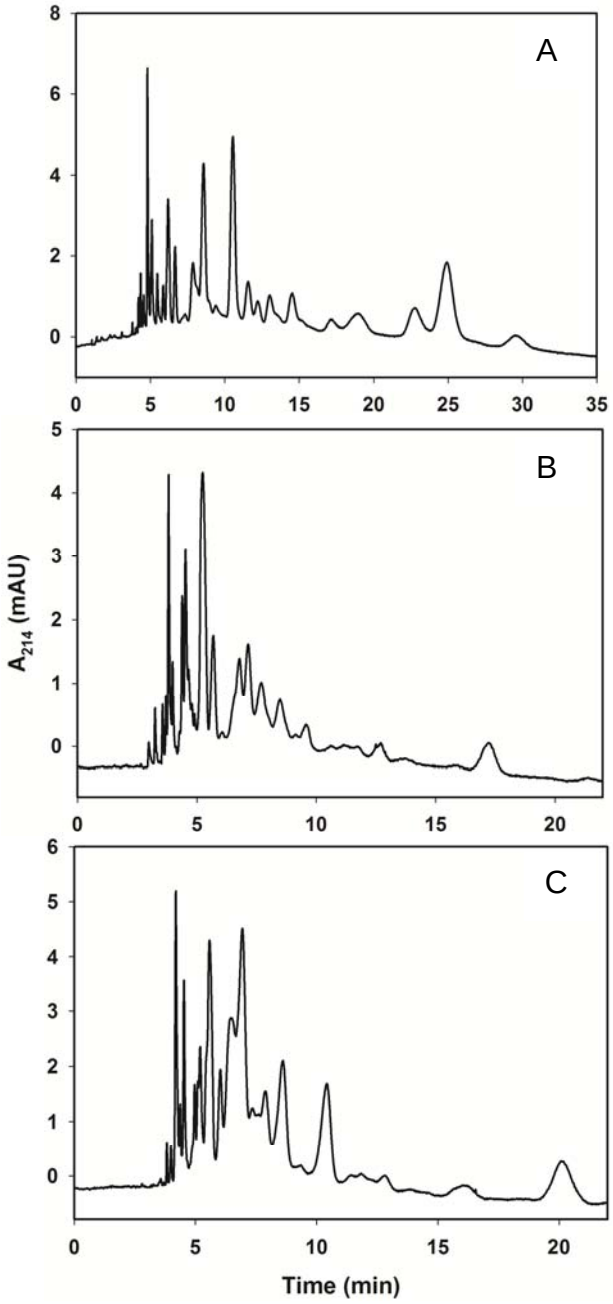

Figure 4. *Electrochromatograms of the separation of tryptic digest of chicken white lysozyme in (A), cytochrome C in (B) and β-casein in (C). Capillary columns, 20 cm effective length, 27 cm total length × 100 μm ID. Other conditions as in Fig.3 A.*

.

References

1. Svec, F., *J. Chromatogr. A* **2010**, *1217*, 902-924.
2. Ku, Z., ccaron, erová, Szumski, M., Buszewski, B., Jandera, P., *J. Sep. Sci.* **2007**, *30*, 3018-3026.
3. Svec, F., Huber, C. G., *Anal. Chem.* **2006**, *78*, 2100-2107.
4. Trojer, L., Lubbad, S. H., Bisjak, C. P., Bonn, G. K., *J. Chromaogr. A* **2006**, *1117*, 56-66.
5. Huang, H.-Y., Huang, I.-Y., Lin, H. Y., *J. Sep. Sci.* **2006**, *29*, 2038-2048.
6. Huang, H.-Y., Liu, Y.-C., Cheng, Y.-J., *J. Chromatogr. A* **2008**, *1190*, 263-270.
7. Svec, F., *Electrophoresis* **2009**, *30*, S68-S82.
8. Karenga, S., El Rassi, Z., *Electrophoresis* **2010**, *31*, 991-1002.
9. Szumski, M., Buszeweski, B., *J. Sep. Sci.* **2007**, *30*, 55-66.
10. Bisjak, C. P., Lubbad, S. H., Trojer, L., Bonn, G. K., *J. Chromatogr. A* **2007**, *1147*, 46-52.
11. Bisjak, C. P., Trojer, L., Lubbad, S. H., Wieder, W., Bonn, G. K., *J. Chromatogr. A* **2007**, *1154*, 269-276.
12. Karenga, S., El Rassi, Z., *J. Sep. Sci.* **2008**, *31*, 2677-2685.
13. Okanda, F., El Rassi, Z., *Electrophoresis* **2005**, *26*, 1988-1995.
14. Li, L., Hayakawa, T., Yonetake, K., Ueda, M., *Macromole. Chem. Phys.* **2000**, *201*, 1667-1672.
15. Graham Solomons, T. W., Fryhle, C. B., Organic Chemistry, John Wiley & Sons, Inc **2008**, pp. 650 - 653.
16. Reubsaet, J. L. E., Vieskar, R., *J. Chromatogr. A* **1999**, *841*, 147-154.

17. Meza-Nieto, M. A., Vallejo-Cordoba, B., Gonzalez-Cordova, A. F., Felix, L., Oycoolea, F. M., *J. Dairy Sci.* **2007**, *90*, 582-593.

CHAPTER VI

CONTROLLING RETENTION, SELECTIVITY AND MAGNITUDE OF ELECTROOSMOTIC FLOW BY SEGMENTED MONOLITHIC COLUMNS CONSISTING OF OCTADECYL AND NAPHTHYL MONOLITHIC SEGMENTS–APPLICATIONS TO RP-CEC OF BOTH NEUTRAL AND CHARGED SOLUTES

Introduction

The electroosmotic flow (EOF) in CEC has the same function as the mechanical pump used in HPLC. Similar to the pressure driven flow in HPLC, the EOF in CEC is the driving force that brings about differential migration thus allowing the rapid and efficient separation of neutral and charged solutes in a single CEC run. Contrary to the "bullet shaped" flow profile in HPLC that gives rise to band broadening, the flat flow profile of EOF is particularly favorable as it does not contribute to band broadening.

Since high EOF velocity is required for rapid separations by CEC, ways of increasing the EOF velocity should be developed to further enhance the CEC technique. Traditionally, the major approach for controlling the magnitude and direction of EOF has

been the intentional inclusion of fixed charges on the surface of the stationary phase to support EOF [1-3]. This approach however, suffers from electrostatic attraction/repulsion of charged solutes of opposite/equal signs as that of the stationary phase charges. While possessing the same charge sign as the stationary phase leads to solute repulsion and consequently little or no retention that translates into poor selectivity, solutes having charges of opposite sign to the stationary phase will undergo electrostatic attraction leading to band broadening and in some cases irreversible adsorption of polyionic solutes (e.g., proteins and peptides) to the stationary phase fixed charges [4, 5].

As early as 1999, the problem of electrostatic interactions of charged solutes with the stationary phase charged groups of opposite charge sign was recognized and addressed by Yang and El Rassi who introduced packed segmented capillaries for the control and manipulation of EOF [6]. These packed capillaries had one segment packed with octadecyl silica (ODS) and served as the separation segment while the other segment was packed with bare silica and functioned as the EOF accelerator segment [6]. Later on, Wen *et. al*. demonstrated that an equi-diameter open tubular auxiliary column offered a greater enhancement of EOF velocity than a packed segment [7].

Later in 2005, Okanda and El Rassi [8] introduced a neutral stearyl acrylate monolith for the separation of a wide range of neutral and charged species including peptides and proteins at zero electrostatic interactions thus yielding high separation efficiency of ~600,000 plates/m for proteins [9]. This stearyl monolith produced a relatively strong EOF velocity despite the fact that it was devoid of fixed charges. The EOF was the result of the adsorption of mobile phase ions, which imparted the monolith with the zeta potential necessary to support the EOF. In further contributions to neutral

monolithic columns void of any fixed charges and which are capable of generating moderate EOF over a wide range of pH and ACN concentration, Karenga and El Rassi introduced an octadecyl acrylate monolith (ODM) and a naphthyl methacrylate monolith (NMM) [10, 11] (see Chapter II and IV, respectively) each of which produced sufficient EOF to carry out the separation of a wide range of species. While the ODM exhibited the regular reversed phase behavior based solely on hydrophobic interaction, the NMM column exhibited a reversed phase mechanism controlled by both hydrophobic interaction and π-π interactions with neutral and charged aromatic solutes. The ODM yielded higher EOF velocity than the NMM column under otherwise identical operating conditions.

In order to realize the full benefits of ODM and NMM in terms of EOF, retention and selectivity, segmented monolithic capillary (SMC) columns formed from these two different stationary phases, which exhibit different reversed phase retention mechanisms and flow are reported in this investigation. The segmented monolithic columns were made by sequentially filling a capillary column segment first with ODM whose mechanism of retention is purely based on the hydrophobicity of the solute followed by NMM whose retention mechanism is based on a combination of both π-π and hydrophobic interactions. The fact that the two monoliths used in this study were prepared using the same porogenic solvent and crosslinker has facilitated the control of polymerization of the two monoliths in two adjacent separate segments in the same capillary.

Since both monoliths exhibited differences in flow and retention mechanisms, the segmented monolithic capillaries (SMC) provided a better way of tuning EOF, selectivity

and retention by manipulating the fractional length of each segment in the SMCs. The SMCs allowed the separation of a wide range of solutes such as ABs, NAs, benzene derivatives, PAHs and toluene derivatives that are difficult to separate using conventional alkyl ligands. At some fractional length of ODM, the fabricated SMC allowed the separation of charged solutes like peptides and proteins that could not otherwise be achieved on a monolithic column made from the isotropic stationary phase NMM due to the lower EOF exhibited by this monolithic column.

Experimental

Instrumentation

A P/ACE 5010 CE system from Beckman (Fullerton, CA, USA) equipped with a fixed wavelength UV detector and a P/ACE 5510 system were used in this investigation. All electrochromatograms were recorded with a PC running a Gold P/ACE system. The samples were injected electrokinetically at various applied voltages as stated in the figure captions.

Reagents and materials

Trimethylolpropane trimethacrylate (TRIM), octadecyl acrylate (ODA), naphthyl methacrylate (NAPM), 2,2'-azobis(isobutyronitrile) (AIBN), 3-(trimethoxysilyl)propyl methacrylate, alkylbenzenes (ABs), alkyl phenyl ketones, nitroalkanes (NAs), benzene derivatives, polycyclic aromatic hydrocarbons (PAHs), toluene derivatives and analytical-grade acetone were from Aldrich (Milwaukee, WI, USA). Cyclohexanol was purchased from J.T. Baker (Phillipsburg, NJ, USA). Ethylene glycol (EG), and

acetonitrile (ACN) were from Fischer Scientific (Fair Lawn, NJ, USA). Buffer solutions were prepared using monobasic sodium phosphate from Mallinckrodt (Paris, KY, USA). Peptides, egg white lysozyme, horse heart cytochrome C, bovine erythrocytes carbonic anhydrase, bovine milk β-lactoglobulin A and B and bovine milk α-lactalbumin were purchased from Sigma (St. Louis, MO, USA). Fused-silica capillaries with an internal diameter (ID) of 100 µm were from Polymicro Technologies (Phoenix, AZ, USA).

Column pretreatment

The inner wall of the fused-silica capillary was treated with 1.0 M sodium hydroxide for 30 min, flushed with 0.10 M hydrochloric acid for 30 min, and then rinsed with water for 30 min. The capillary inner wall was then allowed to react with a solution of 50% v/v of 3-(trimethoxysilyl)propyl methacrylate in acetone for 6 h at room temperature to vinylize the inner wall of the capillary. Finally, the capillary was rinsed with acetone and water and then dried with a stream of nitrogen.

In situ polymerization

Polymerization solutions weighing 0.5 g each were prepared from 15% NAPM as the monomer, 15% TRIM as the crosslinker and porogenic solvents in the ratios of 30:70 w/w monomers/porogenic solvents [11] (see Capter IV). The mixtures of monomer and crosslinker were dissolved in a ternary porogenic solvent consisting of 52.3% cyclohexanol, 15% ethylene glycol and 2.5 % water. 2,2' Azobis(isobutyronitrile) (1.0 wt% with respect to monomers) was added to the solution. The octadecyl monolithic (ODM) columns were fabricated using our previously described method [10] (see chapter II). In brief, polymerization solutions weighing 0.8 g each were prepared from 9.7%

octadecyl acrylate (ODA) as the monomer, 20.5% TRIM as the crosslinker and porogenic solvents cyclohexanol 52.3%, ethylene glycol 15% and 2.5% water. AIBN (1.0 wt% with respect to monomers) was added to the solution. The polymerization solution was warmed in a water bath at 40 °C for ~1 min to facilitate the dissolution of the NAPM/ODA and TRIM in the porogenic solvent. The polymerization solution was then purged with nitrogen for 3 min. A 30 cm pretreated capillary was filled with the polymerization solution consisting of ODA/TRIM/porogenic solvent up to 5, 10, 15 or 20 cm by immersing the inlet of the capillary into the solution vial and applying vacuum to the outlet until the meniscus reached the marked level to prepare a segmented monolithic column filled with 25, 50, 75 or 100 % length of ODM, respectively. Upon filling the column to the predetermined and marked length with ODM, the inlet was quickly immersed into solution vial containing NAPM/TRIM/porogenic solvent and vacuum applied once again to fill the segmented capillary with 20, 15, 10 and 5 cm NAPM/TRIM/porogenic solvent to prepare a segmented monolithic column filled with 100, 75, 50 or 25 % length of NMM. The capillary was coiled several times in order to minimize diffusion at the border section between the two monoliths, sealed using a GC septum and then submerged in a 60 °C water bath for 12 h. The resulting monolithic column was washed with an 80:20 v/v acetonitrile:water mixture using an HPLC pump. A detection window was created at 1-2 mm after the end of the polymer bed using a thermal wire stripper. Finally, the column was cut to a total length of 27 cm with an effective length of 20 cm. A schematic representation of the SMC described above is shown in Fig. 1.

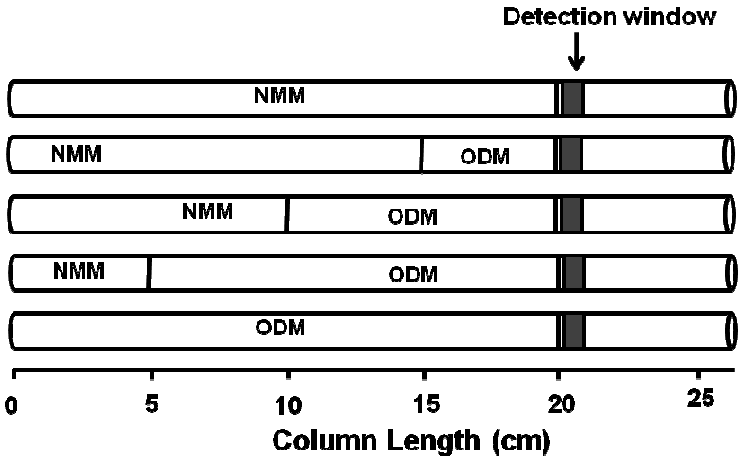

Figure 1. *Schematic representation of the segmented monolithic columns prepared in this study showing each segment filled with NMM and ODM.*

CEC procedures

Before running the monolithic column on the instrument each day, it was equilibrated with the running buffer using a syringe pump for 30 min. Thereafter, the column was placed in the CEC instrument and equilibrated with the mobile phase by applying a stepwise increase in voltage up to 25 kV. The column was further equilibrated at the running voltage until a stable current and baseline were observed. Separations were performed at 25°C at several voltages as stated in the figure captions. Mobile phases were prepared by adjusting the pH of the aqueous solution before the ACN was added. The samples were injected electrokinetically at various applied voltages as stated in the figure captions.

Results and discussion

Effect of the fractional length ODM/NMM in the segmented capillary on EOF

The effect of the fractional length of ODM/NMM in the segmented monolithic column on EOF was investigated at 70% ACN, 5 mM phosphate at pH 7 using thiourea as the EOF marker. An earlier study from our laboratories had shown that ODM generates a faster EOF than NMM under otherwise the same mobile phase composition and running voltage [10, 11]. Filling the monolithic column with a segment containing NMM followed by a segment containing ODM would make the column bearing an EOF accelerator, which is in this case the ODM, and would result in an average EOF that can be manipulated by changing the length of the column segment filled with the EOF accelerator. Figure 2 shows the variation of EOF with the fractional length of capillary segment filled with ODM and NMM. As can be seen from Fig. 2, and as described by equation (1) below, the EOF increases linearly from 0.93 mm/s for a monolithic column filled completely with NMM to 1.18, 1.44, 1.62 and 1.89 at fractional lengths of 0.25, 0.50, 0.75 and 1.0 in ODM, respectively.

The above behavior is in full agreement with the relationship introduced by Nashabeh and El Rassi in 1992 and 1993 [12, 13] for the description of the EOF in coupled fused silica capillaries for rapid capillary electrophoresis of proteins. The EOF velocity in two coupled capillaries (here two adjacent segments) is a weighted average of the intrinsic EOF velocities in the tandem segments, and is given by:

$$\nu_{av} = \frac{\nu_1 l_1}{l_t} + \frac{\nu_2 l_2}{l_t} \qquad (1)$$

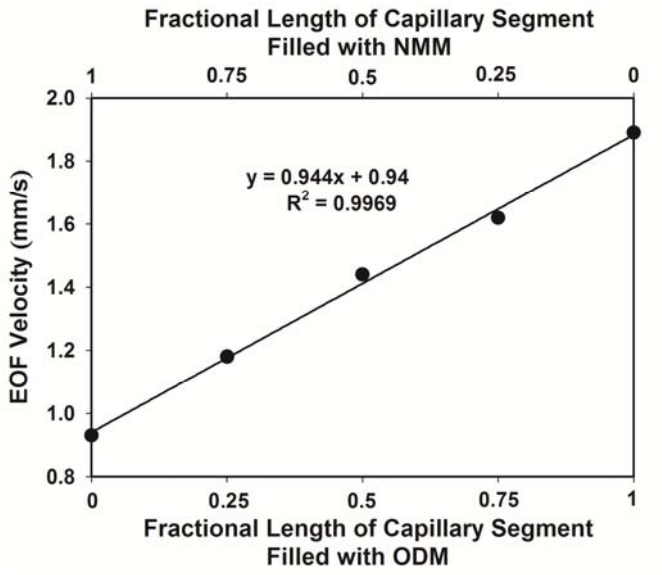

Figure 2. *Variation of EOF velocity (mm/s) with fractional length of capillary filled with ODM/NMM. Capillary column, 20 cm effective length, 27 cm total length × 100 μm ID; mobile phase, 70% ACN, 5 mM sodium phosphate monobasic, pH 7.0; running voltage, 20 kV. EOF tracer, thiourea.*

where ν_1 and ν_2 are the EOF velocities in columns 1 and 2, respectively and l_1, l_2 and l_t are the length of each segment and the total column length, respectively. The above equation (eq. 1) can be rearranged into the following form:

$$\nu_{av} = (\nu_1 - \nu_2)\frac{l_1}{l_t} + \nu_2 \qquad (2)$$

A plot of ν_{av} against l_1/l_t gives a straight line with a slope of $\nu_1 - \nu_2$ and an intercept of ν_2. Also, equations (1) and (2) fitted very well the EOF data obtained with segmented packed

capillary columns having octadecyl-silica and bare silica segment described earlier by Yang and El Rassi in 1999 [6].

Dependence of the retention factor of some representative homologous series on the fractional length of ODM and NMM in the SMCs - Case of alkylbenzenes, alkyl phenyl ketones and nitroalkanes

For a capillary composed of two segments, the k' of a given solute follows in principle the simple additive relationship:

$$k' = \frac{1}{V_M}(V_1 K_1 + V_2 K_2) \qquad (3)$$

where V_M is the volume of the mobile phase in the segmented column, V_1 and V_2 are the volumes of monolith (i.e., sorbent) in segment 1 and segment 2, respectively, and K_1 and K_2 are the equilibrium constants for the partitioning of the solute between the stationary phases in segment 1 and segment 2 and the mobile phase, respectively. Equation 3 translates into a relationship that expresses the k' for a given solute on the SMCs as the weighted average of the retention factor of the solute in the tandem segments, and is given by:

$$k' = \frac{k'_1 l_1}{l_t} + \frac{k'_2 l_2}{l_t} \qquad (4)$$

where k'_1 and k'_2 are the retention factors obtained with the single segment columns filled with monolith 1 and monolith 2, respectively. Equation 4 can be rearranged as follows:

$$k' = (k_1' - k_2')\frac{l_1}{l_t} + k_2' \qquad (5)$$

Three homologous series, namely alkylbenzenes (ABs), alkyl phenyl ketones (APKs) and nitroalkanes (NAs) were chosen to characterize the segmented capillary columns due to the fact that they offer varying degree of nonpolar character and π electrons density. While ABs are the most nonpolar homologous series, APKs are of a relatively medium nonpolarity, and the least nonpolar are NAs (they possess a polar nitro functional group). Although ABs and APKs possess an aromatic benzene ring with 6 π electrons, the benzene ring in ABs is more π donating than the benzene ring in APKs because the former have the weakly activating alkyl chains (i.e., electron-donating chains) whereas the latter have the carbonyl functional group that is an electron withdrawing group, which can partially cancel the effect of the electron donating alkyl chains [14]. The NAs have only 2 π electrons, which make them the compounds of the least π electrons density. The retention of the three different homologous series on the NMM column would result from a combination of some π-π and hydrophobic interactions while their retention on ODM is purely based on hydrophobic interactions.

In order to investigate the effect of varying the length of ODM and NMM in the SMCs on the retention of ABs, APKs and NAs, a mixture of some selected homologous from each series was electrochromatographed on all the SMCs containing 0, 5, 10, 15 and 20 cm length ODM (corresponding to 20, 15, 10 5 and 0 cm NMM) under otherwise the same electrochromatographic conditions. Plots of k' against the fractional length of ODM in the capillary segment are illustrated in Fig. 3. At a first glance, the k' values of ABs, APKs and NAs are higher at 0 cm ODM (i.e., NMM column) than on the ODM

column (20 cm ODM column). As noted previously, this is due to the presence of π-π interaction on the NMM column [11] (see Chapter IV). In all cases, the dependence of the k' values of the solutes on the fractional length of the ODM or NMM segment follows the linear behavior predicted by Eq. 5. The slopes of these lines give an estimate of the difference between the k' values of each solute obtained on single segment monolith (SSM), e.g., the NMM and the ODM, whereas the y-intercepts are the k' values obtained on SSM no. 2. By knowing the k' values on the individual SSM column, the k' values for each solute can be predicted for any SMC.

The homologous series have allowed the confirmation of the linear dependence of the k' values of the solutes on the fractional length of the given segment in the SMC. The electrochromatographic system moves from one retention mechanism to another passing through an intermediate mechanism which is a weighted average of the individual mechanisms, thus allowing the adjustment of the analysis time as well as the selectivity of solutes of varying retention properties, see the next sections.

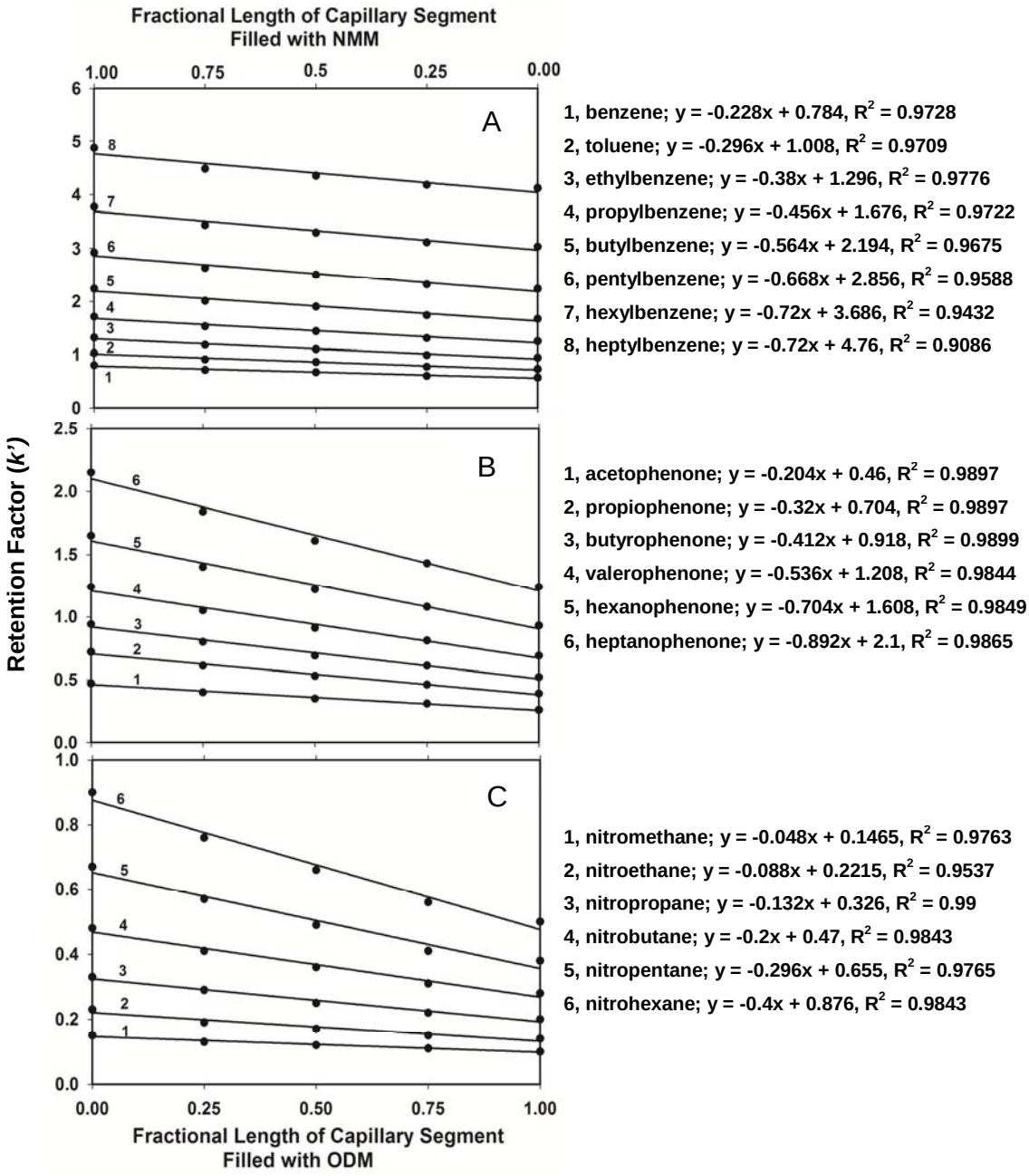

Figure 3. *Plots of retention factor k' against fractional length of capillary filled with ODM/NMM for AB in (A), APK in (B) and NA in (C). Capillary column, 20 cm effective length, 27 cm total length × 100 μm ID; mobile phase, 70% v/v ACN, 5 mM sodium phosphate monobasic, pH 7.0; running voltage, 20 kV; electrokinetic injection for 3 s at 10 kV. EOF tracer, thiourea.*

Dependence of k' and selectivity of solutes of varying electron-donating/electron-withdrawing substituents

Case of benzene derivatives. It has already been reported in a previous study by Karenga and El Rassi that NMM retains solutes by a combination of π-π and hydrophobic interactions [11] (see Chapter IV) while ODM retains solutes purely based on their hydrophobicity [10], see Chapter II. A segmented monolith prepared from these two different monoliths would therefore exhibit a combination of these two interaction mechanisms and which are expected to vary in magnitude as the length of each monolith is varied across the SMCs.

To investigate the variability of retention mechanism on the SMC columns, a mixture containing benzaldehyde, benzonitrile, nitrobenzene, toluene and *m*-dinitrobenzene was electrochromatographed on all the SMCs containing 0, 5, 10, 15 and 20 cm length ODM (corresponding to 20, 15, 10, and 0 cm NMM) at 50% ACN, 1 mM phosphate, pH 7 and 20 kV. These probes possess different functional groups that either impart the solute with a given polarity or affect the solute π-electron density leading to different solute retention in columns exhibiting either π-π and/or hydrophobic interactions. As shown in Fig. 4, the five solutes are completely resolved on a 20 cm NMM column with the order of elution being benzaldehyde, benzonitrile, nitrobenzene, toluene and *m*-dinitrobenzene. The k' values for these solutes on this NMM column are highest compared to k' values obtained on other SMC columns and tend to decrease linearly with increased length of ODM in accordance with eq. 5. On increasing the length of ODM from 0 to 5 cm, the elution order is maintained but with a shortening of the analysis time to only 12 min as compared to the retention time of 24 min at 20 cm

1, benzaldehyde; y = -0.596x + 1.674, R^2 = 0.9977
2, benzonitrile; y = -0.508x + 1.44, R^2 = 0.9949
3, nitrobenzene; y = -1.2x + 2.92, R^2 = 0.9982
4, toluene; y = -0.964x + 3.99, R^2 = 0.9714
5, *m*-dinitrobenzene; y = -3.68x + 5.51, R^2 = 0.9967

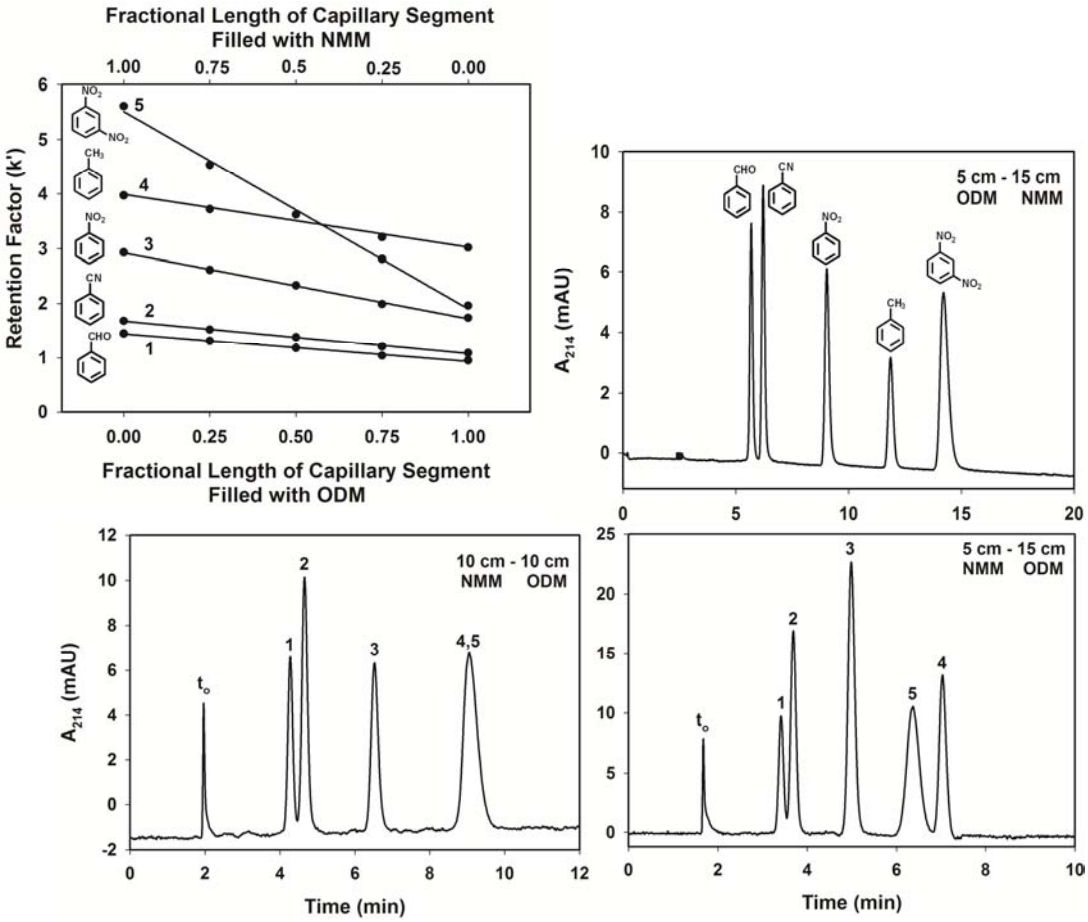

Figure 4. *Plots of retention factor k' against the fractional length of capillary filled with ODM/NMM for benzene derivatives and typical electrochromatograms at different fractional length ODM/NMM as shown in the inserts. Capillary column, 20 cm effective length, 27 cm total length × 100 μm ID; mobile phase, 50% v/v ACN, 1 mM sodium phosphate monobasic, pH 7.0; running voltage, 20 kV; electrokinetic injection for 3 s at 10 kV. EOF tracer, thiourea.*

NMM, which reflects a 50% reduction on analysis time while maintaining good selectivity towards all the solutes.

Two solutes of interest are toluene and *m*-dinitrobenzene, which constitute two representative model solutes to investigate the effect of increasing the length of ODM of the SMC on the π-π interactions. Toluene, which is a benzene ring to which a weak electron donating methyl group is attached, is more hydrophobic than *m*-dinitrobenzene which possesses two strong electron withdrawing groups that lower the π-electron density of its aromatic ring [14]. When the aromatic ring of *m*-dinitrobenzene becomes π-electron deficient, it becomes a soft Lewis acid that can accept π-electrons from the π-electron rich naphthyl ligand on the stationary phase, which in this case becomes a soft Lewis base [15]. Therefore, in a monolithic column that has π-π interaction as the predominant interaction mechanism such as NMM, *m*-dinitrobenzene would be more retained than toluene while the reverse is true for a column exhibiting hydrophobic interactions as the major retention mechanism. On moving to a column made from 10 cm length ODM and 10 cm NMM, both *m*-dinitrobenzene and toluene coeluted and the separation is complete in 10 min, see Fig. 4. On increasing the length of the ODM segment further to 15 cm the two solutes have switched order, whereby now *m*-dinitrobenzene elutes before toluene as the operating retention mechanism has switched majorly to hydrophobic interaction. The retention time at this length of ODM has been reduced to 7 min as shown in Fig. 4.

This experiment has shown that the length of ODM and NMM segments in the SMC columns exhibiting either π-π, hydrophobic or a combination of both interactions

can be varied systematically in order to obtain the selectivity required for achieving a given separation within a satisfactory analysis time.

Case of toluene derivatives. Similarly to the benzene derivatives, a group of 7 toluene derivatives including *p*-toluidine, *p*-tolualdehyde, *p*-tolunitrile, toluene, *p*-nitrotoluene, 2,3-dinitrotoluene, and 2,4,6-trinitrotoluene allowed the illustration of the effect of varying the segment lengths of NMM and ODM in the SMC columns on the separation selectivity and analysis time. Due to the difference in the number and nature of the substituents, the toluene derivatives differ in their π electron density and as well as in hydrophobicity, thus constituting good model solutes to evaluate the effect of the segmented monoliths on selectivity and analysis time. Figure 5 shows the plots of k' versus the fractional length of the segmented capillaries. In all cases, the dependence of k' on the fractional length of the SMC is linear and follows eq. 5. As shown in Fig. 5, a SSM such as the ODM column does not offer the selectivity required (α = 1.01) to resolve toluene and 2,4,6-trinitrotoluene whereas the SSM made of NMM offers a selectivity that is relatively very high (α = 3.51) and beyond what is needed for a good separation within a short analysis time.

In fact, the analysis time with the NMM column is 21.5 min as compared to 6 min on the ODM column. A compromise in selectivity (α = 1.68) and analysis time of 12 min is achieved on a SMC consisting of 15 cm ODM segment and 5 cm NMM segment

1, *p*-toluidine; y = -0.0889x + 0.5, R^2 = 0.9453

2, *p*-tolualdehyde; y = -0.288x + 0.812, R^2 = 0.9657

3, *p*-tolunitrile; y = -0.356x + 0.926, R^2 = 0.9674

4, toluene; y = -0.292x + 1.314, R^2 = 0.9537

5, *p*-nitrotoluene; y = -0.696x + 1.526, R^2 = 0.9904

6, 2,3-dinitrotoluene; y = -0.908x + 1.622, R^2 = 0.9821

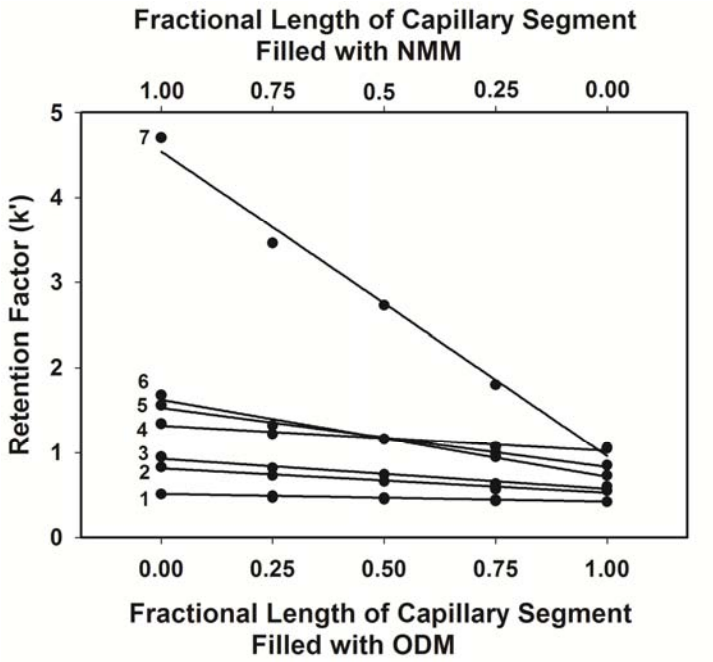

Figure 5. *Plots of retention factor k' against the fractional length of capillary filled with ODM/NMM for toluene derivatives. Capillary column, 20 cm effective length, 27 cm total length × 100 μm ID; mobile phase, 70% v/v ACN, 1 mM sodium phosphate monobasic, pH 7.0; running voltage, 15 kV; electrokinetic injection for 3 s at 10 kV. EOF tracer, thiourea.*

Case of PAHs. Since PAHs contain π-electrons and possess a hydrophobic backbone, they constitute model solutes that can be used to study the selectivity and retention offered by segmented capillaries containing two different stationary phases

exhibiting different retention mechanisms. A mixture containing ten PAHs namely: benzene, 1-cyanonaphthalene, 2-nitrobiphenyl, naphthalene, 1-nitronaphthalene, biphenyl, fluorene, phenanthrene, fluoranthene and pyrene was electrochromatographed using a mobile phase containing 70% ACN, 5 mM phosphate at 20 kV on all the segmented capillary columns filled to different lengths with ODA. A plot of the k' values obtained against length ODM in the segmented monolith is shown in Fig. 5.

Again, the plots are linear as predicted by eq. 5. Generally, the k' values obtained for the 10 PAHs under investigation on a SMC containing 0 cm length ODM (i.e., NMM column) are higher than the k' values obtained for the 10 PAHs on the other SMCs. It is also evident from the plot that at 0 cm length ODM (i.e., NMM column), 2-nitrobiphenyl and naphthalene co-eluted. Although with the NMM column, the retention mechanism is largely based on π-π interactions, these secondary interactions are not sufficient enough to provide baseline resolution of these two solutes. However, as the length ODM in the SMC was increased to 5 cm, these two solutes were well resolved, an indication that a combination of π-π and hydrophobic interactions in different proportions is necessary to achieve their complete resolution. While it took 24 min for all the solutes to be eluted on the NMM column, it took only 17 min for the same solutes to be eluted on a SMC made from 5 cm length ODM and 15 cm NMM, Fig.5. The elution order on both these SMCs was consistent with the elution order listed in the opening sentence of this paragraph. The results discussed above once again demonstrate the applicability of SMC in offering less retention times as well as different and increased selectivity towards various solute probes.

On separating the same PAHs mixture on a SMC with 10 cm length ODM and 10 cm NMM, the SMC is unable to resolve naphthalene and nitronaphthalene (each solute has 10 π-electrons), and these two solute probes co-eluted. Since 1-nitronaphthalene bears a nitro group, it renders it less hydrophobic than its counterpart naphthalene which is on the other hand hydrophobic and which would be expected to elute later than 1-nitronaphthalene on a column that is retaining solutes based on their hydrophobicity. This is some further evidence that at this length ODM, neither π-π nor hydrophobic interactions dominate but they both balance each other. The elution time for the solutes has been reduced to only 13 min. On increasing the length ODM further to 15 cm, there is a complete switch to the elution order of 1-nitronaphthalene and naphthalene whereby now 1-nitronaphthalene elutes before naphthalene since the SMC at this point exhibits hydrophobicity as the dominating retention mechanism. This elution order is maintained on a monolith made of 20 cm length ODM. It can also be seen from Fig. 5 that the k' values obtained on the monolithic column obtained from 20 cm length ODM are the lowest. This observation is not surprising because of the presence of π-π interactions in addition to hydrophobic interactions for PAHs on the NMM column. The elution of the 10 PAHs is completed in 10 and 7 min at 15 and 20 cm length ODM in the SMC, respectively, as shown by the lower two electrochromatograms in Fig. 5.

1, benzene; y = -0.196x + 0.752, R^2 = 0.9335

2, 1-cyanonaphthalene; y = -0.692x + 1.376, R^2 = 0.9852

3, 2-nitrobiphenyl; y = -0.968x + 1.712, R^2 = 0.9789

4, naphthalene; y = -0.616x + 1.726, R^2 = 0.9537

5, 1-nitronaphthalene; y = -1.064x + 1.6, R^2 = 0.9904

6, biphenyl; y = -0.908x + 2.288, R^2 = 0.964

7, fluorene; y = -1.128x + 2.782, R^2 = 0.9634

8, phenanthrene; y = -1.616x + 3.762, R^2 = 0.9689

9, fluoranthene; y = -2.208x + 5.062, R^2 = 0.9748

10, pyrene; y = -2.516x + 5.778, R^2 = 0.967

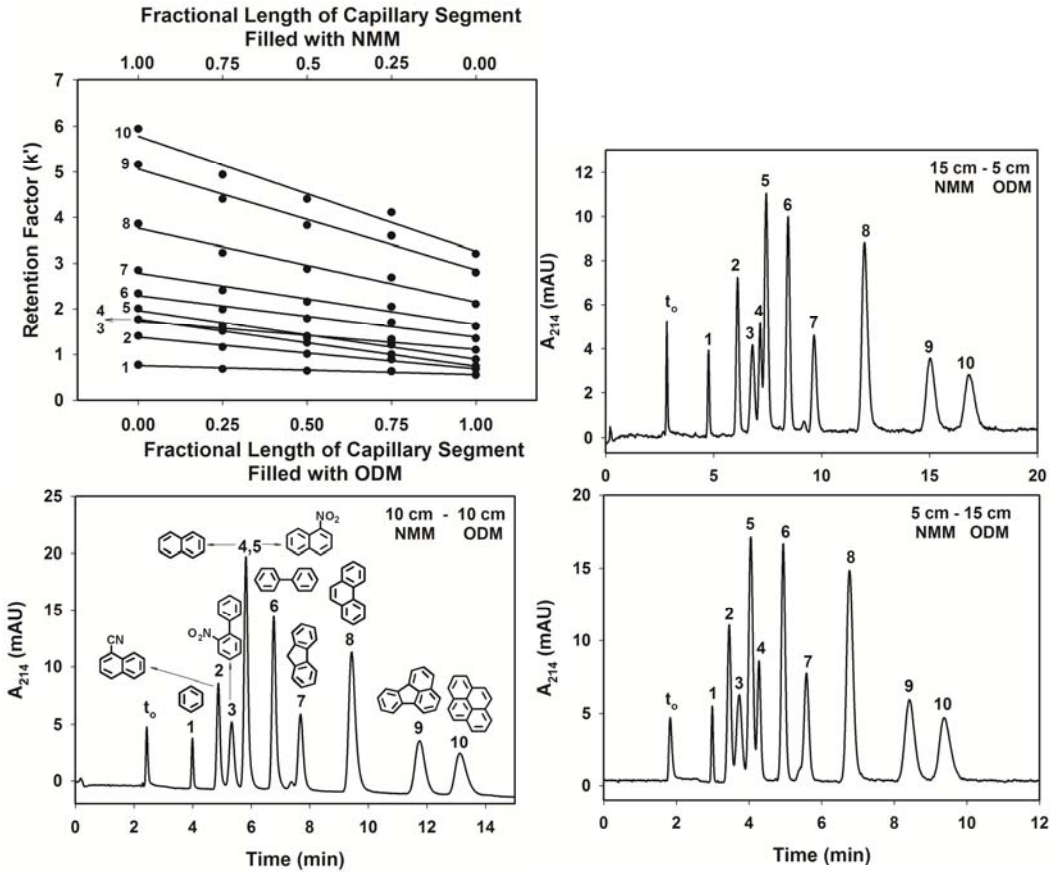

Figure 6. *Plots of retention factor k' against fractional length of capillary filled with ODM/NMM for PAHs and typical electrochromatograms at different fractional length ODM/NMM as shown in the inserts. Capillary column, 20 cm effective length, 27 cm total length × 100 μm ID; mobile phase, 70% v/v ACN, 5 mM sodium phosphate monobasic, pH 7.0; running voltage, 20 kV; electrokinetic injection for 3 s at 10 kV. EOF tracer, thiourea.*

Applications to CEC of charged species–Case of peptides and Proteins

The separation of charged solutes like peptides and proteins in RP-CEC is governed by a dual mechanism that involves a combination of electrochromatographic partitioning and electrophoretic migration. Thus, a monolithic column exhibiting good EOF velocity and combining the two retention mechanisms consisting of π-π and hydrophobic interactions should in principle be suitable for the separation of charged species such as peptides and proteins especially those containing amino acid residues with aromatic side chains such as phenylalanine and tryptophan.

A mixture containing four standard di-peptides: Ala-Phe, Gly-Trp, Gly-Phe, Phe-pro and two standard tri-peptides: Gly-Gly-Leu and Gly-Gly-Ala was run on NMM and ODM columns as well as on the SMC columns using a mobile phase of 50% ACN, 5 mM phosphate, pH 6 and 15 kV, see Fig. 7. The peptides under investigation have pI values of ~6.0 in pure aqueous media. Since the mobile phase used in the run is a hydro-organic mixture, the peptides would not have net zero charges due to the organic solvent, which tends to shift the solute ionization. It is believed that the peptides under study have net negative charges as manifested from the order of their migration, which reflect the presence of both chromatographic partitioning and electromigration. For instance, the tripeptide Gly-Gly-Ala is more retarded than the more hydrophobic Gly-Gly-Leu.

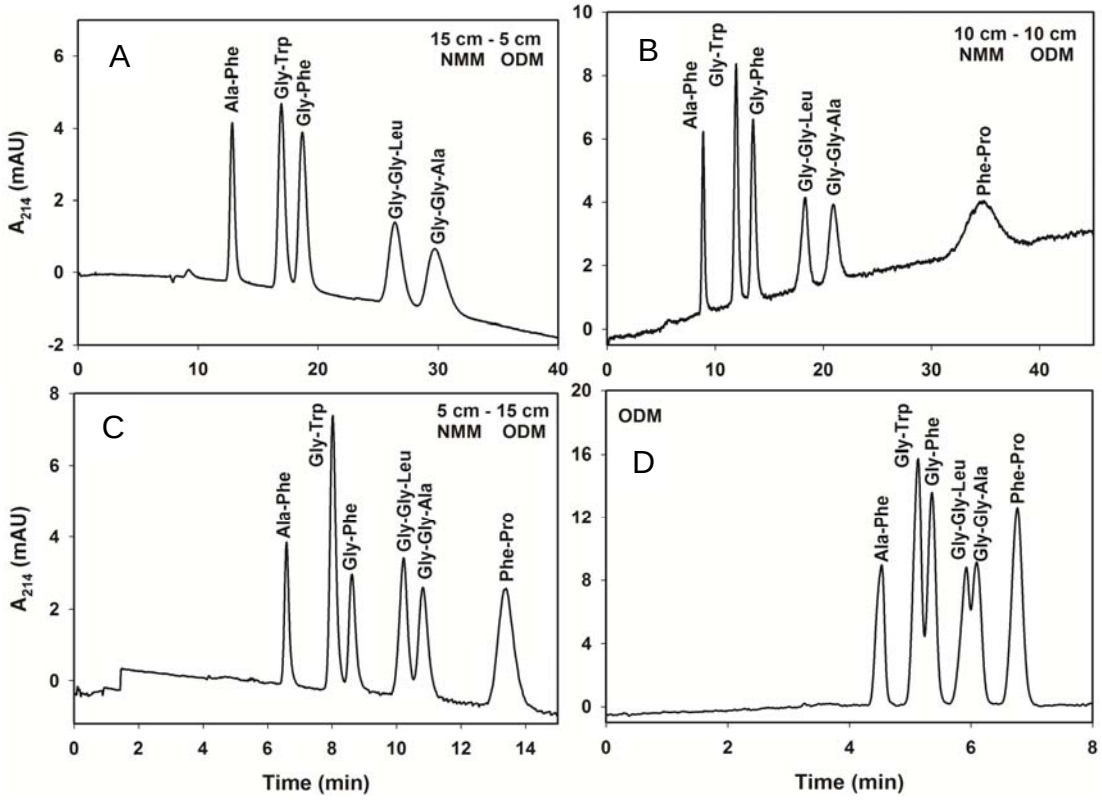

Figure 7. *Electrochromatograms for some standard peptides on SMC filled with different fractional length ODM/NMM. Capillary column, 20 cm effective length, 27 cm total length × 100 μm ID; mobile phase, 50% v/v ACN, 5 mM sodium phosphate monobasic, pH 6.0; running voltage, 12 kV; electrokinetic injection for 3 s at 10 kV.*

The standard peptide mixture was not well separated on either SSC, e.g., NMM or ODM column. The analysis time on the NMM column was relatively long and Phe-Pro was not eluted due to the relatively low EOF velocity (see Fig. 2) observed on the NMM column. By going to an SMC column of 15 cm NMM and 5 cm ODM, the analysis time was still long and Phe-Pro was not eluted too, See Fig. 7A. On the other hand, on the ODM column the mixture was eluted relatively rapidly but the resolution between the two tripeptides Gly-Gly-Leu and Gly-Gly-Ala and the two dipeptides Gly-Trp and Gly-

Phe degraded, se Fig. 7D. A SMC made of 15 cm ODM segment and 5 cm NMM segment exhibited enough flow that allowed a rapid separation of the mixture with very good resolution among the various solutes, See Fig. 7C. The higher retention exhibited by the dipeptide Phe-Pro and the good resolution between the two dipeptides Gly-Trp and Gly-Phe are believed to be due to their aromatic residues Phe and Trp which might establish π-π interactions with the naphthyl moiety of the NMM segment in the segmented capillary column.

The above SMC consisting of 5 cm NMM segment and 15 cm ODM segment was also useful in the separation of 6 standard proteins varying in molecular weights and pI values at pH 7.0, see Fig 8. The 6 proteins span a wide range of pI values from 11 for lysozyme (MW = 14.7 kDa) to 10.2 for cytochrome C (MW = 12.4 kDa) to 5.2 and 5.1 for β-lactoglobulin B and β-lactoglobulin A (both of MW = 18.4 kDa), respectively, to 4.2 trypsin inhibitor (MW = 24 kDa) and to 4.2-4.5 α-lactalbumin (MW = 14.2 kDa). Despite the very small difference in the amino acid sequence of the two β-lactoglobulins, these two closely related variants are very well separated. In fact, the bovine β lactoglobulin A variant differs from the β-lactoglobulin B variant by only two amino acids: aspartate-64 (Asp) and valine-118 (Val). These amino acids are substituted by glycine (Gly) and alanine (Ala) in the B variant [16]. The separation of the 6 standard proteins was achieved in less than 17 min at 12 kV using a mobile phase of 10 mM sodium phosphate at 50% (v/v) ACN.

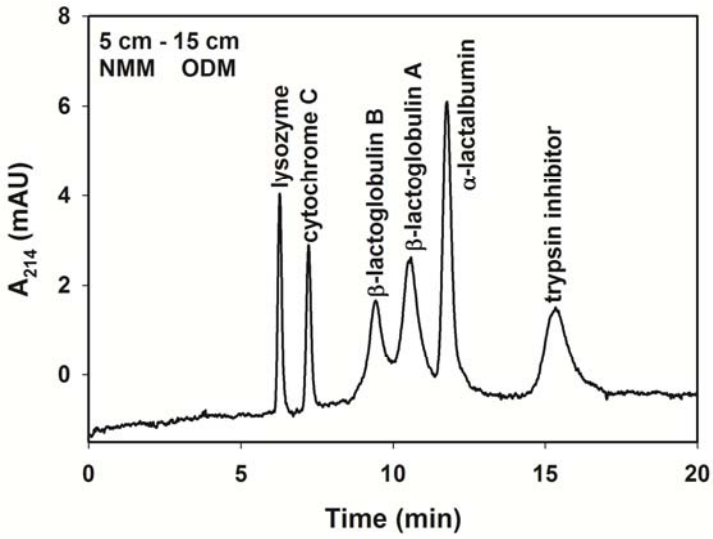

Figure 7 *Electrochromatograms for some standard peptides on SMC filled with different fractional length ODM/NMM. Capillary column, 20 cm effective length, 27 cm total length × 100 μm ID; mobile phase, 50% v/v ACN, 5 mM sodium phosphate monobasic, pH 6.0; running voltage, 12 kV; electrokinetic injection for 3 s at 10 kV.*

Conclusions

Segmented monolithic capillaries consisting of two different monolith segments such as ODM and NMM exhibiting different retention mechanisms have been readily fabricated by the *in situ* polymerization in capillaries filled sequentially with two polymerization mixtures. Since the two monoliths exhibited differences in retention mechanisms and EOF characteristics, the resulting SMC columns offered a unique approach for tuning the EOF, retention and selectivity in a predictable manner for a given separation problem. This facilitated the rapid separation of benzene and toluene derivatives, PAHs, peptides and proteins.

References

1. Bedair, M., El Rassi, Z., *Electrophopresis* **2002**, *23*, 2938-2948.
2. Bedair, M., El Rassi, Z., *J. Chromatogr. A* **2003**, *1013*, 35-45.
3. Svec, F., Peters, E. C., Sykora, D., Frechet, J. M. J., *J. Chromatogr. A* **2000**, *887*, 3-29.
4. El Rassi, Z., *Electrophoresis* **2010**, *31*, 174-191.
5. Szumski, M., Buszeweski, B., *J. Sep. Sci*. **2007**, *30*, 55-66.
6. Yang, C., El Rassi, Z., *Electrophoresis* **1999**, *20*, 18-23.
7. Wen, E., Rathore, A. S., Horvath, C., *Electrophoresis* **2001**, *22*, 3720-3727.
8. Okanda, F., El Rassi, Z., *Electrophoresis* **2005**, *26*, 1988-1995.
9. Zhang, M., El Rassi, Z., J. *Proteome Res.* **2006**, *5*, 2001-2008.
10. Karenga, S., El Rassi, Z., *J. Sep. Sci.* **2008**, *31*, 2677-2685.
11. Karenga, S., El Rassi, Z., *Electrophoresis* **2010**, *31*, 991-1002.
12. Nashabeh, W., El Rassi, Z., J. *High Resolut. Chromatogr.* **1992**, *15*, 289-292.
13. Nashabeh, W., El Rassi, Z., *J. Chromatogr*. **1993**, *632*, 157-164.
14. Graham Solomons, T. W., Fryhle, C. B., Organic Chemistry, John Wiley & Sons, Inc **2008**, pp. 650 - 653.
15. Brindle, R., Klaus, A., *J. Chromatogr. A* **1997**, *757*, 3-20.
16. Meza-Nieto, M. A., Vallejo-Cordoba, B., Gonzalez-Cordova, A. F., Felix, L., Goycoolea, F. M., *J. Dairy Sci.* **2007**, *90*, 582-593.

CHAPTER VII

MIXED LIGAND MONOLITHIC COLUMNS FOR REVERSED-PHASE CAPILLARY ELECTROCHROMATOGRAPHY *VIA* HYDROPHOBIC AND π INTERACTIONS

Introduction

Different approaches are available to manipulate retention and selectivity in CEC. The most practiced approach involves changing the mobile phase composition, including the concentration of the organic modifier, pH and the nature of the buffer and its concentration [1-3]. Another alternative to achieving better selectivity and consequently separation, which is usually undertaken when changing the mobile phase composition does not produce the selectivity needed will be to change the mode of chromatography by changing the nature of the stationary phase. An even more convenient approach is to consider a stationary phase that is a hybrid of two modes of chromatography, which is often referred to as mixed mode chromatography. However, in CEC the mixed mode approach has limitation specially when one of the modes is based on ion exchange and the other mode is dominated by nonpolar interaction because the presence of fixed

charges on the surface of the stationary introduces the nuisance of electrostatic attraction/repulsion towards charged solutes and may result in irreversible adsorption, low selectivity and/or low separation efficiency. Recognizing this serious limitation, we have embarked on developing mixed ligand monolithic (MLM) columns whereby one ligand offers purely hydrophobic interaction while the second ligand offers in addition to hydrophobic interaction a more specific interaction the so called π-π interactions. As will be shown here, the MLM columns provided a unique selectivity that was not achievable by a single ligand monolith (SLM) or single mode stationary phase.

The MLM columns are based on the *in situ* co-polymerization of different compositions of octadecyl acrylate (ODA) and 2-naphthyl methacrylate (NAPM) monomers with the crosslinker trimethylolprpanetrimethacrylate (TRIM) at fixed composition in the presence of a ternary porogenic solvent containing cyclohexanol, ethylene glycol and water. While the ODA ligand exhibits solely nonpolar interactions, the NAPM ligand displays both nonpolar and π-interactions for chromatographic retention with certain solutes. The combination of these two ligands should lead to a monolith characterized by a retention mechanism composed of hydrophobic and π-π interactions toward neutral, polar and charged solutes.

As one could envision, it has to be noted that when mixing in the polymerization solution the ligands at let us say 1:1 ratio (ODA:NAPM) or any other ratios, it should not be interpreted that the resulting monolith surface will have a surface density at 1:1 ratio of the two ligands or any other prefixed ratios, simply because of the difference in reactivity of ODA and NAPM with the crosslinker as well as among the two monomers and within each monomer. This kind of behavior is known in polymer science as the

reactivity ratio. Thus, a short description of the reactivity ratio as it applies to our investigation is in order.

The extent of copolymerization of vinyl monomers having alkyl, aryl or other side chains is controlled by the reactivity ratios of the various monomers involved. The notion of general reactivity or thermodynamic reactivity was advanced by Alfrey and Price in 1947 [4] as it governs reactivity in part, as it must in all chemical processes, and also there may be a polar contribution to reactivity that results from mutual attraction or repulsion between two given reactants. In this treatment, each reactant was given a parameter Q for the monomer and P for the free radical, both of which together denote the general reactivity and another parameter e describing the permanent electric charge carried by the reacting species. For a given reaction between a radical (species 1) and a monomer (species 2), the rate constant k_{12} was postulated to relate the four relevant reactivity parameters, and is given by

$$\boldsymbol{k}_{12} = \boldsymbol{P}_1\boldsymbol{Q}_2 \exp(-\boldsymbol{e}_1\boldsymbol{e}_2) \qquad (1)$$

Assuming that the reactivity of a growing polymeric radical depends only on the nature of the terminal radical unit, the similarity equations for the basic propagation rate constants, k_{11}, k_{21} and k_{22} can be derived. The reactivity ratios r_1 and r_2 are used to eliminate the parameter P for the free radical, and are given by

$$\boldsymbol{r}_1 = \frac{\boldsymbol{k}_{11}}{\boldsymbol{k}_{12}} = \frac{\boldsymbol{Q}_1}{\boldsymbol{Q}_2}\exp[-\boldsymbol{e}_1(\boldsymbol{e}_1 - \boldsymbol{e}_2)] \qquad (2)$$

$$\boldsymbol{r}_2 = \frac{\boldsymbol{k}_{22}}{\boldsymbol{k}_{21}} = \frac{\boldsymbol{Q}_2}{\boldsymbol{Q}_1}\exp[-\boldsymbol{e}_2(\boldsymbol{e}_2 - \boldsymbol{e}_1)] \qquad (3)$$

This led to the so-called Q-e scheme. Despite its shortcomings (see ref. [5]), the Q-e scheme allows at a reasonable approximation the codification of co-polymerization

results in terms of the Q and e values thus leading to a deciding utility and is in good harmony with experimental data. In fact, the free radical copolymerization reactivity ratios (r_1 and r_2) for various monomers are compiled in the Polymer Handbook [6], which constitute the only source for predicting radical copolymerization in use today.

For the purpose of the present investigation on MLM, the use of the notion of reactivity ratio is to delineate the difference in reactivity of the two monomers ODA and NAPM used for the fabrication of MLM. The reported reactivity ratios in the literature refer to two monomers and are not available for polymerization systems composed of three different monomers as in the case of MLM where one monomer, TRIM, makes up the crosslinker and the other two reacting monomers ODA and NAPM constitute the ligands. To judge, at least in a qualitative terms, the extent of the reactivity of ODA and NAPM with TRIM, it would be useful to resurrect to values of reactivity ratios reported in the literature for ODA and NAPM vis-à-vis a given monomer (e.g., methyl methacrylate MMA or styrene). This would allow expressing the differences in the reactivity of both monomers ODA and NAPM toward TRIM. For instance, in the radical copolymerization of MMA (Monomer 1) with ODA (Monomer 2), r_1 and r_2 were reported to be equal to 2.36 and 0.48, respectively [7] while in the radical copolymerization of MMA (Monomer 1) with NAPM (Monomer 2) the r_1 and r_2 values were found to be equal to 0.33 and 1.93, respectively [8]. These two copolymerization systems used very closely related solvents benzene and toluene, which would minimize the effect of the nature of the solvent on reactivity. Relatively speaking, and for the same monomer (in this case MMA), the ODA is much less reactive than its counterpart NAPM; compare 0.48/2.36 = 0.20 to 1.93/0.33 = 5.85. That is by a factor of 30. It has to

be stressed that these reactivity ratios are for binary systems, and therefore may not apply directly to a ternary as the one under study. Nevertheless, these values reveal that the reactivity ratio for NAPM is greater than that for ODA.

For a binary MLM consisting of two ligands, ODA (ligand 1) and NAPM (ligand 2), and whose surface ligand densities are δ_1 and δ_2, respectively, the retention factor k' for a given solute obtained on the MLM column is a weighted average of the k'_1 and k'_2 of that solute obtained on each SLM (i.e., NMM and ODM) and the fractional surface densities of each ligand δ_1/δ_t and δ_2/δ_t as follows:

$$k' = \frac{\delta_1}{\delta_t} k'_1 + \frac{\delta_2}{\delta_t} k'_2 \qquad (4)$$

which can be rearranged to

$$k' = (k'_1 - k'_2)\frac{\delta_1}{\delta_t} + k'_2 \qquad (5)$$

Given the fact that the surface fractional ligand density is directly proportional to the mole fraction of the particular monomer χ used in the in situ polymerization solution, equation 2 can be written as

$$k' = (k'_1 - k'_2)\chi_1 + k'_2 \qquad (6)$$

Despite the potential difference in the reactivity ratios of the two monomers furnishing the two ligands of the MLM, a plot of k' of a given solute versus the mole fraction χ_1 of ligand 1 (ODA here) is in principle a straight line simply because the ligand surface density increases progressively at a fixed steepness with mole fraction regardless of the reactivity ratio of the monomers. According to equation 6, if $k'_1 > k'_2$, the slope of the line is positive. Conversely, the slope of the line is negative. If k'_1 and k'_2 are nearly the same, the slope is zero and k' is virtually independent of the mole fraction.

The rationale behind the fabrication of a MLM is to provide a column with a given surface density in retentive ligands and whose performance supersedes that of a monolith made from only one of the individual ligand (i.e., SLM). In other words, a column made from mixing different ligands should yield a hybrid column with better performance in terms of retention and selectivity towards a given set of solutes. In this report, the effects of the ligand density in the MLM columns on retention factor k', and selectivity for a wide range of solutes differing in polarity and π electrons density are evaluated. Also, the effect of the ligand density on the magnitude of the electroosmotic flow (EOF) velocity is examined.

Experimental

Instrumentation

A P/ACE 5010 CE system from Beckman (Fullerton, CA, USA) equipped with a fixed wavelength UV detector was used in this investigation. All electrochromatograms were recorded with a PC running a Gold P/ACE system. The samples were injected electrokinetically at various applied voltages as stated in the figure captions.

Reagents and materials

Trimethylolpropane trimethacrylate (TRIM), octadecyl acrylate, 2-naphthyl methacrylate (NAPM), 2,2' azobis(isobutyronitrile) (AIBN), 3-(trimethoxysilyl)propyl methacrylate, alkylbenzenes (ABs), alkyl phenyl ketones (APKs), polycyclic aromatic hydrocarbons (PAHs), phenols, anilines, and analytical-grade acetone were from Aldrich (Milwaukee, WI, USA). Cyclohexanol was purchased from J.T. Baker (Phillipsburg, NJ,

USA). Ethylene glycol (EG), dodecanol, HPLC-grade methanol (MeOH) and acetonitrile (ACN) were from Fischer Scientific (Fair Lawn, NJ, USA). 1-Naphthol was from Eastman Kodak (Rochester, NY, USA). Buffer solutions were prepared using sodium phosphate monobasic from Mallinckrodt (Paris, KY, USA). Egg white lysozyme, horse heart cytochrome C, bovine milk β-lactoglobulin A and B and bovine milk α-lactalbumin, peptides and trypsin TPCK from bovine pancreas were purchased from Sigma (St. Louis, MO, USA). Tryptic protein digestion (e.g., chicken white lysozyme) was performed after protein reduction and alkylation using the Promega protocol. Fused-silica capillaries with an internal diameter (ID) of 100 µm were from Polymicro Technologies (Phoenix, AZ, USA). In all cases, the pH value refers to the pH of the aqueous buffer before mixing with acetonitrile.

Column pretreatment

The inner wall of the fused-silica capillary was treated with 1.0 M sodium hydroxide for 30 min, flushed with 0.10 M hydrochloric acid for 30 min, and then rinsed with water for 30 min. The capillary inner wall was then allowed to react with a solution of 50% v/v of 3-(trimethoxysilyl)propyl methacrylate in acetone for 6 h at room temperature to vinylize the inner wall of the capillary. Finally, the capillary was rinsed with acetone and water and then dried with a stream of nitrogen.

In situ polymerization

For the SLM, polymerization solutions were prepared from 0.24 mmol functional monomers (NAPM or ODA) and 0.48 mmol TRIM as the crosslinker. The mixtures of monomer and crosslinker were dissolved in a ternary porogenic solvent (0.88 g)

consisting of cyclohexanol 69.2 wt%, dodecanol 26.7 wt% and water 4.1 wt%. While the making of the ODM in terms of the monomer composition was the same as previously described [9] (see Chapter II) that of NMM was different from the recently published composition [10] (see Chapter IV). For the MLM, NAPM and ODA were blended in different mole% (25, 50, 75) while maintaining the total functional monomer amount at 0.24 mmol to prepare MLM containing 25, 50, 75 mole% ODA and 75, 50, 25 mole% NAPM. In all cases AIBN (1.0 wt% with respect to monomers) was added to the solution. The polymerization solution was warmed in a water bath at 40°C for ~1 min to facilitate the dissolution of the NAPM/ODA and TRIM in the porogenic solvent. The polymerization solution was then purged with nitrogen for 3 min. A 30 cm pretreated capillary was filled with the polymerization solution up to 21 cm by immersing the inlet of the capillary into the solution vial and applying vacuum to the outlet to prepare a final column of 27 total length. The capillary ends were then sealed using a GC septum and the capillary submerged in a 60°C water bath for 12 h. The resulting monolithic column was washed with an 80:20 v/v acetonitrile:water mixture using an HPLC pump. A detection window was created at 1-2 mm after the end of the polymer bed using a thermal wire stripper. Finally, the column was cut to a total length of 27 with an effective length of 20 cm.

Results and discussion

Column fabrication and electrochromatographic characterization

Porogens and monomers composition. Since the two ligands used in the fabrication of the MLM columns have previously been used to make single ligand monoliths (SLM) using two different macroporogens either dodecanol or cyclohexanol [9, 10], it was necessary to determine the best macroporogen that will yield an efficient MLM with a good permeability in a pressure driven flow, which would facilitate the washing and conditioning of the resulting MLM columns.

As a starting point, the mole% ODA in the polymerization solution was varied from 0-25 (i.e., mole% NAPM was varied from 100 – 75) while dodecanol was used as the macroporogen. The resulting columns were found to have a good permeability in a pressure driven flow. To further gain insight into the effect of increasing the mole% ODA (at > 25%), which corresponds to decreasing the mole% NAPM (at < 75%), on the retention of solutes, more monolithic columns were fabricated at 50, 75 and 100 mole% ODA (50, 25 and 0 mole% NAPM) using dodecanol as the macroporogen. However, these columns were found to have no permeability in a pressure driven flow. Therefore, the less polar macroporogen dodecanol was replaced with the more polar macroporogen ethylene glycol (EG) and the resulting monolithic columns had good flow permeability. Ethylene glycol was therefore adopted as the macroporogen of choice in fabricating the MLM columns for this study.

Variation of the EOF with ligand composition of the MLM. Before the fabricated MLM columns could be exploited in CEC, it was important to investigate and understand

each column's performance in terms of EOF. In this regard, the EOF of the various MLM columns was measured using thiourea as the EOF marker under otherwise the same electrochromatographic conditions. As shown in Fig. 1, an increase in mole% ODA from 0 to 50% (i.e., decreasing the mole% of NAPM from 100 to 50%), the EOF increased sharply from 0.8 mm/s to 2.0 mm/s and then leveled off (at 2.1 mm/s) on a further increase of mole% ODA to 75 and 100 (i.e., decrease of mole% NAPM to 25 and 0). From these results, one can conclude that ODA has a higher binding capacity than NAPM for the mobile phase phosphate ions that are responsible for the generation of EOF.

The magnitude of the EOF is also affected by the pore size distribution of the monolith. The sharp increase and leveling off of the EOF at increased mole % ODA (i.e., at decreased mole% NAPM) may reflect a shift in the pore size distribution toward the macroporous size, which would eliminate/reduce double layer overlap in narrow pores thus resulting in increased EOF. In other words, the increased surface density of the MLM in ODA ligand may favor the formation of larger pores.

Mapping the CEC retention of alkylbenzenes, alkyl phenyl ketones and nitroalkanes homologous series. Having concluded that EG was the best macroporogen for fabrication of the MLM columns with different mole% ODA and NAPM in the polymerization solution, and after understanding each column's performance in terms of EOF, it was necessary to evaluate the MLMs performance using solutes with different

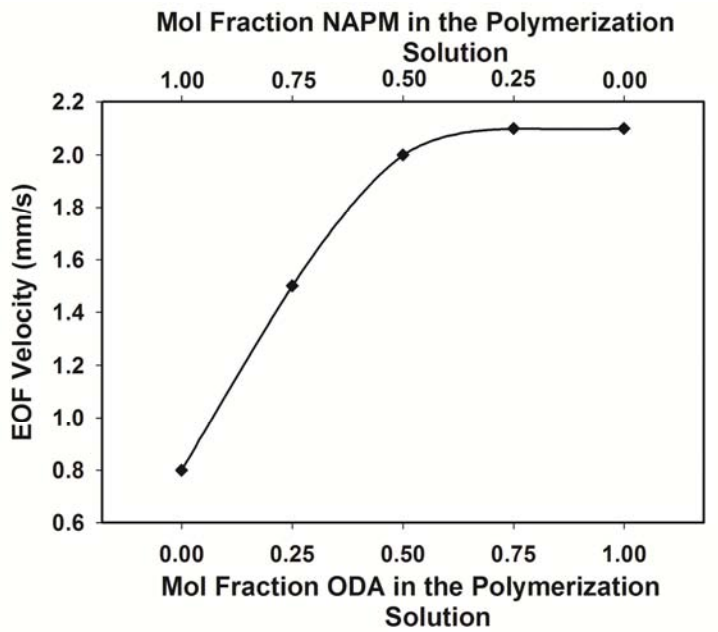

Figure1. *Variation of EOF velocity (mm/s) with mole fraction ODA/NAPM in the polymerization solution. Capillary column: 20 cm effective length, 27 cm total length × 100 μm id, mobile phase: 70% ACN, 5 mM sodium phosphate monobasic, pH 7.0, running voltage: 20 kV. EOF tracer: thiourea.*

π electron density as well as hydrophobicity such as the ABs, APKs and NAs. As stated in Chapter 5, while ABs are the most nonpolar homologous series, APKs are of a relatively medium nonpolarity, and the least nonpolar are NAs (they possess a polar nitro functional group). Although ABs and APKs possess an aromatic benzene ring with 6 π electrons, the benzene ring in ABs is more π donating than the benzene ring in APKs because the former have the weakly activating alkyl chains (i.e., electron-donating chains) whereas the latter have the carbonyl functional group that is an electron withdrawing group, which can partially cancel the effect of the electron donating alkyl chains [11]. The NAs have only 2 π electrons, which make them the compounds of the

least π electrons density. The retention of the three different homologous series *via* the naphthyl ligands would result from a combination of some π-π and hydrophobic interactions while their retention *via* the octadecyl ligands is purely based on hydrophobic interactions.

The results in terms of k' vs. the mole fraction of ODA and NAPM in the polymerization solutions used in preparing the MLM columns for the three homologous series are shown in Fig. 2. As shown in this figure, the k' values for ABs are the highest followed by APKs and then NAs are the least. As described in the introduction, and according to equation 6, the larger the difference in the k' values for a given solute obtained on the individual SLM columns (i.e., ODM and NMM), the steeper the slope of the line. On the other hand, the closer the k' values of a given solute obtained on the 2 SLM columns, the less dependent the k' values of that solute (obtained on the MLM columns) on mole fraction will be. As shown in Fig. 2A, the plots of the k' values of the ABs versus the mole fraction of ODA or NAPM are quasi linear with R^2 in the range of 0.92 to 0.95. This linear behavior is also seen for the upper two homologous of APKs ((i.e., hexanophenone and heptanophenone), see Fig. 2B.

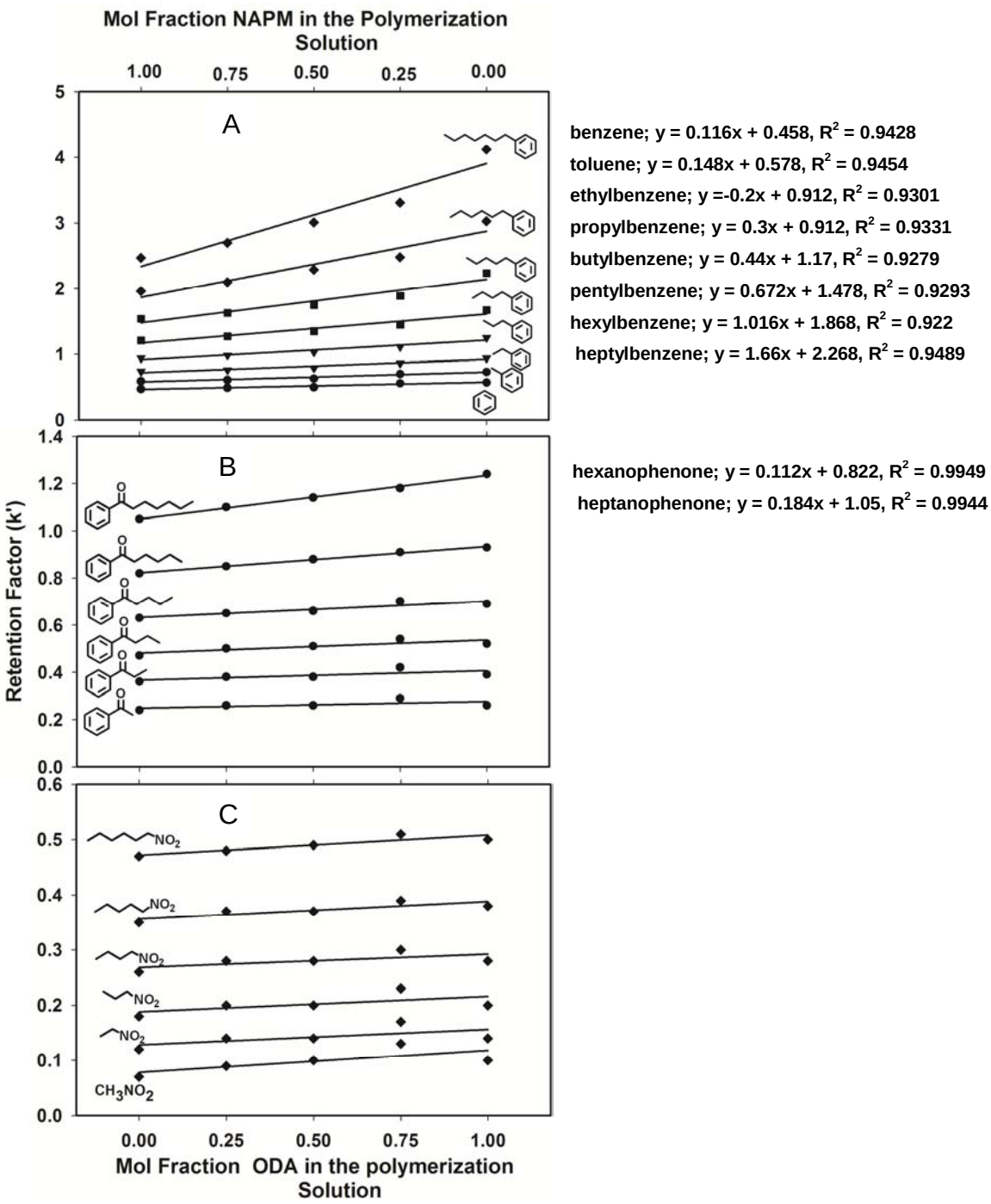

Figure 2. *Plots of retention factor (k') against mole fraction ODA/NAPM in the polymerization solution for ABs in (A), APKs in (B) and NAs in (C). Capillary column: 20 cm effective length, 27 cm total length × 100 μm id, mobile phase: 70% ACN, 5 mM sodium phosphate monobasic, pH 7.0, running voltage: 20 kV. EOF tracer: thiourea.*

For all the solutes including the NAs and the first 4 APKs, the k' is virtually independent of the mole fraction of ODA or NAPM. The observed fluctuations in the k' values of NAs and the first 4 APKs are within the experimental errors.

In short, different solutes would then respond differently to the surface density of naphthyl and octadecyl ligands in the MLM columns. This observation led to mapping the CEC retention of other solutes that are different in their polar character and π electrons content, see the following sections.

Mapping the CEC retention behavior of some representative polycyclic aromatic hydrocarbons (PAHs). In order to further gain insight into the effect of the composition of the MLM column on solute retention, a mixture consisting of eight PAHs probes, namely 1-cyanonaphthalene, naphthalene, 1-nitronaphthalene, biphenyl, fluorene, phenanthrene, fluoranthene and pyrene was separated on the six monolithic columns under investigation. PAHs are model solutes that are characterized by possessing both hydrophobicity and π electrons. Thus, they are ideal for gauging the surface density of the MLM in both the C18 ligand and the naphthyl ligand. As can be seen in Fig. 3, and with the exception 1-nitronaphthalene, the retention of these solutes on the ODM column is higher than on the NMM column under otherwise the same CEC conditions. The 1-nitronaphthalene exhibits more interaction with the NMM than with the ODM column due primarily to the nitro substituent, which confer to the naphthalene ring both less hydrophobic interaction with the ODA ligands and stronger π-π interaction with the naphthyl ligands. As can be seen in Fig. 3, and with the exception of 1-nitronaphthalene,

2, naphthalene; y = 0.244x + 0.88, R^2 = 0.962

4, biphenyl; y = 0.144x + 1.206, R^2 = 0.9337

5, fluorene; y = 0.212x + 1.406, R^2 = 0.966

6, phenanthrene; y = 0.236x + 1.866, R^2 = 0.9378

7, fluoranthene; y = 0.412x + 2.37, R^2 = 0.9669

8, pyrene; y = 0.564x + 2.626, R^2 = 0.979

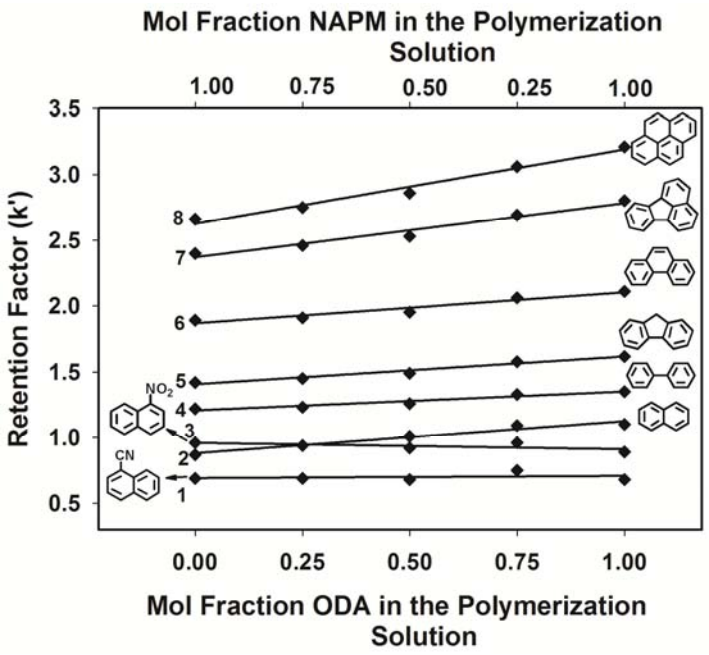

Figure 3. *Plots of retention factor (k') against mole fraction ODA/NAPM in the polymerization solution for polycyclic aromatic hydrocarbons. Capillary column: 20 cm effective length, 27 cm total length × 100 μm id, mobile phase:70 % ACN, 5 mM sodium phosphate monobasic, pH 7.0, running voltage 20 kV. Solutes: 1; 1-cyanonaphthalene; 2; naphthalene, 3; 1-nitronaphthalene; 4; biphenyl; 5; fluorene; 6; phenanthrene; 7; fluoranthene; 8; pyrene. EOF tracer: thiourea.*

the k' values of naphthalene, biphenyl, fluorene, phenanthrene, fluoranthene and pyrene increased quasi linearly with the ODA mole fraction, a behavior that is very similar to that of ABs and is predicted by equation 6. The k' values of 1-cyanonaphthalene on the

ODM and NMM are virtually the same (0.68 vs. 0.9), and as a result the k' values of this solute obtained on the various MLM columns is virtually independent of the mole fraction of ODA and NAPM, see Fig, 3.

In short, while the PAHs without substituents but differing in the π electron density and the hydrophobicity follow more or less the same retention behavior on the MLM columns similar to that of the ABs, the solutes with polar substituents (e.g., 1-nitronaphthalene and 1-cyanonaphtahlene) follow another retention trend; that is a steady slight decrease in k' for 1-nitonaphthalene and a virtually constant k' for 1-cyanonaphthalene with increasing mole fraction of ODA.

Modulating the separation selectivity by MLM

Toluene derivatives. Aromatic compounds with different substituents on the benzene ring represent model solutes that can be used to characterize the retentive properties of the MLM columns that have π electrons density and/or hydrophobic character in different proportions. The substituent on the benzene ring can be an electron withdrawing substituent (referred to as deactivating substituents) thus decreasing the aromatic ring's π electron density. The now deficient aromatic ring becomes a soft Lewis acid that can accept π electrons from a π electron rich ligand (i.e., a soft Lewis base) [12]. This additional form of interaction makes such a solute to be preferentially retained in a column that has π interaction as a second participating separation mechanism relative to a column in which the predominant separation mechanism is based on the hydrophobicity of the solute. The substituent can also impart a certain polarity to the solute thus decreasing the retention of that solute on a column that separates solutes based on their hydrophobicity.

In a series of experiments, 7 toluene derivatives, namely toluene, *p*-toluidine, *p*-tolualdehyde, *p*-tolunitrile, *p*-nitrotoluene, 2,3-dinitrotoluene and 2,4,6-trinitrotoluene were separated on the MLM columns under investigation. The methyl group acts as a weakly activating group, which makes the benzene ring of the toluene more π-donating than benzene itself (i.e., soft Lewis base). At 0 mole fraction ODA (i.e., an SLM corresponding to the NMM column), the retention of 2,4,6-trinitrotoluene was significantly higher (by a factor of 2.3) than that of the solutes toluene, *p*-nitrotoluene and 2,3-dinitrotoluene, which co-eluted, see Fig. 4. The retention order of *p*-toluidine, *p*-tolualdehyde and *p*-tolunitrile followed that of the electron donating/electron withdrawing capability of the substituents (amino, aldehyde and nitrile groups) on the toluene ring, see Chapter 4. This order remained the same as the mole fraction of ODA was increased from 0 to 1. Briefly, an amino group is a strong activating group (i.e., strong electron donating group) that makes the benzene ring a more π-donating then the benzene itself. This is the case of *p*-toluidine, whereby the k' value of this solute is less than that of tolualdehyde and tolunitrile. A cyano group is a moderately deactivating group but stronger than the aldehyde group. This is reflected in the magnitude of retention of *p*-tolualdehyde and *p*-tolunitrile on the NMM column (k' = 0.44 for *p*-tolualdehyde vs. k' = 0.5 for *p*-tolunitrile). At 0.25-mole fraction ODA (i.e., 0.75 mole fraction NAPM), *p*-nitrotoluene and 2,3-dinitrotoluene changed retention order with 2,3-

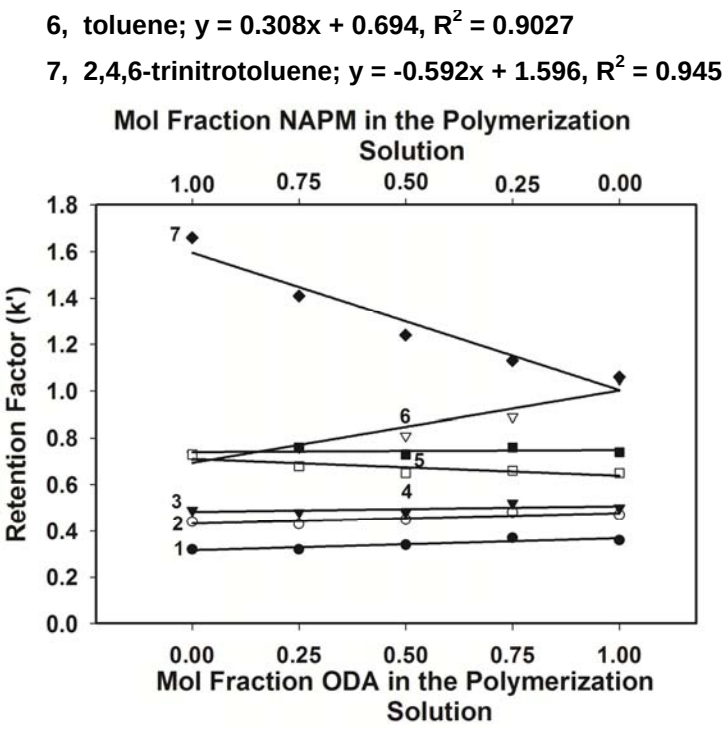

Figure 4. *Plots of retention factor (k') against mole fraction ODA/NAPM in the polymerization solution for toluene derivatives. Capillary column: 20 cm effective length, 27 cm total length × 100 μm id, mobile phase:70 % ACN, 1 mM sodium phosphate monobasic, pH 7.0, running voltage 15 kV. Solutes:1, p-toluidine; 2, p-tolualdehyde; 3, p-tolunitrile; 4, 2,3-dinitrotoluene; 5, p-nitrotoluene; 6, toluene; 7, 2,4,6-trinitrotoluene.*

dinitrotoluene eluting before *p*-nitrotoluene, indicating increased incorporation of ODA ligand in the MLM. This order remained the same as the mole fraction of ODA increased from 0.25 to 1. In this ODA mole fraction range, the k' value of the most polar solute 2,4,6-trinitrotoluene decreased quasi linearly as more ODA ligand was incorporated in the MLM. In other words, as the interaction shifted towards more hydrophobic interaction than π-π interaction, the k' value of the solute decreased linearly in

accordance with equation 6. To a lesser extent, the same trend was observed with *p*-nitrotoluene, see Fig. 4. On the other hand, the k' value of toluene increased linearly as the mole fraction of ODA increased. For the other solutes including *p*-toluidine, *p*-tolualdehyde, *p*-tolunitrile and 2,3-dinitrotoluene, the k' values did not show any virtual dependence on the mole fraction of ODA. The overall picture represents a typical modulation of the k' values and in turn selectivity of solutes varying in polarity and π-electron density. In fact, the selectivity can be readily tuned by varying the composition of the MLM columns in view of equation 6 that allows the prediction of retention and in turn selectivity. For this type of solutes an excellent selectivity is obtained anywhere in the range of mole fraction of 0.5 and 0.8.

Alkylbenzenes and polycyclic aromatic hydrocarbons. A mixture containing 5 ABs and 5 PAHs was electrochromatographed on MLMs containing 0, 25, 50 and 100 mole% ODA in the polymerization solution. At 0 mole% ODA (i.e., NMM column), the 10 solutes were separated within~9 min and there was no good selectivity between 1-nitronaphthalene and butylbenzene (solutes 4 and 5) as seen in Fig. 5. When the same mixture was electrochromatographed on a monolith with 25-mole% ODA, all the 10 solutes were separated within ~ 9 min and with very good selectivity for all the solutes including solute number 4 and 5. Also, heptyl benzene (peak number 8) with its relatively long alkyl chain is now the last eluting peak. For a MLM with 50-mole% ODA, the 10 solutes elute within ~ 7 min but the selectivity for fluorene and 9-

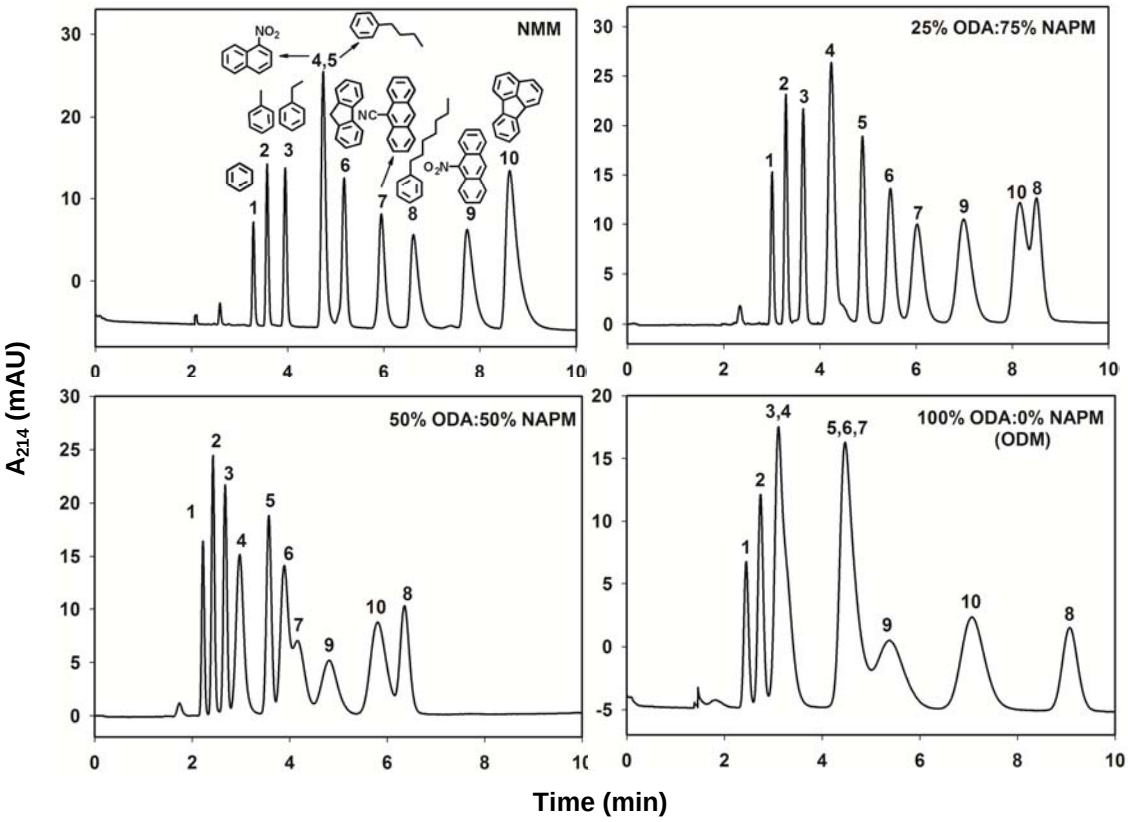

Figure 5. *Electrochromatograms showing the separation of 5 ABs and 5 PAHs on monolithic columns with different mol fraction ODA/NAPM. Capillary column: 20 cm effective length, 27 cm total length × 100 μm ID; mobile phase:70 % ACN, 1 mM sodium phosphate monobasic , pH 7.0, running voltage 20 kV; electrokinetic injection for 3 s at 10 kV. Solutes: 1, benzene; 2, toluene, 3, ethylbenzene; 4, 1-nitronaphthalene; 5, butylbenzene; 6, fluorene;7, 9-anthracenecarbonitrile; 8, heptylbenzene; 9, 9-nitroanthracene; and 10, fluoranthene. EOF tracer: thiourea.*

anthracenecarbonitrile is greatly reduced. A further increase in mole% ODA to 100 (i.e., ODM column) resulted in a further reduction of the selectivity of the column as manifested by the co-elution of ethyl benzene and 1-nitonaphthalene (peaks nos. 3 and 4)

and also the co-elution of butyl benzene, fluorene and 9-anthracenecarbonitrile. From these results, it is evident that for the separation of such a mixture of ABs and PAHs, a MLM consisting of 25 mole% ODA and 75 mole% NAPM would be a good choice offering the best selectivity for the solutes within a reasonable retention time.

Charged solutes

Peptides. The usefulness of the MLM columns under investigation is further demonstrated in the separation of polyionic solutes such as peptides and proteins. Obviously, the retention of such charged species is dependent on both partitioning between the stationary and mobile phases as well as their electrophoretic migration. Six peptides, Ala-Phe, Gly-Trp, Gly-Phe, Gly-Gly-Leu, Gly-Gly-Ala and Phe-Pro were selected as test solutes and separated on four columns with different mole% ODA/mole% NAPM in the polymerization solution using a mobile phase containing 45% ACN, 10 mM NaH_2PO_4 buffer (pH 6.0) at 12 kV. On all the columns tested, the elution order of the di- and tripeptides was Ala-Phe < Gly-Trp < Gly-Phe < Gly-Gly-Leu < Gly-Gly-Ala< Phe-Pro. Under the electrochromatographic conditions used, both chromatographic partitioning between the stationary and mobile phase and the electrophoretic migration are playing roles in the elution order of these peptides. As shown in Fig. 6, major differences in terms of selectivity and retention were observed on the various MLM columns. When an MLM column prepared from 25 mole% ODA and 75 mole% NAPM

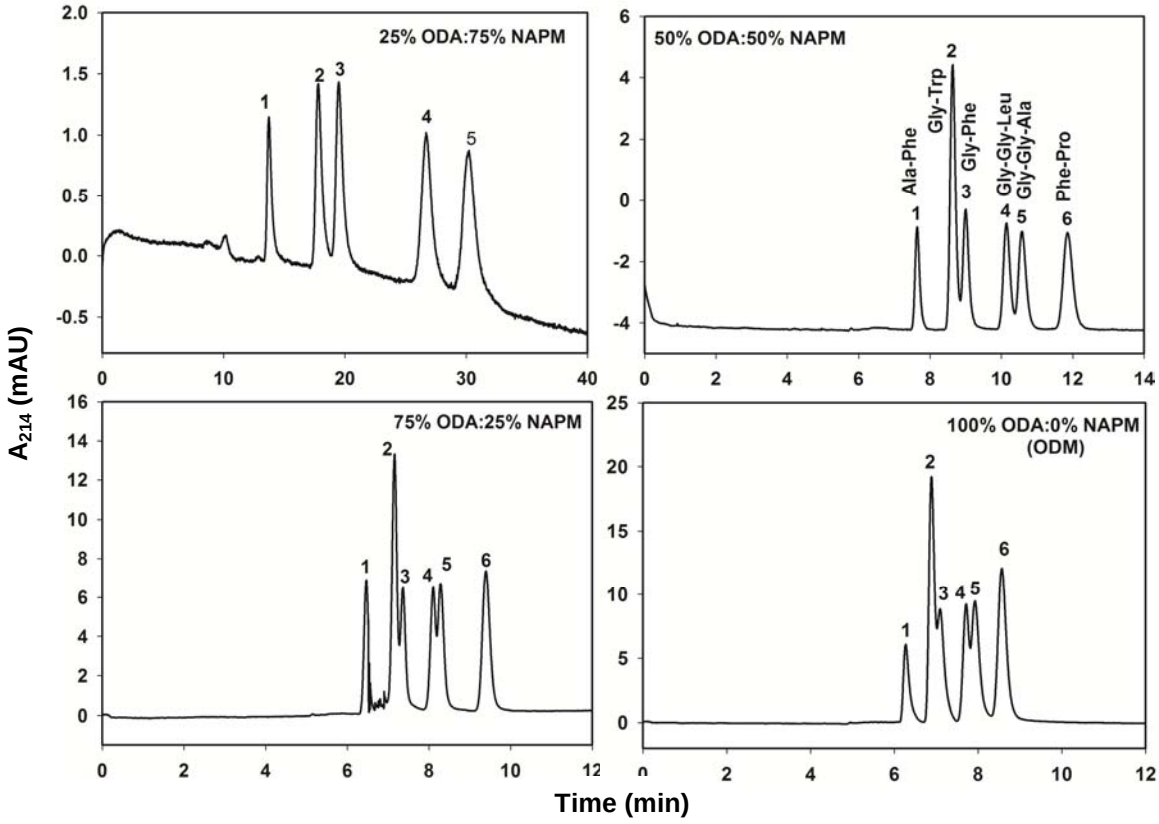

Figure 6. *Electrochromatograms of some standard peptides on monolithic columns made from different mol fraction ODA/NAPM. Capillary columns: 20 cm effective length, 27 cm total length × 100 μm ID; mobile phase, 10 mM sodium phosphate, pH 6.0, at 45% v/v ACN; running voltage, 12 kV; electrokinetic injection for 3 s at 10. Solutes: 1, Ala-Phe; 2, Gly-Trp; 3, Gly-Phe; 4, Gly-Gly-leu; 5, Gly-Gly-Ala; and 6, Phe-Pro.*

was used in the separation of the 6 peptides, it took more than 30 min for five of the peptides to elute and the last dipeptide Phe-Pro was too retained and did not elute under the given CEC conditions or the peak became too diffuse to be detected after allowing the run to go for about 80 min. Because of the relatively slow migration of the peptides on

this MLM column, which gives rise to increased longitudinal molecular diffusion, the peaks are rather broad compared to the peaks observed on the other 3 columns containing increased mole% ODA.

When the same test mixture was separated on a MLM with 50-mole% ODA and 50-mole% NAPM, all six peptides were eluted within 12 min with very good selectivity and efficiency. On a column with 75-mole% ODA and 25-mole% NAPM, the elution time is shortened by 3 min to ~9 min but the selectivity between Gly-Trp and Gly-Phe as well as Gly-Gly-Leu and Gly-Gly-Ala is diminished. This too, is the case at 100-mole% ODA (i.e., ODM column) although the retention time is slightly shorter than the retention at 75-mole% ODA. From these observations, we find that when the column used is a SLM column made up of 75-mole% NAPM it is unable to perform the separation satisfactorily, and an inclusion of 50-mole% ODA perfectly performs the separation with good selectivity and reasonable retention time.

Tryptic peptide mapping. The monolithic columns under investigation were applied to the separation of a complex peptide mixture originating from the tryptic digest of chicken white lysozyme. The electrochromatograms obtained are shown in Fig. 7. The inserts in the electrochromatograms are expanded parts of the early eluting peaks of the peptide map. On the NMM column as well as on the 25 mole% ODA:75 mole% NAPM column, the peptide mapping could not be achieved completely due to the relatively low EOF velocity. The peptide map time became faster and decreased to 30 min on a MLM column made from 50-mole% ODA and 50-mole% NAPM. At 75-mole% ODA, the same separation took about 25 min to complete and only 12 min on the

ODM column. By a closer look at the inserts, which represent an expansion of the first few min of the digest, it is clear that the insert at 50-mole% ODA has more peaks than the other inserts, an indication that at this mole% ODA more selectivity is obtained. These results clearly indicate that the mixing of naphthyl and octadecyl ligands is also useful in the separation of charged solutes. When these interactions are blended at a given composition, good selectivity and retention is achieved for both neutral and charged solutes.

Proteins. Five standard proteins including lysozyme, cytochrome C, β-lactoglobulin A and B and α-lactalbumin spanning a wide range of pI and molecular weights, were separated on the MLM columns under investigation, see Fig. 8. As can be seen in this figure, the MLM column that provided the best separation was that fabricated from 50% mole ODA and 50 Mole% NAPM. At lower ODA composition (i.e., at < 50 mole %) some of the proteins could not be eluted from the MLM column. Columns fabricated from 75-mole% ODA and 25-mole% NAPM and from 100-mole% did not provide sufficient selectivity although the proteins were eluted in less than 6 min.

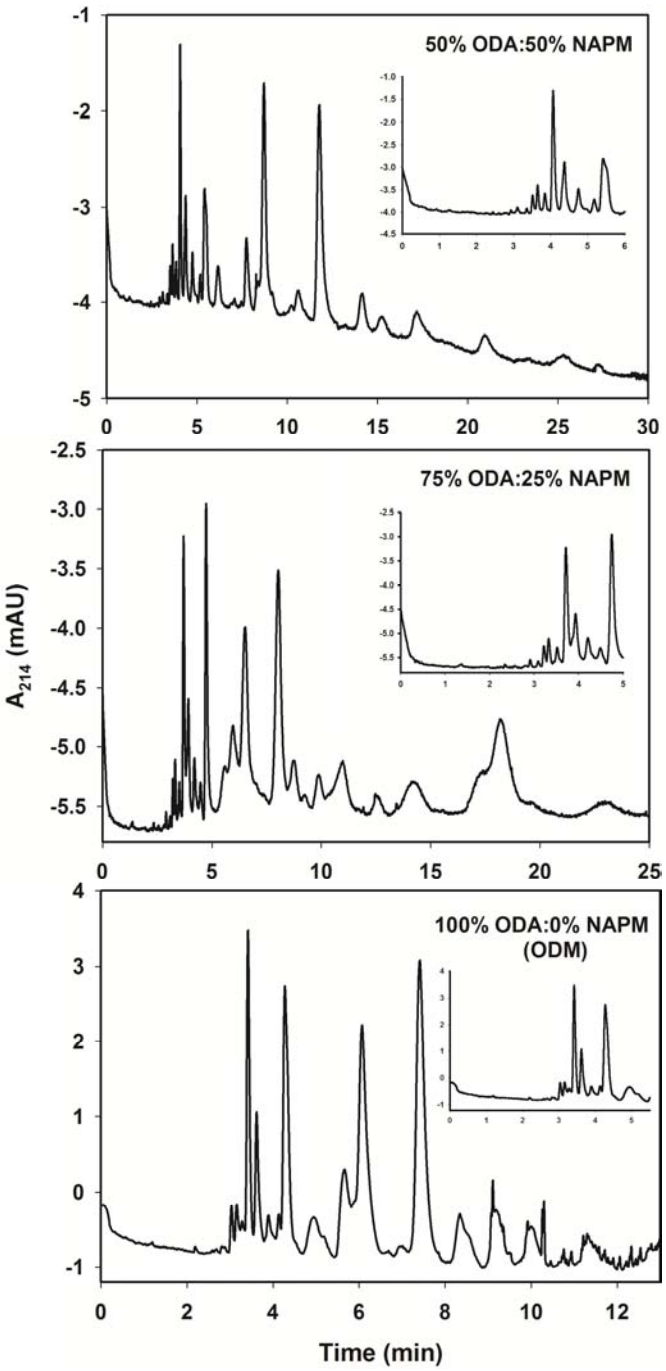

Figure 7. *Electrochromatograms of the separation of a tryptic digest of chicken white lysozyme on monolithic columns made from different mol fraction ODA/NAPM. Capillary columns: 20 cm effective length, 27 cm total length × 100 μm ID. Other conditions as in Fig. 6.*

Conclusions

The fabrication of MLMs for reversed phase CEC of various neutral and charged solute probes has been described. Plots of the values of the retention factor k' of solutes versus the mole fraction of the functional monomers (i.e., the monomer furnishing the chromatographic ligands), used in the polymerization solutions yielded straight lines. Obviously, when the k' of a given solute was nearly the same on ODM and NMM, the k' value of that solute on the MLM columns was virtually independent of the mole fraction of the functional monomers. The larger the difference in the k' values of a given solute on ODM and NMM columns, the steeper was the slope of the line for the plot k' vs. mole fraction. On this basis, the retention and selectivity for a given set of solute could be conveniently predicted so that the optimum MLM column could be readily designed. Also, the EOF velocity of the MLM columns varied as a function of the mole fraction of ODA in the polymerization solution. However, the dependence of EOF velocity on the mole fraction of ODA could not be easily predicted due to the fact that the EOF velocity depends also on the pore size distribution of the MLM columns, which also varied with the mole fraction of the functional monomers.

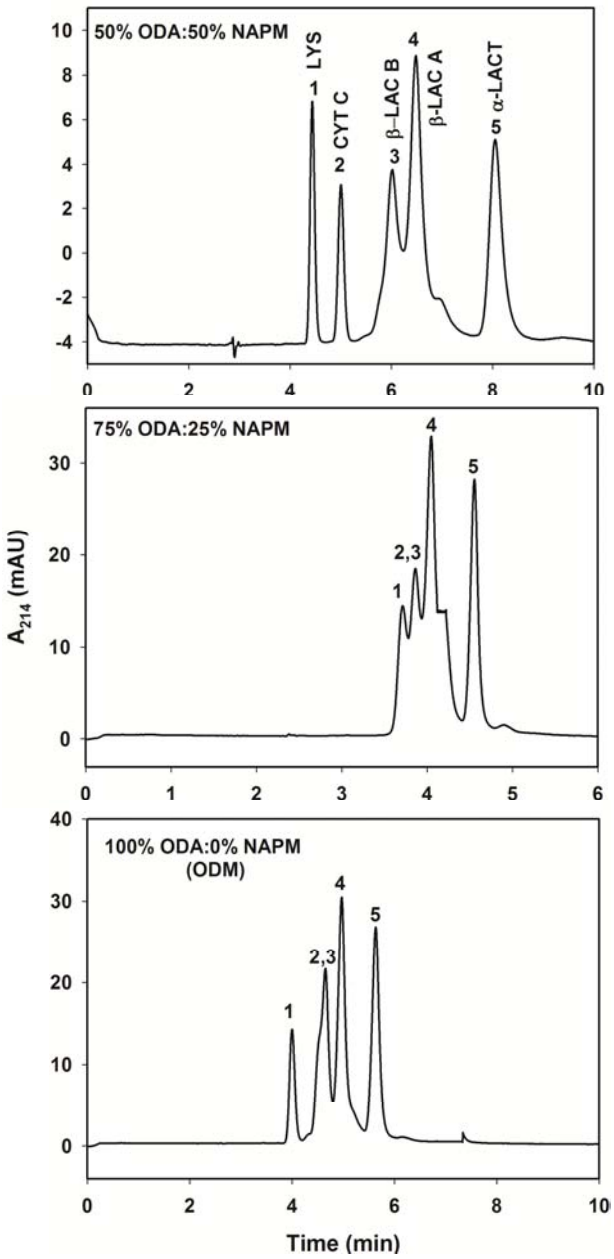

Figure 8. *Electrochromatograms of some standard proteins on monolithic columns made from different mol fraction ODA/NAPM. Capillary columns: 20 cm effective length, 27 cm total length × 100 μm ID; mobile phase, 10 mM sodium phosphate, pH 7.0, at 50% v/v ACN; running voltage, 12 kV; electrokinetic injection for 3 s at 10. Solutes: 1, Lysozyme; 2, Cytochrome C; 3, β-lactoglobulin B, 4, β-lactoglobulin A; and 5, α-lactalbumin*

References

1. Pursch, M., Sander, L. C., *J. Chromatogr. A* **2000**, *887*, 313-326.
2. Dittmann, M. M., Rozing, G. P., J. *Microcol. Sep.* **1997**, *9*, 399-408.
3. Ohyama, K., Fujimoto, E., Wada, M., Kishikawa, N., Ohba, Y., Akiyama, S., Nakashima, K., Kuroda, N., *J. Sep. Sci.* 2005, *28*, 767-773.
4. Alfrey, T., Price, C. C., *J. Polym. Sci.* **1947**, *2*, 101-109.
5. Jenkins, A. D., *J. Polym. Sci.* **1996**, *34*, 3495-3510.
6. Brandrup, J., Immergut, E. H., Grulke, E. A. (Eds.), Polymer Handbook, John Wiley & Sons, New York **1999**.
7. Jordan, E. F., Bennett, R., Shuman, A. C., Wrigley, A. N., *J. Polym. Sci. A-1* **1970**, *8*, 3113-3121.
8. Simionescu, C. I., Natansohn, A., Percec, V., *Colloid & Polymer Sci.* **1981**, *259*, 697-700.
9. Karenga, S., El Rassi, Z., *J. Sep. Sci.* **2008**, *31*, 2677-2685.
10. Karenga, S., El Rassi, Z., *Electrophoresis* **2010**, *31*, 991-1002.
11. Graham Solomons, T. W., Fryhle, C. B., Organic Chemistry, John Wiley & Sons, Inc **2008**, pp. 650 - 653.
12. Reubsaet, J. L. E., Vieskar, R., *J. Chromatogr. A* **1999**, *841*, 147-154.

VITA

Samuel Mukiha Karenga

Candidate for the Degree of

Doctor of Philosophy

Thesis: NEUTRAL MONOLITHIC CAPILLARY COLUMNS WITH ALKYL AND ARYL LIGANDS FOR REVERSED-PHASE CAPILLARY ELECTROCHROMATOGRAPHY

Major Field: Chemistry

Biographical:

Personal Data: Born in Nyeri District, Kenya, on December 29, 1975, the son of Samson Karenga and Agnes Gachanja

Education: Graduated from Giakanja Secondary School, Nyeri, Kenya in November, 1995; received Bachelor of Science degree in Chemistry and Master of Science degree in Chemistry from Egerton University, Njoro, Kenya in October 2002 and November 2009, respectively. Completed the requirements for the Doctor of philosophy degree with major in Chemistry at Oklahoma State University, Stillwater, Oklahoma in July, 2010.

Experience: Worked under dissertation research internship program at International Center for Insect Physiology and Ecology (ICIPE), Nairobi, Kenya, August 2003-April 2005. Employed by Oklahoma State University, Department of Chemistry as a teaching assistant, August 2005 to present.

Professional Memberships: American Chemical Society and California Separation Science Society.

Name: Samuel Mukiha Karenga Date of Degree: July, 2010

Institution: Oklahoma State University Location: Stillwater, Oklahoma

Title of Study: NEUTRAL MONOLITHIC CAPILLARY COLUMNS WITH ALKYL AND ARYL LIGANDS FOR REVERSED-PHASE CAPILLARY ELECTROCHROMATOGRAPHY

Pages in Study: 195 Candidate for the Degree of Doctor of Philosophy

Major Field: Chemistry

Scope and Method of Study:

The broad objective of this dissertation involved an integrated approach for furthering the advancement of reversed-phase capillary electrochromatography (RP-CEC) by providing an improved design of neutral acrylate/methacrylate–based monoliths offering both hydrophobic and π interactions for separating a wide range of solutes including polyionic biomolecules such as peptides and proteins. Being neutral, the monoliths were void of fixed charges that are traditionally incorporated to support EOF but still afforded relatively strong electrosomotic flow (EOF) necessary for mass transport in the absence of annoying electrostatic interactions. Such interactions would otherwise lead to irreversible adsorption of charged analytes to the stationary phase surface, causing band broadening and irreproducible retention times. Towards this end, octadecyl acrylate monoliths (ODM), naphthyl methacrylate monoliths (NMM), segmented monolithic columns (SMC) and mixed ligand monoliths (MLM) were developed and evaluated.

Findings and Conclusions:

The investigation described in this dissertation has significantly contributed to enhancing the scope of RP-CEC by demonstrating its capabilities in areas that had not been largely exploited previously. Although without fixed charges, the neutral monoliths afforded relatively strong EOF through the adsorption of ions from the electrolyte, which imparted the monolith with a given zeta potential to generate the EOF necessary for mass transport. The ODM columns provided hydrophobic interactions while the naphthyl methacrylate columns exhibited both hydrophobic and π interactions. By changing the choice of the crosslinker, the EOF, retention and selectivity of the ODM and NMM were tuned. Similarly, the preparation of SMC and MLM provided a convenient way of tuning the magnitude of EOF, retention and selectivity towards both neutral and charged solutes. The novel stationary phases developed within the framework of this investigation will not only facilitate a solution to many separation problems in life sciences, but also contribute to new concepts that will broaden the utility of RP-CEC in the future.

ADVISER'S APPROVAL: Dr. ZIAD EL RASSI